

**Splicing pattern of Aryl hydrocarbon interacting protein like 1 (AIPL1)  
in relation to Centromere Protein F**

Inaugural Dissertation  
submitted to the  
Faculty of Medicine  
in partial fulfillment of the requirements  
for the PhD-Degree  
of the Faculties of Veterinary Medicine and Medicine  
of the Justus Liebig University Giessen

by  
**Bhupesh Parise**  
of  
Vijayawada, India

Giessen 2013

From the Department of Ophthalmology  
Director: **Prof. Dr. med. Birgit Lorenz**  
Faculty of Medicine, Justus Liebig University Giessen

First Supervisor and Committee Member: **PD Dr. Dipl-Biol. Markus Preising**  
Second Supervisor and Committee Member: **Prof. Visvanathan Ramamurthy PhD**  
Examination Chair and Committee Member: **Prof. Dr. Christine Wrenzycki**  
Committee Member: **Prof. Dr. Lienhard Schmitz**

Date of Doctoral Defense: 26.02.2014

*“Tamaso ma jyotir Gamaya ...” (lead us from darkness to light)*

*In Sanskrit from the discussion of the life force ‘Prana’ in Brihadaranyaka Upanishad  
(1.3.28) (800–2000 bc)*

To my parents with so much love

## Table of Contents

<b>Abbreviations.....</b>	<b>Vi</b>
<b>List of figures.....</b>	<b>X</b>
<b>Tables.....</b>	<b>Xi</b>
<b>1. INTRODUCTION.....</b>	<b>1</b>
1.1 Visual pigments: Role of rods and cones.....	2
1.1.1 Visual cycle.....	2
1.2 Inherited retina degenerations: Lebers Congenital Amaurosis (LCA).....	3
1.3 Aryl Hydrocarbon Interacting Protein Like 1 AIPL1.....	5
1.3.1 Role of TPR motifs in AIPL1.....	6
1.3.2 Chaperone role of AIPL1.....	7
1.3.3 Role of Phosphodiesterase 6 (PDE6) in retina & Influence of AIPL1 on PDE6.....	7
1.4 Alternative Splicing.....	9
1.4.1 Alternative splicing in AIPL1.....	9
1.4.2 Splicing pattern in AIPL1.....	10
1.5 Centromere protein F.....	11
1.5.1 Leucine Zipper Motifs role in protein interaction.....	13
1.6 Relationship between AIPL1 and Cell cycle regulatory proteins.....	14
1.7 Aim of the study.....	15
<b>2. MATERIALS AND METHODS.....</b>	<b>16</b>
2.1 Materials.....	16
2.1.1 Chemicals and Reagents.....	16
2.1.2 Oligonucleotides.....	18

2.1.3 Vectors.....	18
2.1.4 Cell lines.....	19
2.1.5 Competent cells.....	19
2.1.6 Enzymes.....	19
2.1.7 Antibodies.....	20
2.1.8 Buffers.....	21
2.1.9 Ready Kits.....	23
2.1.10 Molecular weight standards.....	23
2.2 Equipment and devices.....	24
2.2.1 Computer aided data processing.....	25
2.3 Methods of molecular biology.....	26
2.3.1 Polymerase chain reaction (PCR).....	26
2.3.2 Agarose gel electrophoresis.....	28
2.3.3 Isolation of DNA from agarose gels.....	28
2.3.4 Cloning.....	29
2.3.4.1 Restrictionendonuclease digestion.....	29
2.3.4.2 Dephosphorylation.....	30
2.3.4.3 Ligation.....	30
2.3.4.4 Transformation.....	31
2.3.4.5 Preparation of competent bacterial cells.....	31
2.3.4.6 Bacterial transformation by electroporation.....	32
2.3.5 Preparation of plasmid DNA.....	32
2.3.5.1 Preparation of plasmid DNA (Miniprep).....	32

2.3.5.2 Preparation of plasmid DNA (Maxiprep).....	33
2.3.6 Quantification of nucleic acid.....	34
2.3.7 Sequence analysis of plasmids.....	34
2.3.8 Preparation of Glycerol stocks.....	34
2.3.9 Over expression of recombinant proteins.....	35
2.3.9.1 Growth of standard <i>E.coli</i> expression cultures (100 ml).....	35
2.3.9.2 Over expression with EnPresso™ Tablet cultivation set.....	35
2.3.10 Protein extraction.....	36
2.3.10.1 Protein extraction from tissue.....	36
2.3.10.2 Bacterial protein extraction.....	36
2.3.10.3 Mammalian protein extraction.....	37
2.3.11 Determination of the protein concentration by Bradford assay.....	37
2.3.12 Purification of His tagged proteins using Ni-NTA resin under native conditions.....	38
2.3.12.1 Buffers for purification under native conditions.....	38
2.3.12.2 Purification of over expressed and extracted recombinant proteins using Ni_NTA resin.....	38
2.3.13 Concentrating protein samples using centriprep® centrifugal filter device .....	39
2.3.14 Gel electrophoresis of proteins-SDS-PAGE.....	40
2.3.14.1 Preparation of His tagged marker.....	40
2.3.14.2 Protein electrophoresis using manually prepared acrylamide gels.....	41
2.3.14.3 Loading and running.....	41
2.3.14.4 SDS-PAGE using precast 8-16 % gradient SERVAGel™ TG.....	41
2.3.15 Polyacrylamide Gel Staining Protocol.....	42
2.3.16 Western Blotting.....	42

2.3.17 Ponceau S staining of proteins on nitrocellulose membranes.....	43
2.3.18 Antibody Hybridization on nitrocellulose membranes.....	44
2.3.19 Stripping and reprobing Western blots.....	45
2.3.20 Mammalian cell culture.....	46
2.3.20.1 HEK293 cell line.....	46
2.3.20.2 HeLa cell line.....	46
2.3.20.3 Culture of cell lines.....	47
2.3.20.4 Long term storage of cell lines.....	47
2.3.21 Heterologous expression in HeLa cells for immunocytochemistry.....	47
2.3.21.1 Transfection of HeLa cells using lipofectamin <sup>®</sup> .....	47
2.3.21.2 Transfection of HeLa cells using Roti <sup>®</sup> -Fect PLUS.....	48
2.3.22 Immunocytochemistry.....	48
2.3.23 Heterologous expression in HEK293 cells and mammalian protein extraction.....	49
<b>3. Results.....</b>	<b>50</b>
3.1 Sub cloning of AIPL1 splice variants into an expression vector.....	50
3.1.1 Identification of human AIPL1 splice variants.....	50
3.1.2 Cloning of splice variants.....	51
3.1.3 Restriction digestion and sequence analysis.....	54
3.2 Over expression of AIPL1 splice variants in a Prokaryotic system using the Enbase <sup>®</sup> Flo cultivation system .....	56
3.2.1 Recombinant protein purification and pull down experiments.....	56
3.2.1.1 SDS_PAGE of Ni_NTA agarose purified probes of SV1-SV5.....	56
3.2.1.2 SDS_PAGE of His tag purified and centriprep concentrated samples of (SV1- SV5).....	57

3.2.3 Immunoblot analysis of <i>AIPL1</i> splice variants.....	58
3.2.3.1 Western blot analysis of <i>AIPL1</i> splice variants (SV1-SV5) expressed in prokaryotic system.....	58
3.2.3.2 Immunoblot detection of His tags in <i>AIPL1</i> splice variants from SV1-SV5.....	60
3.2.3.3 Expression and purification of recombinant proteins in HEK293 cell lines.....	61
3.3 Intracellular localization of human <i>AIPL1</i> splice variants SV1-SV5 in HeLa cells.....	63
3.3.1 Immunohistochemical co-detection of heterologously expressed <i>AIPL1</i> and Intrinsic CENP-F.....	67
<b>5. Discussion.....</b>	<b>72</b>
4.1 Impact of splicing on <i>AIPL1</i> protein function.....	72
4.2 Protein expression and purification studies of <i>AIPL1</i> .....	73
4.2.1 Role of imidazole and FKBP's in protein purification.....	74
4.3 Immunoblot analysis of <i>AIPL1</i> splice variants.....	74
4.4 Choosing CENP-F as a possible interaction partner of <i>AIPL1</i> .....	75
4.5 Features that support interaction between <i>AIPL1</i> and CENP-F.....	75
4.6 Colocalization studies of <i>AIPL1</i> and CENP-F.....	76
4.7 Future aspects in validating <i>AIPL1</i> splice variants and protein interaction studies.....	77
<b>6. Summary.....</b>	<b>78</b>
<b>7. Zusammenfassung.....</b>	<b>79</b>
<b>8. References.....</b>	<b>80</b>
<b>9. Acknowledgements.....</b>	<b>88</b>

## Abbreviations

AIPL1	Aryl hydrocarbon interacting protein like 1
ABCR	ATP-binding cassette (ABC) –transporter gene, retina specific
A. dest	Double distilled water
ad	autosomal dominant
ar	autosomal recessive
aa	Amino acid
bp	Base pairs
BSA	Bovine serum albumin
B-PER	Bacterial Protein Extraction Reagent
CENP-F	Centromere protein F
COD	Cone dystrophy
cDNA	coding DNA
cGMP	cyclic Guanosine Monophosphate
CORD	Cone-Rod dystrophy
CRALBP	Cellular Retinaldehyde-binding Protein
CRX	Cone Rod Homeobox Protein
CSRD	Childhood-onset Severe Retinal Dystrophy
DNA	Deoxyribonucleic Acid
dNTP's	Deoxynucleotide Triphosphates
EDTA	Ethylenediaminetetraacetic Acid

EOSRD	Early-Onset Severe Retinal Dystrophy
ERG	Electroretinography
FKBP	FK506-binding protein family
FKS	Fetal Calf Serum
g	gram
GMP/GDP/GTP	Guanosin-Mono-/-Di-/-Triphosphat
h	hour
HEPES	2-[4-(2-hydroxyethyl)piperazin-1-yl]ethanesulfonic acid
IPTG	Isopropyl $\beta$ -D-1-thiogalactopyranoside
kb	Kilobase pairs
kDa	Kilodalton
l	Liter
LCA	Leber Congenital Amaurosis
mRNA	messenger RNA
M	Mol
MW	Molecular weight
min	Minute
M-PER	Mammalian Protein Extraction Reagent
NUB1	NEDD8 Ultimate Buster 1
nm	Nanometer
nt	Nucleotide
OD	Optical density
PRD	Proline rich domain

PDE6	Phosphodiesterase 6
PAA	Polyacrylamide
PAGE	Poly Acrylamide Gel Electrophoresis
P/Cl	phenol / chloroform / isoamyl alcohol
PCR	Polymerase Chain Reaction
PFA	Paraformaldehyde
RDS	Retinal Degeneration Slow
RNA	Ribonucleic Acid
RP	Retinitis Pigmentosa
RPE	Retinal Pigment Epithelium
RPE65	Retinal Pigment Epithelium Protein 65
RPGR	Retinitis Pigmentosa GTPase Regulator
rpm	revolutions per minute
RT	Room Temperature
S	Second
SDS	Sodium Dodecyl Sulphate
SV	Splice Variant
TPR	Tetratrico peptide repeat motifs
TBE	Tris/Borate/EDTA (Running buffer for gel electrophoresis)
TE	Tris-EDTA
U	Unit
UTR	Untranslated region
UV	Ultraviolet light

V	Volt
v/v	Volume per volume
W	Watt
w/v	weight per volume
X-Gal	5-bromo-4-chloro-indolyl- $\beta$ -D-galactopyranoside

### **Nucleic acids /Nucleotides**

A	Adenine
C	Cytosine
G	Guanine
T	Thymine
U	Uracil
P	Purines (A, G)
Y	Pyrimidines (C, T/U)
N	arbitrary nucleotide

### **Amino acids:**

M	Met	Methionine
N	Asn	Asparagine
P	Pro	Proline
Q	Gln	Glutamine
R	Arg	Arginine
S	Ser	Serine
T	Thr	Threonine
V	Val	Valine
W	Trp	Tryptophan
Y	Tyr	Tyrosine

## List of figures

Figure 1 Structure of the human retina.....	1
Figure 1 a. Schematic representation of the human eye.....	1
Figure 1 b. Cross-section of the human retina.....	1
Figure 2 Schematic representation of the human retina.....	4
Figure 3 Schematic representation of AIPL1 protein.....	6
Figure 4 Potential AIPL1 photoreceptor functions.....	8
Figure 5 Schematic illustration of important functional regions of Centromere protein F.....	12
Figure 6 Schematic illustration of CENP-F in cell cycle.....	13
Figure 7 Western blotting transfer order. Arrow shows direction of transfer .....	43
Figure 8 pCR <sup>®</sup> 2.1-TOPO-TA vector map with AIPL1 cloned into the TA-site.....	51
Figure 9 pQE-Tri-System His. <i>Strep</i> 1 vector map and its elements.....	52
Figure 10 Multiple cloning site of pQE-TrisSystem His. <i>Strep</i> 1.....	52
Figure 11 Vector map of pQE-Tri-SystemHis. <i>Strep</i> 1 Vector containing <i>AIPL1</i> splice variants SV1 - SV5.....	53
Figure 12 Restriction endonuclease analysis of <i>AIPL1</i> splice variant pQE-TriSystem 1 His. <i>Strep</i> clones (SV1 - SV5).....	54
Figure 13 A. Verification of forward frame conservation of the inserts towards start codon of the vector with chosen restriction site EcoRI.....	55
Figure 13 B. Verification of reverse frame conservation of the inserts towards stop codon of the vector with tags 8x His and Strep along with the chosen restriction site HindIII. ....	55
Figure 14 Coomassie-stained SDS-PAGE analysis of over expressed His tagged AIPL1 (SV1 - SV5) purified by Ni-NTA agarose.....	57
Figure 15 Coomassie-stained SDS-PAGE analysis of His tagged AIPL1 purified by Ni-NTA agarose and concentrated samples of E2 fractions of (SV1 - SV5).....	58
Figure 16 A: Ponceau S staining of the nitrocellulose membrane following electrophoretic transfer of proteins by SDS-PAGE gel separation.....	59
Figure 16 B: Western blot analysis of overexpressed and purified His tagged AIPL1 splice variants SV1 - SV5 in prokaryotic system.....	59
Figure 17 Western blot analysis of over expressed and purified His tagged AIPL1 splice variants (SV1 - SV5) in prokaryotic system.....	60
Figure 18 SDS-PAGE of Ni-NTA agarose purified probes (SV1 - SV5) from expression in eukaryotic HEK293 cell lines.....	61

Figure 19 SDS-PAGE of centriprep concentrated probes of AIPL1 SV1 - SV5 from expression in eukaryotic HEK293 cell lines.....	62
Figure 20 Western blot analysis of AIPL1 splice variants (SV1 - SV5) (Eukaryotic).....	62
Figure 21 Heterologues expression of <i>AIPL1</i> splice variants in HeLa cells: Immunofluorescent images showing intracellular localisation of AIPL1 proteins expressed in HeLa cells.....	65
Figure 22 Heterologous expression of His-tagged AIPL1: Immunofluorescent images showing cellular localisation of AIPL1 proteins expressed in HeLa cells.....	67
Figure 23 Immunohistochemical detection of intrinsic <i>CENPF</i> expression and transient <i>AIPL1</i> expression in HeLa cells.....	69
Figure 24 Immunohistochemical detection of intrinsic <i>CENPF</i> expression and transient expression of His-tagged AIPL1 in HeLa cells.....	71

## Tables

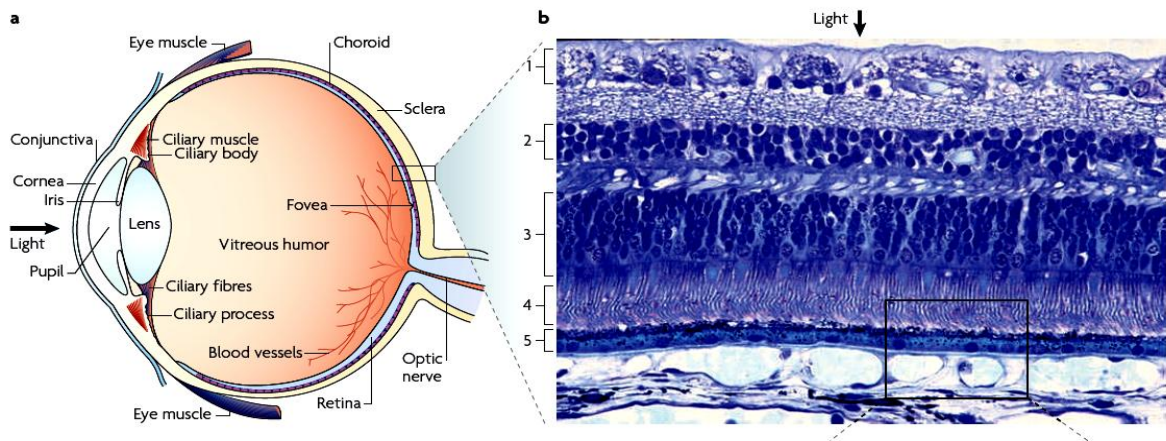
Table 1 List of genes frequently identified underlying LCA and EOSRD.....	3
Table 2 Splicing pattern in AIPL1.....	10
Table 3 Gel mixture.....	41
Table 4 Expected sizes of cloned <i>AIPL1</i> splice variant fragments.....	54

# CHAPTER 1

## I. Introduction

The retina is an anatomical component of the eye where light particles are captured and transmuted into neuronal signals for vision with the help of photoreceptor cells (rods and cones). In the mammalian retina, rods occupy a share of approximately 90% of photoreceptor cells and cones occupy the remaining 10%. Rods operate in dim light whereas cones operate in daylight and perform colour discrimination. The retina is an outpost of the central nervous system where several genes play a role in retinal dystrophies. Leber Congenital Amaurosis (LCA) is a subgroup of a set of early onset severe retinal dystrophies (EOSRD) causing severe visual impairment from birth with legal blindness at the age of 2 years[13]. This study investigates *AIP1* one of the genes underlying LCA.

**Figure 1: Structure of the human retina**



**a. Schematic representation of the human eye retina**

**b . Cross-section of the human retina**

a. Schematic representation of the human eye: Light passes through the pupil, lens and vitreous cavity before reaching the light-sensitive retina. b . Cross-section of the human retina:

(1) Ganglion cell layer - axons form optic nerve connects the retina to the brain (2) Inner nuclear layer, which contains second-order neurons, such as bipolar, amacrine and horizontal cells (3) Outer nuclear or photoreceptor (PR) layer, which contains the cell bodies and nuclei of the rod and cone PRs (4) PR outer segments, which are densely packed with Opsin-containing discs and are separated from the inner segments and cell bodies by a narrow 200 –

500 nm-long connecting cilium (not visible) (5) Retinal pigment epithelium (RPE), a monolayer of cells containing tight junctions that separates the neural retina from the choroid, which supplies blood to the RPE and PRs (outer retina). Notice the inverted orientation, in which light passes through the nerve fibre layers, inner retinal blood vessels and inner cell layers before reaching the light-sensitive PRs, which are located close to their blood supply. [92,105] (Fig reproduced with kind permission of: Nat Rev Genet. 2010 Apr;11(4):273-84. doi: 10.1038/nrg2717)

## **1.1 Visual Pigments: Role of rods and cones**

In photoreceptors 11-*cis* retinal, a chromophore is a light sensitive component linked to an opsin apo-protein. Opsin activates signaling pathways and generates a cellular response to light. Opsins are G-protein coupled receptors with a binding pocket for 11-*cis* retinal. The visual pigment is thus formed when the apo-protein part of the opsin and 11-*cis* retinal combine [70]. The apo-proteins are not photosensitive by themselves. Opsins become photosensitive when 11-*cis* retinal is attached. Rhodopsin is the visual pigment of rod photoreceptors. In addition, three types of cone photoreceptors are present in humans, each one with a specific absorption peak at a wavelength corresponding to red, green, and blue light [12]. When light strikes the visual pigment, the isomerization of 11-*cis* retinal to all-*trans* retinal in the binding pocket transforms the apo-protein into an active conformation and initiates phototransduction. While the newly formed all-*trans* retinal is required for the activation of opsin all-*trans* retinal must be released from opsin and fresh 11-*cis* retinal must be bound to regain light sensitivity [71].

### **1.1.1 Visual cycle**

The conversion of all-*trans*-retinal back to 11-*cis*-retinal requires a complex sequence of biochemical reactions involving several enzymes and retinoid binding proteins. Collectively, these reactions are known as the visual cycle or retinoid cycle. These biochemical reactions take place primarily in the retinal pigment epithelium (RPE). The recovery of 11-*cis* retinal during the visual cycle is important to maintain the sensitivity of the visual system [82] [57,59]. Abnormalities, dysfunction and/or death of retinal photoreceptors constitute the primary cause of visual impairment or blindness in most of the retinal degeneration diseases, such as Lebers's congenital amaurosis (LCA), retinitis pigmentosa and macular degeneration.

## 1.2 Inherited retinal degenerations: Leber Congenital Amaurosis (LCA)

Almost 150 years ago, Theodore Leber [61] described a severe form of vision loss at or near birth, which was later given his name. LCA accounts for at least 5% of all retinal dystrophies and is one of the main causes of blindness in children [44,77,84].

**Table 1: List of genes frequently identified underlying LCA and EOSRD**

Gene	Symbol	Locus	Reference
Retinale Guanylate cyclase 2D	<i>GUCY2D</i>	LCA1	[76]
Retinal pigment epithelium specific protein 65 kDa	<i>RPE65</i>	LCA2	[35]
Spermatogenesis Associated Protein 7	<i>SPATA7</i>	LCA3	[73] [104]
Aryl hydrocarbon receptor interacting protein-like 1	<i>AIPL1</i>	LCA4	[88]
Leber congenital amaurosis 5	<i>LCA5</i>	LCA5	[15]
Retinitis pigmentosa GTPase regulator interacting protein 1	<i>RPGRIP1</i>	LCA6	[21]
Cone-rod homeobox	<i>CRX</i>	LCA7	[28]
Crumbs homolog 1	<i>CRB1</i>	LCA8	[18]
Nicotinamide Nucleotide AdenylylTransferase 1	<i>NMNAT1</i>	LCA9	[11,26,53] [75]
Nephronophthisis 6	<i>NPHP6</i> , <i>CEP290</i>	LCA10	[16]
Inosine monophosphate dehydrogenase 1	<i>IMPDH1</i>	LCA11	[8]
Retinal degeneration 3	<i>RD3</i>	LCA12	[29,79]
Retinol dehydrogenase 12	<i>RDH12</i>	LCA13	[74]
Lecithin retinol acyltransferase	<i>LRAT</i>	LCA14	[93]
Tubby like protein 1	<i>TULP1</i>	LCA15	[19,68]
Potassium Channel, Inwardly Rectifying, Subfamily J, Member 13	<i>KCNJ13</i>	LCA16	[85]

The disease was characterized by a reduced or abolished photoreceptor response to light, wandering nystagmus, and a normal fundus at birth [27] progressing to a typical appearance of retinitis pigmentosa. There has often been a failure to diagnose LCA because of the normal appearance of the fundus in the first months of life, leading to the misdiagnosis of cortical blindness. LCA and related early-onset retinal degenerations are caused by mutations in at

least 23 genes (<http://www.ncbi.nlm.nih.gov/books/NBK1298/>, <http://www.retina-international.org/sci-news/databases/disease-database/leber-congenital-amaurosis/>). All these genes were identified to cause LCA but few of them are rare sometimes identified in very early onset.

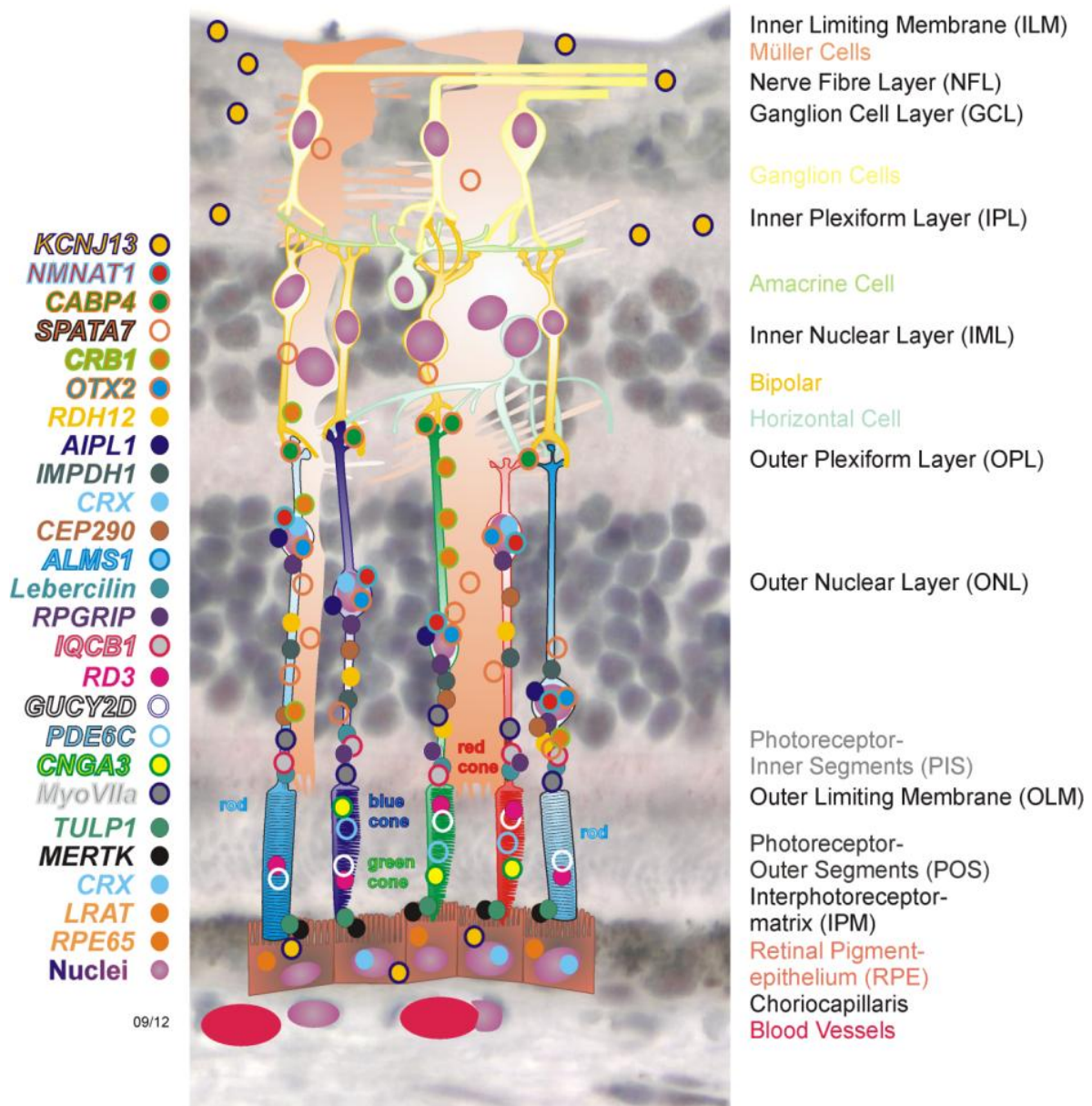


**Figure 2: Schematic representation of the human retina** - showing photoreceptors (PRs), muller glia, microglia, astrocytes, and vessels. The outer nuclear layer (ONL) is composed of the cell bodies of rod and cone PRs, the inner nuclear layer (INL) contains the cell bodies of several types of neurons (horizontal cells, bipolar cells, amacrine cells) as well as the bodies of Muller glia. The ganglion cell layer (GCL) contains ganglion cells. Left panel indicates the

list of genes underlying LCA. (Fig modified from : <http://www.retina-international.org/sci-news/databases/disease-database/leber-congenital-amaurosis/>)

### **1.3 Aryl Hydrocarbon receptor Interacting Protein Like 1 (AIPL1)**

*AIPL1* is the fourth gene linked with LCA [88]. The share of *AIPL1* in LCA is about 7 %. Main features of *AIPL1* are three tetratricopeptide repeat (TPR) domains, a poly proline rich region, and a FKBP506 binding domain.

*AIPL1* expression is limited to photoreceptors and the pineal gland, the gene consists of 6 exons which encodes a 384 amino acid protein containing three tetratricopeptide (TPR) motifs [81,88,97] and belongs to FK506-binding protein (FKBP) family. [88]. Early studies revealed that *AIPL1* is expressed only in rods and performs a function essential for the maintenance of rod photoreceptor [97]. Further studies revealed the presence of AIPL1 in rod and cone photoreceptors of the developing human retina but absent from cone photoreceptors in adult human retina [99]. Later it was disclosed that the presence of AIPL1 is endogenous in adult mouse and human cones, albeit the expression is very low in cone cells compared to rod cells [51]. Human AIPL1 protein sequence contains three tetratricopeptide (TPR) motifs, 34 amino acid motifs that are thought to serve as interfaces for protein-protein interactions [7,20]. TPR motifs are found in proteins that mediate a variety of functions, including protein trafficking or protein folding. These proteins are usually associated with multiprotein complexes [7]. In addition, a Proline-rich region is present at the carboxyl-terminus of the protein, in humans. Similar sequences are found in situations requiring rapid recruitment or interchange of several proteins, such as signaling cascades or initiation of transcription [46].

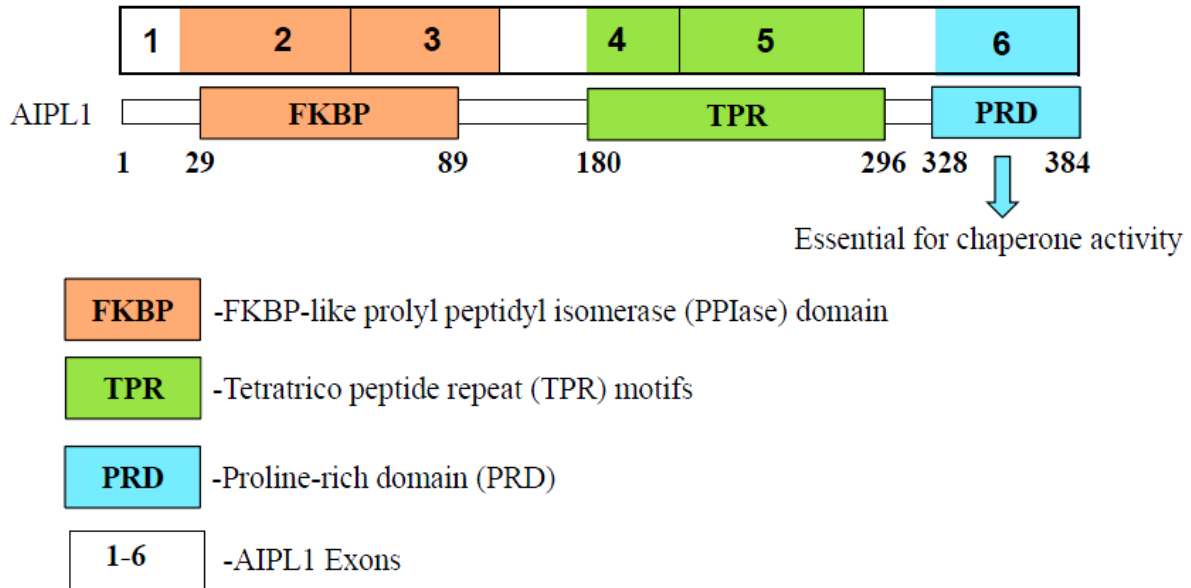


**Figure 3: Schematic representation of AIPL1 protein [62]**

(Fig modified from: Biochemistry. 2013 Mar 26;52(12):2089-96. doi: 10.1021/bi301648q. Epub 2013 Mar 13)

### 1.3.1 Role of TPR motifs in AIPL1

The presence of TPR motifs downstream from a Peptidylprolyl isomerase (PPIase) domain in AIPL1 makes it a close relative of the larger members of the FK-506 binding protein (FKBP) family such as FKBP52 and AIP, which function in the maturation or translocation of steroid receptors and dioxin, respectively [50,78]. The TPR motif is an evolutionary and functionally conserved but degenerate motif found in a number of structurally unrelated proteins. It mediates the binding of specific protein-interaction partners [98]. The TPR motif consists of a 34 aminoacid sequence comprising a pair of anti-parallel alpha helices that are arranged in large superhelical arrays of tandem repeats, forming a contiguous concave surface suitable for binding to a peptide ligand. Proteins containing TPR motifs are widely distributed across multiple classes of proteins involved in a variety of cellular functions [14,87].

The importance of the TPR domain in AIPL1 and its role in protein interactions were investigated by analyzing the mutations within the TPR domain of AIPL1, located between amino acid residues 181 and 330. At this site many LCA-associated mutations of AIPL1 were found [43]. Along with mutations the other aspect which abolished interactions is the removal of the chaperone TPR acceptor site (residues 329-384) (figure 4).

### **1.3.2 Chaperone role of AIPL1**

AIPL1 role as a chaperone was indicated by aligning of AIPL1 with the aryl hydrocarbon receptor interacting protein (AIP), in which AIPL1 shares 49% similarity with AIP [88]. The proteins of the FKBP family function as chaperones and typically do not act at the step of initial polypeptide folding. Rather, these proteins are “specialized chaperons” that assist specific client proteins in later stages of maturation, subunit assembly, transport, and degradation [7,9,106]. AIPL1 interacts with the molecular chaperones Hsp70 and Hsp90. Probing the role of these chaperons in AIPL1 chaperone activity showed that AIPL1 cooperated with Hsp70, but not with Hsp90, to suppress the formation of NUB1 inclusions. It was shown that AIPL1 may use components of the Hsp70 and Hsp90 chaperone machineries to fulfill its important photoreceptor-specific functions [37].

### **1.3.3 Role of phosphodiesterase 6 (PDE6) in retina and influence of AIPL1 on PDE6**

In the retina phosphodiesterase 6 (PDE6) is highly represented and controls cytoplasmic levels of cyclic guanosine monophosphate (cGMP) in outer segments of the rods and cones in response to light [12]. Retinae lacking AIPL1 showed rod photoreceptor degeneration which is due to massive reduction of rod cGMP phosphodiesterase (PDE6) subunits ( $\alpha$ ,  $\beta$  and  $\gamma$ ) but the link between AIPL1 and the stability of PDE6 subunits is not known. Ex-vivo pulse label analysis demonstrated that AIPL1 is not involved in the synthesis of PDE6 subunits [54]. Instead, rod PDE6 subunits are rapidly degraded by proteasomes in the absence of AIPL1. This rapid degradation of PDE6 is due to the essential role of AIPL1 in the proper assembly of synthesized individual PDE6 subunits. It was shown that the catalytic subunit ( $\alpha$ ) of PDE6 associates with AIPL1 in retinal extracts and is needed for the proper assembly of functional rod PDE6 subunits. [54]

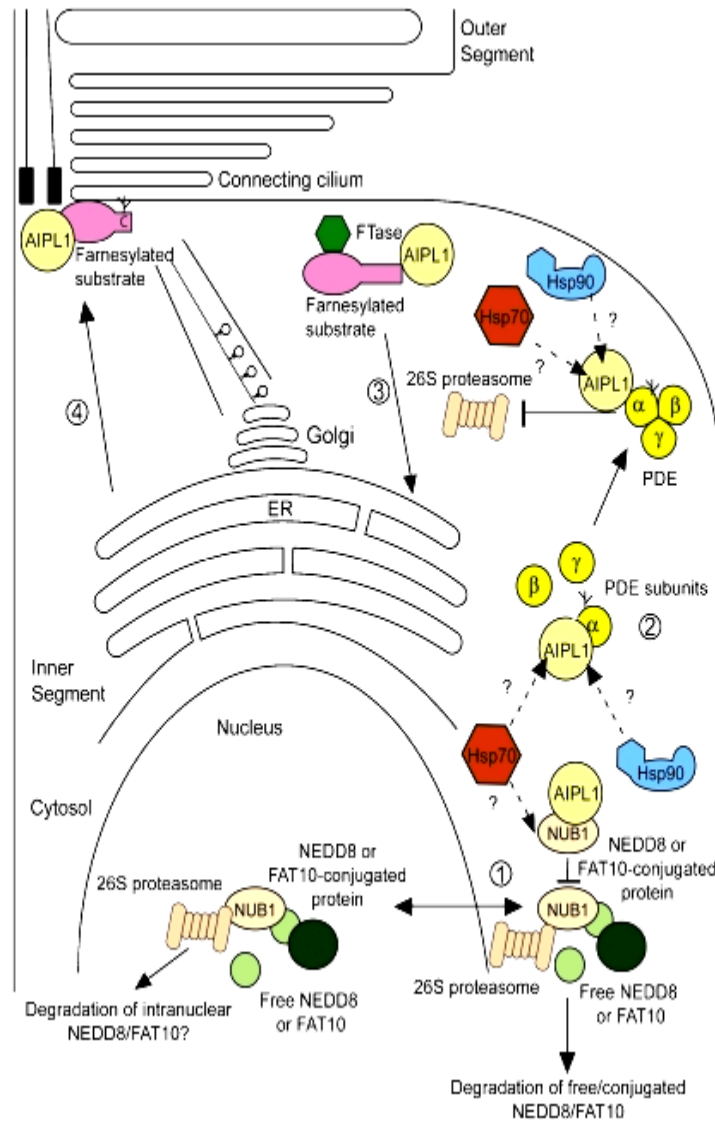


**Figure 4: Potential AIPL1 photoreceptor functions**

(Fig reproduced with kind permission of : Prog Retin Eye Res. Jul 2008; 27(4): 434–449. doi: 10.1016/j.preteyeres.2008.03.001)

Schematic representation showing potential roles of AIPL1 within photoreceptors. AIPL1 is able to modulate the nuclear localization of NUB1, which may affect the NUB1 NEDD8 and FAT10 ‘busting’ activity (1) AIPL1 interacts with and enhances stability of the PDE holoenzyme (2) AIPL1 may enhance transport and stability of farnesylated proteins to the ER (3) or other target membranes (4). AIPL1 is likely to utilize the Hsp70 and Hsp90 chaperone machinery to execute its cellular functions [55].

Through Yeast two-hybrid analysis it was demonstrated that AIPL1 is able to interact with and aid in the processing of farnesylated proteins in a farnesyltransferase-dependent manner [98]. Protein prenylation directs protein-membrane interactions and is important for the maintenance of retinal and photoreceptor cytoarchitecture. AIPL1 may protect the

farnesylated protein from proteasomal degradation, or chaperone the targeted translocation of the farnesylated protein to an appropriate target membrane or to the ER for further processing.

#### **1.4 Alternative splicing**

Alternative splicing enables one gene to produce multiple mature transcripts with different sequences [38]. Genome-wide analyses revealed that 40 - 60% of human genes undergo alternative splicing [69]. Alternative splicing gives rise to functionally different proteins with specific biological function [90] and the regulation of alternative splicing is important for diverse biological processes. There are several types of alternative splice events, which vary in frequency. In vertebrates, the inclusion or skipping of entire exons are the most frequent alternative splice event [49]. Defects in splicing are associated with cancer [45,47,48] and other human diseases [103]. The advancements in proteomics have revealed many novel splice variants of the genes responsible for retinal disorders. Recent studies on alternative splicing and retinal degeneration reported mutations in alternatively spliced retina-specific exons of the widely expressed Retinitis pigmentosa GTPase regulator (*RPGR*) and *COL2A1* (collagen, type II, alpha 1) genes underlying X-linked RP and ocular variants of Stickler syndrome, respectively [64].

##### **1.4.1 Alternative splicing in *AIPL1***

Alternative splicing of *AIPL1* was shown to be common among mammals and affects regions encoding functionally important protein domains [41]. In addition, the alternatively spliced exons have been found to harbor mutations underlying LCA. Since alternative splicing is thought to broaden the functional range of a gene, the question arises to what extent the *AIPL1* isoforms functionally differ and whether this affects the impact of mutations occurring in the alternatively spliced *AIPL1* exons [41].

Besides a major full length mRNA, the alternative splice variants were less abundant. SV2 and SV3 appear rarely whereas the frequency of SV4 and SV5 is very rare[42]. Given that *AIPL1* is involved in both, cell cycle progression and photoreceptor maturation, different splice variants of *AIPL1* may be required to fulfill specialized functions in these pathways. Interestingly, the alternatively spliced exons do harbor LCA-causing mutations in man. In case of LCA due to exon 2, 3 or 5 mutations, fully functional minor *AIPL1* isoforms are supposed to be generated because mutations would be excluded from mature alternative transcripts (Exon 2 p.Gly64Arg, Exon 3 p.Thr114Ileu and Exon 5 p.Glu226Glu). This may

attenuate the resulting disease phenotype in comparison with mutations occurring in constitutively spliced exons (Exon 2 p.W178\* and Exon 5 p.Gly262Ser). Recently the prevalence of sequence variants in *AIPL1* was presented [95]. The study investigated the likelihood of disease causation of the identified variants, subsequently undertaking a detailed assessment of the phenotype of patients with disease causing mutations. The study reported that despite the associated phenotype being characterized by early onset severe visual loss in patients there was some evidence of a degree of retinal structure and functional preservation, which was most marked in the youngest patient. It was suggested that there are patients who have a reasonable window of opportunity for gene therapy in childhood. The identified splice variants of *AIPL1* present transcriptional in-frame deletions of the protein coding region, presumably giving rise to different isoforms of the AIPL1 protein. Interestingly, the alternative splicing events seem to affect important protein functions since the peptidyl–prolyl–isomerase domain and the binding site of cell cycle regulator NUB1 are involved [2,40].

#### 1.4.2 Splicing pattern in *AIPL1*

Gene expression analysis with qPCR revealed the presence of six different splice variants in *AIPL1* [41].

Splice variant	Sequence features (skipped peptide)	% of total transcript*	ORF length	MW of predicted isoform
1	All 6 exons included	50-80	1.155 bp / 384 aa	43.9 kd
2	Exclusion of exon 2 (aa 33-92)	10-20	975 bp / 324 aa	36.8 kd
3	Exclusion of exon 3 (aa 93-155)	10-20	966 bp/ 321 aa	35.0 kd
4	Exclusion of exon 5 part (aa 215-238)	5-10	1.083 bp / 360 aa	40.9 kd
5	Exclusion of exon 2 part (aa 33-54)	Rare	1.089 bp / 362 aa	41.2 kd
6	Exclusion of exon 2 part (aa 33-40), Exclusion of exon 5 part (aa 215-238)	Very rare	1.059 bp / 352 aa	39.9 kd

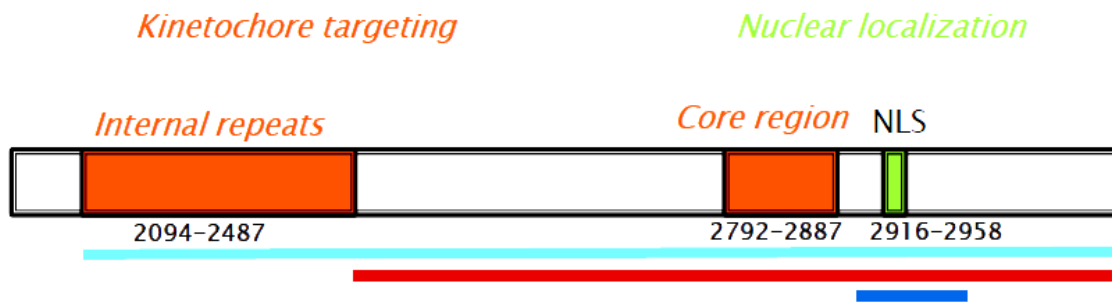
\*estimated from RT-PCR and cloning frequency

**Table 2: Splicing pattern in *AIPL1***

## **1.5 Centromere Protein F**

The centromere is an essential structure that is required for the accurate segregation of genetic material during mitosis and meiosis. It serves as a platform upon which the kinetochore assembles, thus, it is a vital structure for mitotic spindle attachment that is required to guide chromosomal movements during cell division [32]. CENP-F, also named as mitosin, is a large human protein of 3113 amino acid residues initially identified as cell-cycle dependent kinetochore-associated protein in human cells using human autoimmune serum [83]. Its expression and localization is cell cycle dependent [22]. The protein level is low in G1 phase but elevated from S to early M phase [110].

CENP-F is a large protein interacting with different partners through distinct protein domains. It possesses 11 leucine zipper motifs [110], which are potential dimerization motifs found in DNA-binding proteins [60]. Several such motifs in the C-terminus are involved in its kinetochore-targeting and interaction with Activating Transcription Factor 4 (ATF4) [107,108]. Residues 2961-3001 of CENP-F bind to Retinoblastoma protein (Rb) [5,110] whereas residues 2930-2958 contain a strong nuclear localization signal (NLS) [109].



C-terminal farnesylation motif (CAAX)

N- and C- terminal putative phosphorylation sites for Cdks and MAP kinases

Spindle pole localization

2094 – 3113

Homo and heterodimerization

2490 – 3113

Putative chromatin binding region

2902 – 3037

**Figure 5: Schematic illustration of important functional regions of CENP-F [101]**

(Fig reproduced with kind permission of : Chromosoma. 2006 Aug;115(4):288-95. Epub 2006 Mar 25)

CENP-F encodes a protein that associates with the centromere-kinetochore complex [66,101]. The protein is a component of the nuclear matrix during the G2 phase of interphase. In late G2, the protein associates with the kinetochore and maintains this association through early anaphase. Small GTPase Rab5 takes part in chromosome congression and regulates localization of CENP-F to the kinetochores [86]. CENP-F localizes to the spindle midzone and the intracellular bridge in late anaphase and telophase, respectively, and is predicted to be subsequently degraded [63]. The localization of this protein suggests that it may play a role in chromosome segregation during mitosis. It is thought to form either a homodimer or heterodimer. CENP-F represents the first transiently associated kinetochore protein that has been identified acting as an antigen in autoimmune disease [83]. Autoantibodies against this protein have been found in patients with cancer or graft versus host disease [10].

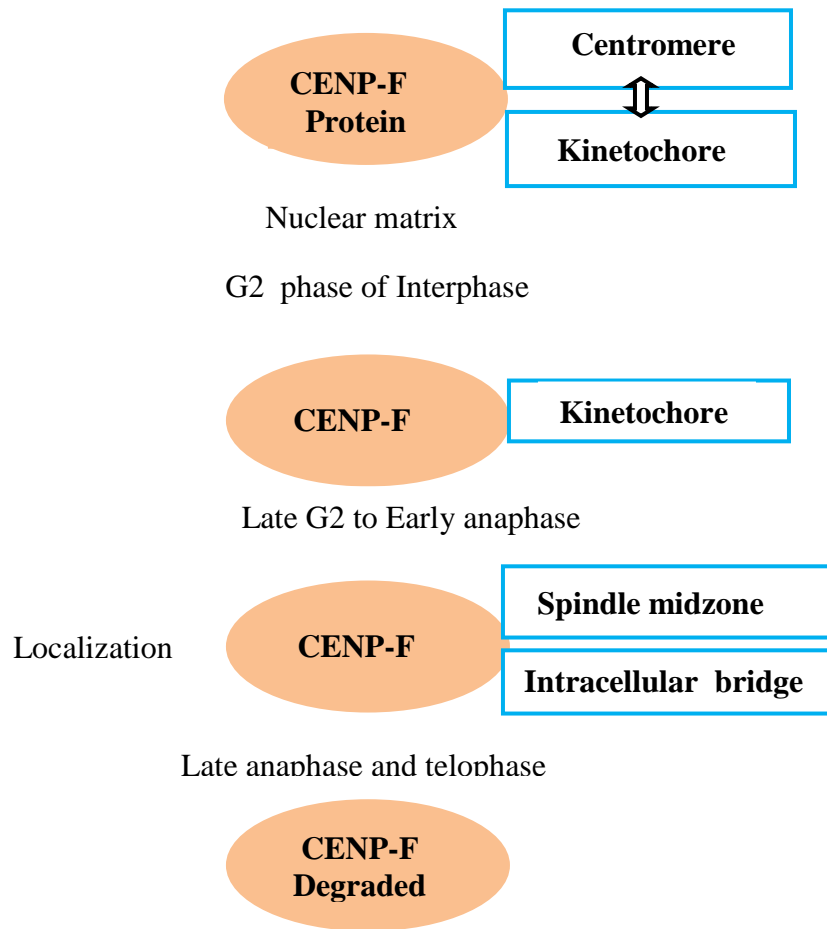


**Figure 6: Schematic illustration of CENP-F in cell cycle**

(Fig according to: Ref: <http://www.ncbi.nlm.nih.gov/gene/1063>)

### 1.5.1 Leucine Zipper Motifs role in protein interactions

In mitotin/CENP-F family proteins, one of the striking structural characteristics is the richness in leucine zipper motifs [33,63,109]. These motifs may mediate protein-protein interactions with other proteins. Leucine heptad repeats are frequently involved in protein-protein interactions and are found three times in the mitotin C terminus. The C terminus of mitotin is essential for its role in influencing cell cycle progression [110]. They may regulate the signaling for kinetochore localization by conveying a conformational change within mitotin. Removal of the region containing the leucine heptad repeats abolishes the homodimerization and heterodimerization capacity of the C terminus. Protein-protein interactions via leucine heptads in the C terminus may regulate the signaling for kinetochore localization by conveying a conformational change within mitotin.

## **1.6 Relationship between AIPL1 and cell cycle regulatory proteins**

During photoreceptor maturation, retinal degeneration observed in LCA patients with *AIPL1* mutations may result from a defect in the regulation of cell cycle progression. *AIPL1* interaction with NUB1 may function in the regulation of cell cycle progression and mutation in *AIPL1* may lead to photoreceptor cell death by disrupting the normal regulation of the cell cycle [1]. The expression of *AIPL1* in developing photoreceptors and the early onset of vision loss in patients with LCA suggests that *AIPL1* function is critical during the period of rod and cone photoreceptor development [99].

For maintenance of the retinal cytoarchitecture and photoreceptor structure, protein modification by prenylation is essential in vision. *AIPL1* interacts with farnesylated proteins and is important in the processing of farnesylated proteins in the retina [81]. Farnesylation is a specific type of prenylation, the addition of a farnesyl or geranylgeranyl residue to specific proteins. Several retinal proteins, cGMP phosphodiesterase (PDE), transducin, and rhodopsin kinase (RK) are known to be farnesylated [3,30,39,58]. The second possible role of *AIPL1* is the control of photoreceptor proliferation and differentiation. *AIPL1* plays a dual role during retinal development, regulating retinal progenitor cell proliferation and or cell fate specification during early stages of development and rod morphogenesis during later stages of development. This hypothesis is consistent with the severity and timing of onset of the *AIPL1*-associated LCA in children.

### **1.7 Aim of the study:**

Previous studies of Aryl hydrocarbon interacting protein like 1 (AIPL1) revealed several splice variants at the mRNA level of AIPL1 in human tissue samples [41]. In these studies the splice variants could not be resolved at the protein level. Here a differentiation of the splice variants at the protein level was approached by separated expression of cloned splice variants compared to human tissue samples.

Further an interaction with the cell cycle regulator protein NUB1 (NEDD8 Ultimate Buster 1), which plays a role in controlling many biological events, particularly cell cycle progression, by down regulating NEDD8 expression was reported[1]. Yeast two hybrid studies identified the C-terminal portion of another cell cycle protein - Centromere protein F (CENP-F) - to interact with AIPL1 [41]. Interaction of AIPL1 and CENP-F would support an early onset of disease like in LCA. In addition, various molecular features of both AIPL1 and CENP-F further supported such an interaction. Investigations of an interaction between these two proteins using both prokaryotic and eukaryotic models were approached using expression of AIPL1 in human cell lines with intrinsic expression of the housekeeping gene CENP-F.

# CHAPTER 2

## 2. MATERIALS AND METHODS

### 2.1 Materials

#### 2.1.1 Chemicals and Reagents

All chemicals used for the study were of reagent grade if not otherwise stated.

<b>Name</b>	<b>Supplier</b>	<b>Order no</b>
Acrylamide/Bis-acrylamide Solution 30%, 37:1	Serva, <i>Heidelberg</i>	10688.01
Agarose (small DNA low melt)	Biozym, <i>hess. Oldendorf</i>	870093
Ampicillin	Sigma-Aldrich, <i>München</i>	A9518
Ammonium persulphate (APS) (NH <sub>4</sub> ) <sub>2</sub> S <sub>2</sub> O <sub>8</sub>	Merck, <i>Darmstadt</i>	001201-0500
Alkaline Phosphatase	Roche Diagnostics, <i>Mannheim</i>	713023
Accutase	PAA, <i>Pasching</i>	L 11-007
Bromophenolblue	Merck, <i>Darmstadt</i>	11746.0005
5-Bromo-4-chloro-3-indolylphosphat-p- tolidin (BCIP-T)	MBI-Fermentas, <i>St. Leon-Rot</i>	R0821
BSA 10X	Pierce, Thermo Fisher, <i>Schwerte</i>	37520
B-PER Bacterial Protein Extraction Reagent	Pierce, Thermo Fisher, <i>Schwerte</i>	78248
CHAPS 3-(3-Cholamidopropyl)- dimethylammonio)-1-propanesulphonate	Merck, <i>Darmstadt</i>	1.11662.0010
Coomassie Plus Protein Assay Reagent	Pierce, Thermo Fisher, <i>Schwerte</i>	23238
4',6-diamidino-2-phenylindole (DAPI)	Invitrogen, <i>Darmstadt</i>	D1306
Dimethylformamid (DMF)	Roth, <i>Karlsruhe</i>	T921.1
Dimethylsulfoxid (DMSO)	Sigma-Aldrich, <i>München</i>	D5879
DMEM (High Glucose without L-Glutamin)	PAA, <i>Pasching</i>	E15-009
DMEM (High Glucose)	Gibco BRL, <i>Darmstadt</i>	41965-070
DMEM with Glucose + L-Glutamin	PAN Biotech, <i>Aidenbach</i>	720107
DMEM with L-Glutamin	BRL / Life technologies, <i>Darmstadt</i>	41965-021

Ethidium bromide	Sigma-Aldrich, <i>München</i>	E 8751
Ethylenediaminetetraacetic acid (EDTA)	Roth, <i>Karlsruhe</i>	8043.2
ECL Plus Western Blotting Detection Reagents	GE Healthcare, <i>Solingen</i>	RPN2209
Ethanol abs. p.A., 99.8% (C <sub>2</sub> H <sub>6</sub> O)	Roth, <i>Karlsruhe</i>	9065.2
Formaldehyde (CH <sub>2</sub> O)	Merck, <i>Darmstadt</i>	1.04003.1000
Formamid (CH <sub>3</sub> NO)	Merck, <i>Darmstadt</i>	822279.100
Fluorescence Mounting Medium	DAKOCytomation, <i>Hamburg</i>	S3023
Glycerine (C <sub>3</sub> H <sub>8</sub> O <sub>3</sub> )	Roth, <i>Karlsruhe</i>	7530.1
Glycin (C <sub>2</sub> H <sub>5</sub> NO <sub>2</sub> )	Roth, <i>Karlsruhe</i>	3908.2
Hydrochloric acid (HCL)	Merck, <i>Darmstadt</i>	1.00317.1000
Imidazol (C <sub>3</sub> H <sub>4</sub> N <sub>2</sub> )	Merck, <i>Darmstadt</i>	8.14223.0250
Isopropyl β-D-1-thiogalactopyranoside (IPTG)	MBI-Fermentas, <i>St. Leon-Rot</i>	R0392
Isopropanol (C <sub>3</sub> H <sub>8</sub> O)	Roth, <i>Karlsruhe</i>	6752.1
Kanamycin	Sigma-Aldrich, <i>München</i>	K1377
Lipofectamine® LTX and PLUS™ Reagents	Invitrogen, <i>Darmstadt</i>	15338-100
Lumi-Phos WB Chemiluminescent Substrate (AP)	Pierce, Thermo Fisher, <i>Schwerte</i>	34150
Luminol	Sigma-Aldrich, <i>München</i>	A4685
Luria Broth Base	Invitrogen, <i>Darmstadt</i>	12795027
Lysozyme	Sigma-Aldrich, <i>München</i>	L 6876
3-(N-morpholino) propanesulfonic acid (MOPS, C <sub>7</sub> H <sub>15</sub> NO <sub>4</sub> S)	Fluka, <i>München</i>	69947-100G
Methanol (CH <sub>4</sub> O)	Roth, <i>Karlsruhe</i>	4627.2
M-PER Mammalian Protein Extraction Reagent	Pierce, Thermo Fisher, <i>Schwerte</i>	78503
Sodium Chloride (NaCl)	Merck, <i>Darmstadt</i>	1.06404.5000
4 Nitroblue-tetrazolium chloride (NBT)	MBI-Fermentas, <i>St Leon-Roth</i>	R0841
Sodium hydroxide (NaOH)	Roth, <i>Karlsruhe</i>	6771.1
Nitrocellulose Transfer Membrane 300 mm x 3 m, 0.2 µm	Whatman, <i>Dassel</i>	10401396
NucleoSpin Extract II	Macherey Nagel, <i>Hilden</i>	740609.250

Phenol (C <sub>6</sub> H <sub>5</sub> OH)	Roth, <i>Karlsruhe</i>	0038.1
Paraformaldehyde	Merck, <i>Darmstadt</i>	8.18715.0100
Ponceau S Solution	Sigma-Aldrich, <i>München</i>	P 7170
Para Hydroxy Coumarin acid (C <sub>9</sub> H <sub>8</sub> O <sub>3</sub> )	Sigma-Aldrich, <i>München</i>	C9008
Roti Load 1 reducing	Roth, <i>Karlsruhe</i>	K929.1
Roti load 2 Non reducing	Roth, <i>Karlsruhe</i>	K930.1
Sodium dodecyl sulphate (SDS), Ultra pure	Roth, <i>Karlsruhe</i>	232601
Tetracycline	Sigma-Aldrich, <i>München</i>	T3383
Tetra methylene diamine (TEMED)	Roth, <i>Karlsruhe</i>	2367.01
Thiourea (CH <sub>4</sub> N <sub>2</sub> S)	Roth, <i>Karlsruhe</i>	HN37.2
Triton X-100	Roth, <i>Karlsruhe</i>	3051.3
Tris (hydroxymethyl) aminomethane	Merck, <i>Darmstadt</i>	1.08382.2500
Tween 20	Roth, <i>Karlsruhe</i>	9127.1
Xylenecyanol	Merck, <i>Darmstadt</i>	10590.0005
Xylol (C <sub>8</sub> H <sub>10</sub> )	Roth, <i>Karlsruhe</i>	9713.3

### 2.1.2 Oligonucleotides

Primers for PCR

Gene	Primer	Nr	Seq
AIPL1	AIPL1-For	787	GATCCGAATTCGCATGGATGCCGCTCTGCTC
AIPL1	AIPL1-Rev	788	TGGTGAAGCTTGTGCTGCAGCGAGTGCCCTG

### 2.1.3 Vectors

Vector		Order no	
pCR2.1 TOPO	Invitrogen, <i>Darmstadt</i>	K4560.01	TA cloning
pQE-TriSystem His-Strep 2	Qiagen, <i>Hilden</i>	32942	Over expression
pCMV6-AC-GFP	Origene, <i>Rockville, USA</i>	PS100010	Expression mammalian cells

### 2.1.4 Cell lines

HEK293 Cell line LGC standards (ATCC), *Wesel* CRL-1573

HeLa Cell line LGC standards (ATCC), *Wesel* CCL-2.1

### 2.1.5 Competent cells

Type of cells	Genotype	Supplier	Order no
E.Coli XL1 Blue	recA1 endA1 gyrA96 thi-1 hsdR17 supE44 relA1 lac [F' proAB lacIqZΔM15 Tn10 (Tetr)]	Stratagene, <i>Heidelberg</i>	200249
E.Coli M15	NaI <sup>S</sup> , Str <sup>S</sup> , Rif <sup>S</sup> , Thi <sup>-</sup> , Lac <sup>-</sup> , Ara <sup>+</sup> , Gal <sup>+</sup> , Mtl <sup>-</sup> , F <sup>-</sup> , RecA <sup>+</sup> , Uvr <sup>+</sup> , Lon <sup>+</sup> .	Qiagen, <i>Hilden</i>	34210
One Shot <sup>®</sup> TOP10 cocomp <sup>™</sup> <i>E.coli</i> electrocomp. <i>E.coli</i>	F <sup>-</sup> <i>mcrA</i> Δ( <i>mrr-hsdRMS-mcrBC</i> ) φ80 <i>lacZ</i> ΔM15 Δ <i>lacX74 recA1 araD139</i> Δ( <i>ara-leu</i> )7697 <i>galU galK rpsL</i> (Str <sup>R</sup> ) <i>endA1</i> <i>nupG</i>	Invitrogen, <i>Karlsruhe</i>	C 4040-52

### 2.1.6 Enzymes

Function	Enzyme	Supplier	Order no
DNA- Amplification	Phusion <sup>®</sup> Hot Start II DNA Polymerase	Thermo Scientific, <i>Schwerte</i>	F-549S
DNA-Restriction	EcoRI  HindIII	NEB, <i>Frankfurt</i>  NEB, <i>Frankfurt</i>	R0101  R0104
DNA-Ligation	T4-DNA-Ligase	NEB, <i>Frankfurt</i>	M0202S

### 2.1.7 Antibodies

<b>Antibody</b>	<b>Lable</b>	<b>Host</b>	<b>Type</b>	<b>Supplier</b>	<b>Order No</b>
Mouse polyclonal to AIPL1		Mouse	Polyclonal	Abcam, <i>Cambridge, UK</i>	ab68636
His Ab-Rabbit polyclonal to 6X His tag	HRP	Rabbit	Polyclonal	Abcam, <i>Cambridge, UK</i>	ab 1187
Chicken anti human AIPL1		Chicken	Polyclonal, Egg yolk	Dauids Biotech, <i>Regensburg</i>	
Anti-Human Full length AIPL1 Ab		Rabbit	Polyclonal, Serum	[81]	
Anti-Human C-terminus CENP-F Ab		Rabbit	Polyclonal	Santa Cruz Biotechnology, <i>Heidelberg</i>	sc-22791
Anti-Rabbit IgG (whole molecule) – peroxidase conjugated	HRP	Goat		Sigma-Aldrich, <i>München</i>	A0545
Anti-Mouse IgG (whole molecule)	HRP	Rabbit		Sigma-Aldrich, <i>München</i>	A9044
Anti-Chicken IgY (IgG) (whole molecule)	HRP	Rabbit		Sigma-Aldrich, <i>München</i>	A 9046
Donkey anti-rabbit IgG (H+L)	Alexa	Donkey		Invitrogen, <i>Darmstadt</i>	A21206
	Fluor 488				
Goat anti-chicken IgG (H+L)	Alexa	Goat		Invitrogen, <i>Darmstadt</i>	A11039
	Fluor 488				
Goat IgG anti-chicken IgY	Alexa	Goat		Invitrogen, <i>Darmstadt</i>	A11040
	Fluor 564				
Goat anti-rabbit IgG (H+L)	Alexa	Rabbit		Invitrogen, <i>Darmstadt</i>	A11010
	Fluor 546				

Goat anti- mouse IgG (H+L)

Alexa

Mouse

Invitrogen,

A11001

Fluor 488

*Darmstadt*

### 2.1.8 BUFFERS

10x PBS	1.37 M	NaCl	(80g/l)
	27 mM	KCl	(2g/l)
	100 mM	Na <sub>2</sub> HPO <sub>4</sub>	(14.4g/l)
	18 mM	KH <sub>2</sub> PO <sub>4</sub>	(2.4 g/l)

ad 1 l Aq. dest

pH adjusted to 7.2 with HCl

Sterilized and autoclaved.

### 5x SDS-PAGE sample buffer

0.225 M Tris	(2.72g/100 ml)
50% glycerol	(50ml/100 ml)
5% SDS	(5g/100 ml)
0.05% bromophenol blue	(0.05g/100 ml)
0.25 M DTT	(3.8 g/100 ml)

dissolved in Aq. bidest, pH 6.8

**Western Transfer buffer (1x)**

50 mM Tris base	(6.06 g/l)
380 mM Glycine	(28.5 g/l)
0.001 % SDS	(1 g/l)
Methanol	(200 ml)

dissolved in Aq. bidest

**10x TBE buffer**

890 mM Tris base	(108 g/l)
890 mM Boric acid	(55 g/l)
20 mM EDTA	(5.84 g/l)

dissolved in Aq. bidest, pH 8.0

**1x TE Buffer**

10 mM Tris	(1.21 g/l)
1 mM EDTA	(0.29 g/l)

dissolved in Aq. bidest, pH 8.0 using HCl

**LB medium**

25 g of Luria Broth(Invitrogen) was dissolved in 1 l of deionized water and autoclaved at 121 °C for 15 min Stored at room temperature.

### 2.1.9 READY KITS

<b>Name</b>	<b>Supplier</b>	<b>Order no</b>
OneStep RT-PCR Kit	Qiagen, <i>Hilden</i>	210210
Long range two step RT-PCR kit	Qiagen, <i>Hilden</i>	205922
TOPO-TA Cloning Kit	Invitrogen, <i>Darmstadt</i>	K4560-01
Illustra triplePrep Kit	GE Healthcare, <i>Solingen</i>	28-9454-34
Just Spin Gel Extraction	Genaxxon Bioscience, <i>Ulm</i>	S5337.0250
Ni-NTA agarose	Qiagen, <i>Hilden</i>	30210
Espresso tabletised media sets	Enbase, Biosilta, Oulu, Suomi	ENP1000
Pierce <sup>®</sup> BCA Protein Assay Kit	Thermo Scientific, <i>Schwerte</i>	23236
His Mag Sepharose Ni	GE-Healthcare, <i>Solingen</i>	28-9799-17
6x DNA Loading Dye	Fermentas, <i>St. Leon-Rot</i>	#R0611
Resuspension Buffer S1	Macherey-Nagel, <i>Hilden</i>	740516.1
Lysis Buffer S2	Macherey-Nagel, <i>Hilden</i>	740517.1
Neutralization Buffer S3	Macherey-Nagel, <i>Hilden</i>	740518.1
Qiagen Plasmid Mini Kit	Qiagen, <i>Hilden</i>	12123
QIAfilter Plasmid Midi Kit	Qiagen, <i>Hilden</i>	12243
Qiagen Plasmid Maxi Kit	Qiagen, <i>Hilden</i>	12163
NucleoSpin Extract II	Macherey-Nagel, <i>Hilden</i>	740609.250

### 2.1.10 Molecular weight standards

<b>Name</b>	<b>Supplier</b>	<b>Order no</b>
Spectra <sup>™</sup> Multicolor Broad Range	Fermentas	SM1841
GeneRuler 1kb DNA Ladder	Fermentas	SM3011

## 2.2 Equipment and devices

<b>Function</b>	<b>Type</b>	<b>Supplier</b>
Blotelutor	B44	Biometra <sup>®</sup> , <i>Göttingen</i>
Centrifuge	4K15	Sigma, <i>Osterode, Harz</i>
	Rotor 12169-H	
Centrifuge	1-15 PK	Sigma, <i>Osterode, Harz</i>
	Rotor 12024-H	
Electrophoresis chambers	Compact S	Biometra <sup>®</sup> , <i>Göttingen</i>
Electrophoresis power supply	Model PS9009	Biometra <sup>®</sup> , <i>Göttingen</i>
Balances	ALC models 98648-012-74	ACCULAB, Sartorius, <i>Göttingen</i>
Fluorescence microscope	BZ-8100 <sup>E</sup>	Keyence, <i>Neu-Isenburg Hessen</i>
Geldryer	Mididry D62	Biometra <sup>®</sup> , <i>Göttingen</i>
Inverted Microscope	Model IT400	VWR, <i>Darmstadt</i>
Incubator	CO <sub>2</sub> Incubator C150	Binder, <i>Tuttlingen</i>
Ice machine	AF80	Scotsman, <i>Berlin</i>
Laminar air flow	MSC ADVANTAGE 1.2	Fischer scientific, <i>Langenselbold</i>
Photometer	Biophotometer	Eppendorf, <i>Hamburg</i>
Mini Centrifuge	MCF-2360	LMS, Tokyo, Jp
ROTATOR	STR4	Stuart Scientific, Chelmsford, UK
Magnetic stirrer	RCT CL	IKAMAG <sup>®</sup> RCT CLASSIC, <i>Staufen</i>
Mini Rocking Platform	WT16	Biometra <sup>®</sup> , <i>Göttingen</i>
Mini-Tumbling Table	WT17	Biometra <sup>®</sup> , <i>Göttingen</i>
Multiporator <sup>®</sup>	Electrofusion	Eppendorf, <i>Hamburg</i>
Themocycler	T Professional Basic	Biometra <sup>®</sup> , <i>Göttingen</i>
	T-Professional Gradient	
Power Pack	P25 T	Biometra <sup>®</sup> , <i>Göttingen</i>
Polyacrylamide Gel	Minigel-Twin	Biometra <sup>®</sup> , <i>Göttingen</i>
electrophoresis Apparatus		
PAGE Apparatus for precast gels	E260	SERVA, <i>Heidelberg</i>
Homogenizer	Precellys <sup>®</sup>	peQLab Biotechnologie, Erlangen

Shaker	CERTOMAT <sup>®</sup> MO II	Sartorius, <i>Göttingen</i>
Blockthermostat	TB2 Thermoblock	Biometra <sup>®</sup> , <i>Göttingen</i>
Thermomixer	Thermomixer Comfort	Eppendorf, <i>Hamburg</i>
UV-Illuminator	BioDoc Analyze Gel Analysis (BDA)	Biometra <sup>®</sup> , <i>Göttingen</i>
Water bath	TW12	Julabo, <i>Seelbach</i>

### 2.2.1 Computer aided data processing

<b>Software</b>	<b>Web links</b>
Chromas lite	<a href="http://www.mybiosoftware.com/sequence-analysis/1979">http://www.mybiosoftware.com/sequence-analysis/1979</a>
Gentle	<a href="http://gentle.magnusmanske.de/">http://gentle.magnusmanske.de/</a>
Vector NTI 11	<a href="http://de-de.invitrogen.com/site/de/de/home/Products-and-Services/Applications/Cloning/vector-nti-software.html">http://de-de.invitrogen.com/site/de/de/home/Products-and-Services/Applications/Cloning/vector-nti-software.html</a>
Image J	<a href="http://imagej.en.softonic.com/">http://imagej.en.softonic.com/</a>
CLC work bench 6	<a href="http://www.clcbio.com/products/clc-genomics-workbench/">http://www.clcbio.com/products/clc-genomics-workbench/</a>
BZ-II Analyzer	<a href="http://www.keyence.de/">http://www.keyence.de/</a>

## **2.3 Methods of molecular biology**

### **2.3.1 Polymerase chain reaction (PCR)**

The polymerase chain reaction (PCR) is used to amplify DNA to generate millions of copies of a particular DNA sequence. PCR relies on thermal cycling, consisting of cycles of repeated heating and cooling of the reaction for DNA melting and enzymatic replication of the DNA. Primers (oligonucleotides) complementary to the margins of the target sequence along with a DNA polymerase are key components to enable selective and repeated amplification. Almost all PCR applications employ a heat-stable DNA polymerase, such as Taq polymerase, an enzyme originally isolated from the bacterium *Thermus aquaticus*. The PCR involves three temperature incubation steps that are repeated. In the first step called denaturation, the two strands of the target DNA molecule are separated (denatured) by heating the DNA up to 98 °C. This breaks the hydrogen bonds between the bases, yielding two separate strands. In the second step, called annealing, two primers forward and reverse hybridize to complementary sequences on the single strands. Annealing temperatures range between 50 °C and 72 °C. During the third step, called extension, the primers are extended by a thermostable DNA polymerase at 72 °C. As PCR progresses, the DNA generated itself is used as a template for replication, setting in motion a chain reaction in which the DNA template is exponentially amplified. PCR can be extensively modified to perform a wide array of genetic manipulations. PCR amplified DNAs, were used for cloning to generate recombinant molecules. Further used to study the functional genomics, gene expression, protein structure–function relationships and protein-protein interactions.

## Phusion® Hot Start II

Component	20µl reaction	Final conc.
Aq. bidest	13.4µl	
5x Phusion® HF Buffer	4 µl	1 x
10 mM dNTPs	0.4 µl	200 µM each
Primer a (AIPL1-F)	0.5 µl	0.5 µM
Primer b (AIPL1-R)	0.5 µl	0.5 µM
Template DNA	0.4 µl (150 ng/µl)	
DMSO	0.6 µl	(3%)
Phusion® Hot Start II DNA Polymerase (2 U/µl)	0.2 µl	0.02 U/µl

Cycle step	Temp.	Time	Cycles
Initial denaturation	98°C	30 s	1
Denaturation	98°C	5-10 s	
Annealing	60°C	30 s	30
Extension	72°C	40 s	
Final extension	72°C	10 min	1
	4°C	Hold	

### **2.3.2 Agarose gel electrophoresis**

Gel electrophoresis is the standard lab procedure for separating DNA by size for visualization and purification.

#### **Preparation of a Standard 1% Agarose Gel**

1g of agarose powder was mixed in an Erlenmeyer flask along with 100 ml of 1x TBE buffer. The flask was heated in microwave for 2 min until the agarose was completely dissolved. Later agarose solution was cooled down for 5 min and ethidium bromide (EtBr) was added to a final concentration of approximately 0.3 µg/ml. EtBr binds to the DNA and allows visualization of the DNA under ultraviolet (UV) light. Agarose was poured into a gel tray with the well comb and placed the gel at 4 °C for 15 minutes until it had completely solidified.

#### **Loading Samples and Running an Agarose Gel**

To all the samples 6x DNA Loading dye (Fermentas) at 20% of the sample volume was added and vortexed. Once solidified, the agarose gel was placed into the gel chamber (electrophoresis unit) and filled with 1x TBE buffer until the gel was covered. Molecular weight ladder of 350 ng was loaded into the first lane of the gel followed by samples into the additional wells of the gel. Gel run was carried at 100 V for 1 h until the dye line was approximately 80% of the way down the gel. Then the gel was carefully removed from the gel chamber. DNA fragments were visualized using the BioDocAnalyze Gel Analysis (BDA) with UV light.

### **2.3.3 Isolation of DNA from agarose gels**

For isolation of DNA from agarose gels, Genaxxon's justSpin<sup>®</sup> columns were chosen due to the following advantages.

The columns did not require special agaroses. No melting or lysis procedures are necessary to dissolve the agarose. There was no requirement of additional buffers or solutions, vacuum manifolds or repeated centrifugation procedures. No desalting procedures were necessary and the columns could be used for small- and big-sized DNA.

The isolated DNA could be used directly for subsequent experiments.

The DNA band was excised from the agarose gel with a clean, sharp scalpel (as the volume of the elute is proportional to the gel slide dimensions, the excised gel block was kept as small as possible). The excised agarose slice was placed in the spin column on top of the column media in a 1.5 ml tube. The tube was placed in a centrifuge (Sigma, type model 1-15PK, rotor 12024-H) and centrifuged at 5867 g for 10 min at room temperature. The elute containing the DNA could be used directly for cloning experiments or other applications without further purification or precipitation steps.

### **2.3.4 Cloning**

PCR products were cloned into plasmid vectors using specific restriction endonuclease sites. Isolated vector plasmid DNA was digested by restriction enzymes and analyzed by gel electrophoresis. Glycerol stocks were prepared for positive clones.

#### **2.3.4.1 Restrictionendonuclease digestion**

Double stranded DNA molecules hydrolyze at specific sites with the help of restriction endonucleases. Endonucleases recognize specific sequences in a DNA sequence and cut at these sites in a reproducible fashion hydrolyzing the backbone of DNA between deoxyribose and phosphate groups. Amplification of DNA was done with a primer set possessing an EcoRI site in the forward and a HindIII site in the reverse primer. Amplified PCR products were cloned into the expression vector digested with the same restriction sites EcoRI and HindIII. Restriction digestion of recombinant DNA with EcoRI and HindIII confirmed the presence of all the inserts and the vector backbone.

#### **Reaction mix – Table**

Sample	7.5 µl
Restriction endonuclease 1	(5 U) 0.5 µl
Restriction endonuclease 2	(5 U) 0.5 µl
Restriction buffer	1.0 µl
Aq. Bidest	10.5 µl
Total	20.0 µl

Restrictionendonuclease digestion was carried out for 1 hr at 37 °C the temperature optimum of endonucleases.

#### **2.3.4.2 Dephosphorylation**

To prevent self ligation of a vector dephosphorylation was carried out using Antarctic phosphatase.

Restriction digestion mix	20 µl
Antartic phosphatase	(5U) 1 µl
Antartic phosphatase buffer	2.5 µl
Aq. Bidest	1.5 µl
Total	25.0 µl

Dephosphorylation was carried out for 30 min at room temperature. For inactivating the restriction enzyme the assay was kept in a heat block at 65 °C for 5 min.

#### **2.3.4.3 Ligation**

Two crucial procedures in cloning are ligation of insert to the vector DNA and transformation of the ligation product i.e. the recombinant molecule into bacteria. Ligation was accomplished using the enzyme DNA ligase, usually from the bacteriophage T4. It requires ATP and magnesium ions to catalyze the formation of phosphodiester bond between juxtaposed 5' phosphate and 3' hydroxyl termini in double-stranded DNA or RNA. T4 DNA ligase will join blunt end and cohesive end termini as well as repair single stranded nicks in duplex DNA, RNA or DNA/RNA hybrids.

### Reaction mix – Table

Vector	1.0 $\mu$ l
Insert	5.0 $\mu$ l
5 X ligase buffer	4.0 $\mu$ l
T4 DNA ligase	1.0 $\mu$ l
Aq. Bidest	9.0 $\mu$ l
Total	20.0 $\mu$ l

Ligation was carried out at room temperature for 1 hour.

#### 2.3.4.4 Transformation

#### 2.3.4.5 Preparation of competent bacterial cells

In a 15 ml reaction tube 5  $\mu$ l Glycerol stock (XL1-Blue) and 5 ml LB medium as given in (2.1.8) supplemented with a bacterial strain specific antibiotic (tetracycline resistance coded on the F plasmid) were incubated at 37 °C for overnight in an orbital shaker at 180 rpm.

100 ml LB medium in a 500 ml Erlenmeyer flask supplemented with the required antibiotic were inoculated with 2 ml overnight culture and were grown at 37 °C and 180 rpm in an orbital shaker for 2 hours until an OD<sub>600</sub> of 0.6 was reached. The OD<sub>600</sub> was tested for every 30 minutes using a spectrophotometer. Later, the cell suspension was filled into 50 ml tubes and kept on ice for 30 min. Subsequently the reaction tubes were placed in a centrifuge (Sigma, model 4K15, rotor 12169-H) and centrifuged at 5100 g for 5 min at 4 °C. Afterwards the supernatant was discarded.

The pellet was resuspended in 50 ml ice cold 1 mM HEPES and centrifuged at 5100 g for 5 min at 4 °C. The supernatant was discarded and the pellet resuspended in 25 ml cold 1 mM HEPES. The pellet was centrifuged for 5 min at 5100 g and 4 °C. The supernatant was discarded, and the pellet was resuspended in 10 ml cold 10% glycerine.

Centrifugation was repeated and the pellet was resuspended in 5 ml cold 10% glycerine.

After a further centrifugation the pellet was resuspended in 1 ml cold 10 % glycerine. The cells could be used directly for transformation. 100  $\mu$ l aliquots were prepared from the rest of

the cell suspension and froze them in liquid nitrogen and stored at -80 °C for later applications.

#### **2.3.4.6 Bacterial transformation by electroporation:**

Plasmid DNA was diluted to 5 ng/μl with Aq. bidest, and competent cells were thawed on ice. 1.5 μl (7.5 ng DNA) were incubated with 50 μl competent *E.coli* cells on ice in 0.2 ml tubes for 15 - 30 min. Electroporation cuvettes were cooled on ice. After incubation, the suspension was filled into the cooled (cuvettes avoiding any air bubbles). The transformation was performed at 2000 V using a multiporator (Eppendorf), and the transformed sample was flushed out of the cuvette with 1 ml LB-medium into a 1.5 ml tube. The transformed sample was incubated at 37 °C for 1 hour, 180 rpm and 100 μl of the sample was plated on LB-Agar supplemented with vector specific antibiotic. LB-agar plates were incubated overnight at 37° C

#### **2.3.5 Preparation of plasmid DNA**

##### **2.3.5.1 Preparation of plasmid DNA (Miniprep)**

Overnight cultures were prepared by picking bacterial colonies from an LB plate into 5 ml of LB medium supplemented with appropriate antibiotics. Bacterial cultures were incubated overnight at 37 °C with shaking.

DNA was extracted from 1.5 ml of bacterial culture using the Macherey and Nagel Mini Prep buffers. Bacterial culture was taken into a 1.5 ml reaction tube and pelleted at 5000 g for 5 min in a centrifuge. The supernatant was discarded and the pellet was resolved in 100 μl of resuspension buffer (S1). 100 μl of lysis buffer (S2) was added, and the tube was inverted once. In the next step 100 μl of neutralization buffer (S3) was added, and the tube was inverted once again. The set up was centrifuged at 10,000 g for 10 min, and the supernatant was removed into a fresh tube. 700 μl of ice cold absolute ethanol was added to the supernatant and centrifuged for 30 min at maximum speed 15,000 g at 4 °C.

Later the supernatant was discarded and 200 μl of 70% ethanol were added to the pellet and centrifuged for 5 min at full speed and 4 °C. Next the supernatant was discarded and the pellet was air dried for 5 min. The pellet was dissolved into 40 μl of TE buffer and proceeded for measuring DNA concentration and analytical digestion.

### **2.3.5.2 Preparation of plasmid DNA (Maxiprep)**

Maxi preps were prepared according to the manufacturer's instructions using the Qiagen Plasmid Maxi kit from 500 ml (low copy) bacterial overnight culture. Bacterial culture was collected into a reaction tube and pelleted at 6000 x g for 15 min at 4 °C in a centrifuge. The supernatant was discarded and the bacterial pellet was homogeneously resuspended in 10 ml buffer P1. 10 ml buffer P2, was added and mixed thoroughly by vigorously inverting 4 - 6 times, and incubated at room temperature for 5 min. 10 ml buffer P3, was added and mixed thoroughly by vigorously inverting 4 - 6 times and incubated on ice for 20 min.

The lysate was centrifuged at 20,000 x g for 30 min at 4°C and the supernatant was recentrifuged at 20,000 x g for 15 min at 4 °C.

Qiagen-tip 500 was equilibrated by applying 10 ml buffer QBT and allowed the column to empty by gravity flow. The supernatant was applied to the Qiagen-tip and allowed to enter the resin by gravity flow. The Qiagen tip was washed with 2 x 30 ml buffer QC. Buffer QC was allowed to move through the Qiagen-tip by gravity flow. DNA was eluted with 15 ml buffer QF into a clean 50 ml tube.

The DNA was precipitated by adding 10.5 ml room temperature isopropanol to the eluted DNA and mixed. The precipitation was centrifuged at 15,000 x g for 30 min at 4°C and carefully the supernatant was decanted. The DNA pellet was washed with 5 ml room temperature 70% ethanol and centrifuged at 15,000 g for 10 min. Carefully the supernatant was decanted. The pellet was air dried for 5-10 min and redissolved DNA in a suitable volume of buffer.

### 2.3.6 Quantification of nucleic acid

The quality and quantity of isolated nucleic acids were determined spectrophotometrically, using an Eppendorf biophotometer. The  $A_{260}/A_{280}$  ratio was indicative of the degree of purity of the nucleic acid. Aq. bidest was used as solvent to suspend the nucleic acids and each sample was placed in a quartz cuvette. With a sample of solvent spectrophotometer was set at zero. For more accurate readings of the nucleic acid sample of interest, the samples were diluted to give readings between 0.1 and 1.0. Contamination of nucleic acid solutions makes spectrophotometric quantitation inaccurate. For an indication of nucleic acid purity  $OD_{260}/OD_{280}$  ratio is calculated. Purified DNA has an  $OD_{260}/OD_{280}$  ratio of ~1.8. Low ratios could be caused by protein or phenol contamination.

### 2.3.7 Sequence analysis of plasmids:

Sequencing of the samples was carried out to verify positive clones. DNA sequencing reactions were performed at Seqlab, Göttingen using Sanger sequencing with dye terminator technology. Seven micro litre containing 700 ng of sample were used for sequencing. Sequences were aligned using Vector NTI and chromatograms were analysed using Chromas lite.

Reaction set up for sequencing:

Sample	5 $\mu$ l
Forward Primer	2 $\mu$ l
<hr/>	
Total	7 $\mu$ l

### 2.3.8 Preparation of Glycerol stocks

For long-term storage and to increase shelf life bacterial cultures were stored using glycerol. 200  $\mu$ l of pure glycerol along with 800 - 1000  $\mu$ l of bacterial solution was added into a cryotube and mixed thoroughly by inverting the tube. The mixture was frozen in liquid nitrogen for 4 - 5 min and then stored at -80 °C.

## 2.3.9 Overexpression of recombinant proteins

### 2.3.9.1 Growth of standard *E.coli* expression cultures (100 ml)

10 ml of the culture medium was inoculated containing both ampicillin (100 µg/ml) and kanamycin (25 µg/ml) in a 50 ml flask, and the cultures were grown overnight at 37 °C. 100 ml of prewarmed media (with antibiotics) was inoculated with 5 ml of overnight cultures and grown at 37 °C with vigorous shaking until an OD<sub>600</sub> of 0.6 was reached. 1 ml sample was taken immediately before induction. This sample was the noninduced control; Cells were pelleted and resuspended in 50 µl 5x SDS-PAGE sample buffer (reducing) and stored frozen (-20 °C) until SDS-PAGE analysis. Expression of the protein was induced by adding 1 M IPTG to a final concentration of 1 mM. Cultures were incubated for an additional 4 – 5 h. A second 1 ml aliquot was collected. This was the induced sample, Cells were pelleted and resuspended in 100 µl 5x SDS-PAGE sample buffer (reducing) and stored frozen at -20 °C until SDS-PAGE analysis. The cells were harvested by centrifugation at 4000 x g for 20 min. Further extraction of protein was carried out from the harvested cell pellet using B-PER kit (PIERCE). Initially 1 ml fractions of the pellets of non-induced control and induced sample were resuspended in 5x SDS-PAGE sample buffer for performing SDS-PAGE. At the end the whole bacterial culture was centrifuged and the pellet was resuspended in B-PER. The supernatant with extracted protein was used for protein purification using Ni\_NTA agarose. Further these samples were dissolved in 5x SDS-PAGE sample buffer before loading.

### 2.3.9.2 Over expression with EnPresso™ Tablet cultivation set

For expressing recombinant protein in bacteria enpresso Enbase® kits were used because higher volumetric yields of soluble recombinant proteins could be obtained due to controlled physiological state. The higher volumetric yields enabled the use of lower culture volumes and could thus significantly reduce the amount of time and effort needed for downstream processing or process optimization.

Enbase® Medium contained two tablets with media components and a polysaccharide complex as substrate, a booster tablet with complex additives for optimal pH conditions and EnZ I'm: mixture of filter sterilized enzymes.

Preculture was set up in a 1.5 ml reaction tube with 1 ml LB medium including Ampicillin (100 µg/ml), Kanamycin (50 µg/ml) and 1 µl of glycerol stock. The culture set up was incubated at 37 °C and vigorous shaking for 6 hours. The Enbase® medium tablets were resolved in 50 ml of sterile water in a sterile 500 ml flask until tablets were dissolved. The

required antibiotics were added to the medium that was inoculated with 500 µl of the pre-culture and 25 µl of EnZ 1'm from the kit. The flask was fastened with an AirOtop seal. Further the culture was incubated at 30 °C at 200 rpm overnight. After overnight culture, inducing agent (IPTG), booster tablet (black bag) and 50 µl of EnZ 1'm were added and incubation continued for protein production. Protein was harvested after 6 hours of cultivation.

### **2.3.10 Protein extraction**

#### **2.3.10.1 Protein extraction from tissue**

Protein extraction from tissue was carried out using the GE Healthcare illustra triplePrep Kit. According to the manufacturer's instructions with illustra triple prep DNA, RNA and protein can be isolated simultaneously. Tissue homogenization and lysis were carried out using Precellys 24 homogenizer in precellys-glas-kit 0.5 mm beads in 2.0 ml tubes. The mini column (orange o-ring) was placed into a 2 ml collection tube provided. Homogenized lysate was transferred into the mini column and spun it for 1 min at 11000 g. The entire flow through was transferred to a new 1.5 ml micro centrifuge tube and 600 µl of protein precipitation buffer type 1 were added and mixed vigorously and incubated for 5 min at room temperature to precipitate the proteins. Further spun it for 10 min at 16000 g. As much supernatant as possible was carefully removed by pipetting and protein wash was done by adding 1 ml of distilled water to the protein pellet. The pellet was actively dispersed by pipetting up and down for 5 times and spun for 1 min at 16 000 g. Protein resuspension was carried out by adding 300 µl of 2-D DIGE buffer for easy protein re-suspension and incubated for 5 min at room temperature. Protein resuspended in 2-D DIGE buffer was used for SDS-PAGE by mixing with 1 volume of 20% SDS. Sample loading buffer (i.e 1 volume of 2x Laemmli buffer) was added and incubated at 70 °C for 10 min before gel loading.

#### **2.3.10.2 Bacterial protein extraction:**

After overexpression of protein in bacterial cells using 1 M IPTG 1 ml of the culture was collected and centrifuged at 8000 g for 5 min and pelleted. Later, the pellet was processed towards extraction of protein using B-PER Bacterial protein Extraction Reagent (Pierce). The cells were resuspended in 300 µl of B-PER reagent by vigorous vortexing the mixture until the cell suspension was homogeneous. The suspension was centrifuged (Sigma, type model 4K15, rotor Nr.12169-H) at 11,627 g for 8 min to separate the soluble proteins from the

insoluble proteins. Collect the supernatant (soluble fraction) and resuspend pellet (insoluble fraction) in 300 µl of B-PER reagent. To determine the solubility of recombinant protein, 10 µl of each the soluble and insoluble fractions were used for SDS-PAGE and western blotting assays

### **2.3.10.3 Mammalian protein extraction:**

Protein was expressed in HEK293 cell lines in 6 well plates for 24 hrs. A GFP probe (pCMV6-AC-GFP) was used as a positive control to determine transfection efficiency. Depending on the transfection efficiency protein extraction was carried out using Mammalian Protein Extraction reagent (M-PER<sup>®</sup>) from PIERCE. Culture medium was carefully removed from the adherent cells and 200 - 400 µl of M-PER were added per well. The lysate was collected and transferred to a microcentrifuge tube. Samples were centrifuged at 14,000g for 5 - 10 min to pellet the cell debris. The supernatant was transferred to a fresh tube for further analysis.

### **2.3.11 Determination of protein concentration by Bradford Assay**

The Bradford protein assay is a spectroscopic analytical method used to measure the protein concentration in a solution. The concentration of the protein is measured dependent on the amino acid composition of the protein. This assay is a colorimetric protein assay, which is based on absorbance shift of the dye Coomassie Brilliant Blue G-250 in which under acidic conditions the red form of the dye is converted into its blue form by assaying the binding to the protein.

The concentration of protein in each sample was measured using the Coomassie Plus Kit. A 50 µl aliquot of unknown sample was diluted into a cuvette with 1.5 ml of Coomassie Plus reagent and mixed well. The reaction mix was incubated for 10 min at room temperature. Subsequently the absorbance of dye was measured at 595 nm with a spectrophotometer. The photometer was set zero with buffer according to the extraction technique, used as blank and subsequently absorbance of the samples was measured to calculate the protein concentration against a standard. Equal amounts of protein were loaded in subsequent assays.

## **2.3.12 Purification of His tagged proteins using Ni-NTA resin under native conditions.**

### **2.3.12.1 Buffers for purification under native conditions**

#### **Lysis buffer**

50 mM	NaH <sub>2</sub> PO <sub>4</sub>	(6.90 g/l)
300 mM	NaCl	(17.54 g/l)
10 mM	imidazole	(0.68 g/l)

ad 1 l Aq. dest

pH adjusted to 8.0 using NaOH.

#### **Wash buffer**

50 mM	NaH <sub>2</sub> PO <sub>4</sub>	(6.90 g/l)
300 mM	NaCl	(17.54 g/l)
20 mM	imidazole	(1.36 g/l)

ad 1 l Aq. dest

pH adjusted to 8.0 using NaOH.

#### **Elution buffer**

50 mM	NaH <sub>2</sub> PO <sub>4</sub>	(6.90 g/l)
300 mM	NaCl	(17.54 g/l)
250 mM	imidazole	(17.00 g/l)

ad 1 l Aq. dest

pH adjusted to 8.0 using NaOH.

### **2.3.12.2 Purification of over expressed and extracted recombinant proteins using Ni\_NTA resin**

After over expression and protein extraction the desired products were purified using Ni/NTA resin. 500 µl of lysis buffer with a concentration of 20 mM imidazole was added to 4 ml of B-PER extracted protein lysate followed by the addition of 1.2 ml of 50% Ni-NTA slurry and mixed gently at 4 °C for 1 h. Imidazole in the lysis buffer suppressed the binding of non-tagged contaminating proteins and lead to increased purity after fewer wash steps. If the tagged protein did not bind under these conditions, the concentration of imidazole was reduced to 1 - 5 mM.

A 5 ml pipette tip was packed with glass wool, which acted as a filter. Later, the protein lysate with Ni-NTA slurry mixture was loaded onto the column and the flow through was collected. The flow-through was saved for SDS-PAGE analysis.

The column was washed twice with wash buffer (4 ml) and the wash fractions W1 and W2 were collected for further analysis. In the final step the elution of protein was carried out four times using 0.5 ml elution buffer. Finally 10 % of glycerol was added to the samples and stored at -20 till performing a SDS-PAGE. For lysis and washing the buffer contained 20 mM imidazole and for elution 500 mM, imidazole were used. Based on the results the concentration of the imidazole was adjusted.

### **2.3.13 Concentrating protein samples using the centriprep<sup>®</sup> centrifugal filter devices**

Centriprep centrifugal filter devices are disposable ultrafiltration devices used for purifying, concentrating, and desalting biological samples. Centriprep devices consist of a sample container with a twist-lock cap, a filtrate collector containing a low adsorptive Ultracel YM regenerated cellulose membrane, plus an air-seal cap for sample isolation.

A centriprep device with Ultracel YM-30 membrane was used for concentrating the samples. Samples were centrifuged twice for 5 min at 1500 g. After the second centrifugation concentrate is collected into a suitable container. Protein concentration of the samples was measured and further analysis of samples was performed.

#### **10x SDS Running buffer: (1 liter)**

250 mM Tris	(30.2 g/l)
1.92 M Glycine	(144.0 g/l)
1 % SDS	(10 g/l)

pH 8.3

### **1x SDS-PAGE sample buffer**

0.045 M Tris.Cl	(0.5 g / 100 ml)
10% glycerol	(10 ml / 100 ml)
1% SDS	(1 g / 100 ml)
0.01% bromophenol blue	(0.01 g / 100 ml)
0.05 M DTT	(0.7 g / 100 ml)

### **Preparation of 6x His Protein Ladder**

6x His Protein Ladder	(lyophilized, 250 µg)
1x SDS-PAGE sample buffer	250 µl

### **2.3.14 Gel electrophoresis of proteins - SDS-PAGE**

Polyacrylamide gel electrophoresis in the presence of SDS (Sodium dodecyl sulphate) is the most common form of protein gel electrophoresis. SDS is an anionic detergent applied to linearize proteins and to impart a negative charge to linearized proteins. SDS binds to the unfolded proteins giving all proteins a similar shape i.e random coil or extend conformation and a uniform charge-to-mass ratio. Coating proteins with a negatively charged detergent minimizes the effects of a protein's net charge. Therefore, during electrophoresis in the presence of SDS, the mobility of a protein depends primarily upon its size. i.e., mobility is inversely proportional to protein mass.

#### **2.3.14.1 Preparation of His tagged marker**

250 µl of 1x SDS-PAGE sample buffer containing the reducing agent dithiothreitol (DTT) were added to lyophilized 6x His Protein ladder (Qiagen, Hilden) and proteins were allowed to dissolve at room temperature for 30 min. After the proteins were dissolved the whole set up was transferred to a micro centrifuge tube and heated at 98° C for 10 min. Appropriate aliquots were prepared and stored at -20 °C. Any applied aliquot was heated immediately before loading the gel. It is important to perform this heating step for the time, and at the temperature recommended. Insufficient heating leads to detection of protein aggregates as extra bands.

### 2.3.14.2 Protein electrophoresis using manually prepared acrylamide gels

**Table 3: Gel mixture**

Resolving gel		Final conc.	Stacking gel		Final conc.
1.5 M Tris/HCl pH 8.8	3.13 ml	400 mM	0.5 M Tris/HCl pH 6.8	2.5 ml	200 mM
20% SDS	62.5 µl	3.5 mM	20% SDS	25 µl	3.1 mM
30% Acrylamide	5 ml	1.7 M	30% Acrylamide	1.1 ml	844.1 mM
Aq. Dest	4.37 ml	19.4 M	Aq. Dest	1.4 ml	13.9 M
10% APS	100 µl	3.5 mM	10% APS	50 µl	3.9 mM
TEMED	10 µl	6.9 mM	TEMED	7.5 µl	12.9 mM

### 2.3.14.3 Loading and running:

After the preparation of stacking gel and resolving gel, the gel was placed into the electrophoresis chamber (Compact S Biometra<sup>®</sup>, Göttingen) so that the open side of the cassette is facing towards the cathode buffer tank. Electrophoresis buffer is added and the comb was pulled steadily out of the gel. Remaining gel rests above the sample wells were removed eventually. The sample wells were rinsed thoroughly avoiding any air bubbles. Before loading the samples the wells were loaded with 1x sample buffer for the confirmation of lanes and loading the samples proceeded further. 20 - 50 µg of protein sample were loaded per lane, along with suitable positive and negative controls. The gels were run at 120 volts for 90 min. After the gel run was finished electrophoresis chamber, power supply, electrophoresis buffer and the gel cassette were removed. Subsequently gels could be stained or used for blotting.

### 2.3.14.4 SDS-PAGE using precast 8 - 16% gradient SERVAGel<sup>™</sup> TG

SERVAGel<sup>™</sup> TG gels are ready to use Tris-Glycine gels, which are designed for vertical slab gel electrophoresis and suited for discontinuous separation of proteins. These pre-cast gels help in achieving high resolution with excellent band sharpness in less time period. Gel loading and running was carried out as mentioned in **2.3.15.3**.

### 2.3.15 Polyacrylamide Gel Staining Protocol

For staining the SDS-PAGE gels, LabSafe™ GEL Blue was used, which is based on coomassie dye and only stains proteins, leaving a clear background resulting in high band visibility. After SDS-PAGE the gel was washed three times for 5 min in a large volume of deionized water. Subsequently an adequate volume of LabSafe™ GEL Blue stain was added to cover the gel. The gel was shaken gently for 1 hour. Later the stained gel was rinsed in a large volume of deionized water, three times for 10 min each to remove background colour. The stained gel was stored in deionized water.

### 2.3.16 Western Blotting

#### Western transfer buffer:

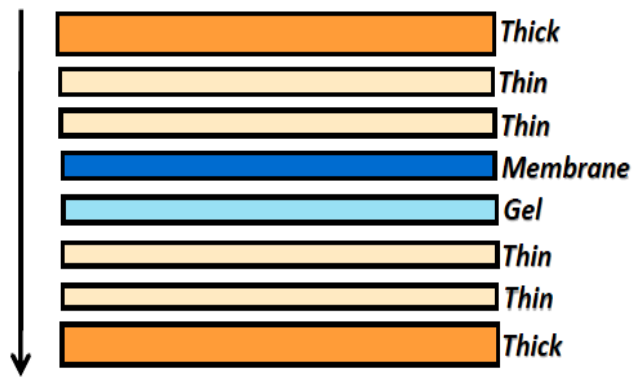
50 mM	Tris base	(6.06 g/l)
380 mM	Glycine	(28.5 g/l)
0.001 %	SDS	(1 g/l)
20% w/v	Methanol	(200 ml/l)

dissolved in Aq. bidest

Nitrocellulose Transfer Membrane 300 mm x 3 m, 0,2 µm	Whatman, Thermo Scientific, <i>Schwerte</i>	10401396
Gel Blotting Paper 460 x 570 mm, 1 mm GB003	Whatman, Thermo Scientific, <i>Schwerte</i>	09-301-404
Gel Blotting Paper 580 x 580 mm, 3 mm GB005	Whatman, Thermo Scientific, <i>Schwerte</i>	09-301-199

Proteins were transferred to nitrocellulose membranes by semi-dry blotting

The order of the blotting filter papers (thick 3 mm GB005 and thin 1 mm GB004), Nitrocellulose Transfer Membran 0.2 µm and gel are as follows



**Order: Thick-Thin-Thin-Membrane-Gel-Thin-Thin-Thick**

**Figure 7: Western blotting transfer order. Arrow shows direction of transfer**

Following gel electrophoresis, the separated proteins were transferred to a solid support for further analysis. Electroblotting was used due to the speed and efficiency of transfer. The gel and blotting membrane were assembled into a sandwich along with several sheets of filter paper which protected the gel and blotting membrane and helped to ensure close contact between their surfaces. 1x western transfer buffer was used for blotting. Filter papers and membrane were precisely cut to the size of the gel and nitrocellulose was prewetted in transfer buffer. Thick and thin filter papers were soaked in transfer buffer and applied directly to the surface of the gel. Blotting was carried out for 1 h at 200 mA followed by confirmation of protein transfer by Ponceau S staining.

### **2.3.17 Ponceau S staining of proteins on nitrocellulose membranes**

To estimate the efficiency of protein transfer after blotting, the membrane was stained with Ponceau S. This stain is reversible and produces pink bands on a light background. The nitrocellulose membrane was washed with Millipore water for 1 min, incubated in Ponceau S solution for 2 - 3 min with constant shaking at room temperature. Subsequently, the membrane was destained by washing with demineralized water to the desired contrast. Finally, it was documented by a digital camera. To remove the stain completely, the membrane was washed again with TBS-T under constant shaking.

### 2.3.18 Antibody Hybridization on nitrocellulose membranes

#### Buffers for antibody hybridization

##### TBST

10% 10X TBS (100 ml/l)

0.1% Tween<sup>®</sup> 20 (1 ml/l)

ad 1 l Aq. bidest.

##### Blocking buffer

5% milk powder in TBST

##### TBS-Triton X 100 (1 liter)

10% 10x TBS (100 ml/l)

0.2 % Triton X 100 (2 ml/l)

ad 1 l Aq. bidest.

##### Blocking buffer for primary and secondary antibodies

5% Nonfat Dried Milk in 100 ml of 1x TBST/TBS-Triton X 100

Dissolved with gentle stirring.

Stored at 4°C

##### Chemiluminiscence detection buffers for horse radish peroxidase (HRP)

###### Solution A (stored at 4°C)

100 mM Tris-HCl (200 ml pH 8.6)

1.4 mM Luminol (0.05 g / 200 ml)

###### Solution B (stored at room temperature in the dark)

6.7 mM Para Hydroxy Coumarin acid (0.011g)

ad 10 ml of DMSO

H<sub>2</sub>O<sub>2</sub> (30%)

1 ml of Solution A was mixed with 0.3 µl H<sub>2</sub>O<sub>2</sub> (30%) and 100 µl Solution B. The solution mix was distributed well on the membrane and incubated for 2 min. For small membranes (Length 7 cm x Width 8 cm) 4 ml Solution A + 1.2 µl H<sub>2</sub>O<sub>2</sub> (30%) + 400 µl Solution B was used.

All incubation and wash steps were performed on a rocking platform or orbital shaker. The membrane was washed twice for 10 min each with TBS buffer at room temperature and subsequently incubated for 1 h in blocking buffer at room temperature.

The membrane was washed twice for 10 min each in TBS-Triton X 100 buffer at room temperature and afterwards for 10 min with TBS buffer at room temperature. The blot was incubated with a primary antibody solution of optimized antibody dilution at room temperature for 1 h. Subsequently the membrane was washed twice for 10 min each time in TBS-Tween/Triton buffer at room temperature. Washing of the membrane was repeated twice for 10 min in TBS buffer at room temperature. The membrane was incubated with an optimized dilution of secondary antibody in blocking buffer for 1 h at room temperature.

Milk powder was used to reduce background. The blot was washed 4 times for 10 min each in TBST at room temperature. Chemiluminescent detection was carried out by reaction, Afterwards the membrane was covered with a thin clear plastic foil, and exposed to X-ray film.

### **2.3.19 Stripping and reprobing Western blots**

#### **Western blot stripping buffer**

##### **Mild stripping:**

Stripping buffer:

0,25 mM	Glycine	(15 g/l)
0.001 % w/v	SDS	(1 g/l)
0.01 %	Tween 20	(10 ml/l)

ad 1 l Aq. bidest.

pH adjusted to 2.2

Removal of primary and secondary antibodies from a western blot membrane is carried out with stripping. It is useful to investigate more than one protein on the same blot.

100 ml of stripping buffer was used to cover the membrane. The blot was incubated at room temperature for 5 – 10 min. The buffer was discarded and the membrane was washed for two times 10 min each with 1x PBS and two times 5 min each with 1x TBS-Tween<sup>®</sup>20. Subsequently the membrane was further proceeded to blocking.

### **2.3.20 Mammalian Cell culture:**

#### **Complete DMEM (Culture medium)**

435 ml DMEM (high glucose)

5 ml Pencillin/Streptomycin (100x) (Final concentration 1x)

10 ml L-Glutamin (4 mM)

50 ml Fetal calf serum (FCS) (Final concentration 10%)

---

500 ml

#### **Freezing medium**

90 ml FBS

10 ml DMSO

100 ml

#### **2.3.20.1 HEK 293 - cell line**

HEK293 is a human embryonic kidney cell line (HEK), the wild type has been transformed by transfection with the adenovirus 5 to a permanently culturable form (293). In 1977, the cell line was established for the first time [34]. The cell line is considered to be well cultivated and is a good basis for studies of proteins expressed by transfection. The cells have an epithelial morphology and grow in an adherent cell layer. The cells were obtained from LGC standards (ATCC) and were cultured in complete DMEM. HEK293 cells were used for overexpression of *AIPL1*.

#### **2.3.20.2 HeLa cell line**

Hela cells are adherently growing human carcinoma cells, which were isolated in 1951 from a cervix epithelial carcinoma of an American patient Henrietta Lacks. This cell line was the first epithelial cell line that has been cultivated continuously and is now known as the standard cell line. The cells were obtained from LGC standards (ATCC) and were cultured in complete DMEM. HeLa cells were used to avoid cell stacks and allowed spreading of cells or extended areas of cytoplasm. HeLa cell lines were used for immunocytochemistry studies.

### **2.3.20.3 Culture of cell lines:**

All cell culture work was done under a clean bench. The cultivation of cells was carried out in 100 mm cell culture dishes by adding 10 ml complete DMEM medium to the cells. Cells were grown in an incubator maintained at 37 °C, 5% CO<sub>2</sub>, and 95% humidity. For passage of adherent cells, the medium was removed with sterile glass pipettes and washed once with 5 ml of 1x PBS. 2 ml of accutase were added to the cells and were incubated for 2 - 5 min. 8 ml of medium was added to the cells detached from the bottom of the cell suspension and approximately 1x 10<sup>6</sup> cells were transferred into a new cell culture dish with 5 ml of medium and placed in an incubator (37 °C, 5% CO<sub>2</sub> and 95% humidity).

### **2.3.20.4 Long term storage of cell lines:**

For storage, the cell lines were frozen. The medium was removed with a sterile glass pipette and 5 ml of accutase was added to the cells. The plates were placed in an incubator for 2 - 5 min. 10 ml of medium were added to the detached cells and cells were resuspended. The cell suspension was transferred to a 15 ml centrifugation tubes and pelleted at 125 g for 10 min. The cell pellet was resuspended at a concentration of about 1x10<sup>6</sup> cells in freezing medium. This suspension was aliquoted (1 ml) in cryotubes. The cryotubes were stored for 24 h at -80 °C and then transferred to liquid nitrogen at -196 °C. Frozen cells could be re-cultured by thawing the cryovials in a water bath at 37 °C. Cells were then pelleted by centrifugation and the DMSO containing medium was removed. The process was repeated washing the cells with 1X PBS before resuspending them in the appropriate medium.

### **2.3.21 Heterologous expression in HeLa cells for immunocytochemistry**

HeLa cells were seeded with sufficient space to spread in eight imaging chamber microscopic slide bottom (PAA, Pasching). The cells were grown in complete DMEM medium at 37 °C and 5% CO<sub>2</sub> over night in an incubator.

#### **2.3.21.1 Transfection of HeLa cells using lipofectamin<sup>®</sup>**

250 ng of pQE-TriSystem His.*Strep* 1 constructs were transiently transfected into 50 - 60% confluent HeLa cells. By using Lipofectamine<sup>™</sup> (Invitrogen, Darmstadt) reagent according to the manufacturer's protocol for HeLa cells.

Plasmid DNA (250 ng) was diluted in 100 µl DMEM medium and vortexed thoroughly. Followed by the addition of 0.5 µl PLUS reagent gently mixed and incubated for 5 min at room temperature. 1.5 µl of Lipofectamine was added to the mix and incubated at room temperature for 30 min, DNA-Lipid complexes were added dropwise to the cells, and the plate was shaken for 10 minutes at 80 rpm. The cells were incubated at 37 °C and 5% CO<sub>2</sub>. Transfected cells were examined 24 hours after transfection.

### **2.3.21.2 Transfection of HeLa cells using Roti<sup>®</sup>-Fect PLUS**

The cells were incubated for 18 - 24 hours at 37 °C at 5% CO<sub>2</sub> in an incubator until they grew 50 - 60% confluent. Nucleic acid and transfection reagent stock solutions were thawed to room temperature and gently swirled. The following solutions were prepared in reaction tubes:

A: 0.5 µg DNA dissolved in 30 µl DMEM medium, which contained neither serum nor antibiotics.

B: 2.5 µl Roti<sup>®</sup>-Fect PLUS dissolved in 30 µl DMEM medium, which contains neither serum nor antibiotics.

Set ups were mixed carefully by pipetting.

Solution A and B were bought together without mixing them and incubated at room temperature for 15 - 20 min so that the nucleic acid/lipid complexes could form. Nucleic acid/lipid complexes were added after 20 min to the cells, and mixed carefully by swivelling gently. The cells were incubated at 37° C in a CO<sub>2</sub> incubator and the transfection medium was replaced with fresh complete medium after 4 hours. pCMV6-AC-GFP was used as a transfection efficiency control vector expressing Green fluorescent protein (GFP). GFP expression and transfection rate were tested 24 hours after transfection. At a transfection rate of more than 70% of the cells immunocytochemistry was subsequently performed.

### **2.3.22 Immunocytochemistry**

4% Paraformaldehyde (PFA) (4.0 g/100 ml)

ad 100 ml 1x PBS

Paraformaldehyde was solved in 1x PBS in a covered flask at 70°C. The solution was swirled for a couple of hours until all the paraformaldehyde was dissolved. Further the solution was

allowed to cool down to room temperature and filtered through a 0.22  $\mu\text{m}$  filter to remove any particulate matter and stored at 4°C.

3% Blocking buffer

BSA	0.3 g
Triton X 100	200 $\mu\text{l}$
1x PBS	10 ml

1X PBS

137 mM NaCl	(8.0g/l)
2.7 mM KCl	(0.2g/l)
10 mM $\text{Na}_2\text{HPO}_4$	(1.44g/l)
1.8 mM $\text{KH}_2\text{PO}_4$	(0.24 g/l)

dissolved in 1 l Aq. bidest and pH adjusted to 7.2 with HCl

Sterilized and autoclaved.

HeLa cells were harvested 24 h after transfection, fixed in 4% PFA for 10 min, and washed 3 times with 1x PBS each for 10 min. Fixed cells were incubated overnight with primary antibody. After extensive washing in 1x PBS for 3 times slides were incubated in secondary antibody solution for 1 h at room temperature in dark conditions. Later, the wells were washed twice with 1x PBS for every 10 min in the dark. Staining with DAPI (4',6-diamidino-2-phenylindole, dihydrochloride) followed. DAPI is a nuclear counterstain for use in multicolour fluorescent techniques. The blue fluorescence of DAPI stands out in vivid contrast to green, yellow, or red fluorescent probes of other structures. DAPI stains nuclei specifically, with little or no cytoplasmic labeling.

### **2.3.23 Heterologous expression in HEK293 cells and mammalian protein extraction**

HEK293 cells were seeded with sufficient space to spread in 6 well plate (Greiner bio-one, CELLSTAR<sup>®</sup>). The cells were grown in complete DMEM medium at 37 °C and 5%  $\text{CO}_2$  over night in an incubator. Further the transfection process was carried out as given in **2.3.21.1 and 2.3.21.2** for HeLa cells. Transfected cells were examined 24 hours after transfection. The cells were further proceeded with protein extraction using M-PER kit as given in **2.3.10.3.**

# CHAPTER 3

---

## 3. RESULTS

Splice variants of human AIPL1 were identified and cloned into pCR<sup>®</sup>2.1-TOPO-TA vector [40]. To visualize the role of these splice variants at protein level they were subcloned into an expression vector pQE-TriSystemHis.*Strep* 1. An expression vector containing the tags His and Strep were chosen for sub cloning followed by over expression, protein purification and further proceeded to protein interaction studies.

### 3.1 Sub cloning of *AIPL1* splice variants into an expression vector:

#### 3.1.1 Identification of human *AIPL1* splice variants

In a previous project splice variants of *AIPL1* were identified by RT-PCR from whole RNA isolated from human retinal tissue [42]. Along with splice variant 1 (full length splice variant) splice variants lacking complete exons 2 or 3 (splice variants 2 and 3), as well as variants showing shortened exons 2 or 5 (splice variants 4 and 5) or both exons 2 and 5 shortened (splice variant 6). Variants 4, 5 and 6 were formed by usage of an alternative acceptor splice sites in exon 2 and 5 which are located more or less further downstream of the regular acceptor splice sites. Detailed specifications of each human *AIPL1* splice variant and encoded protein isoforms are summarized in (table 2). The splice variants were provided cloned into pCR<sup>®</sup>2.1-TOPO-TA for further processing (figure 8). To express the splice variants in cultured human cells the splice variants were subcloned into pQE-TriSystemHis.*Strep* 1 (figure 9).

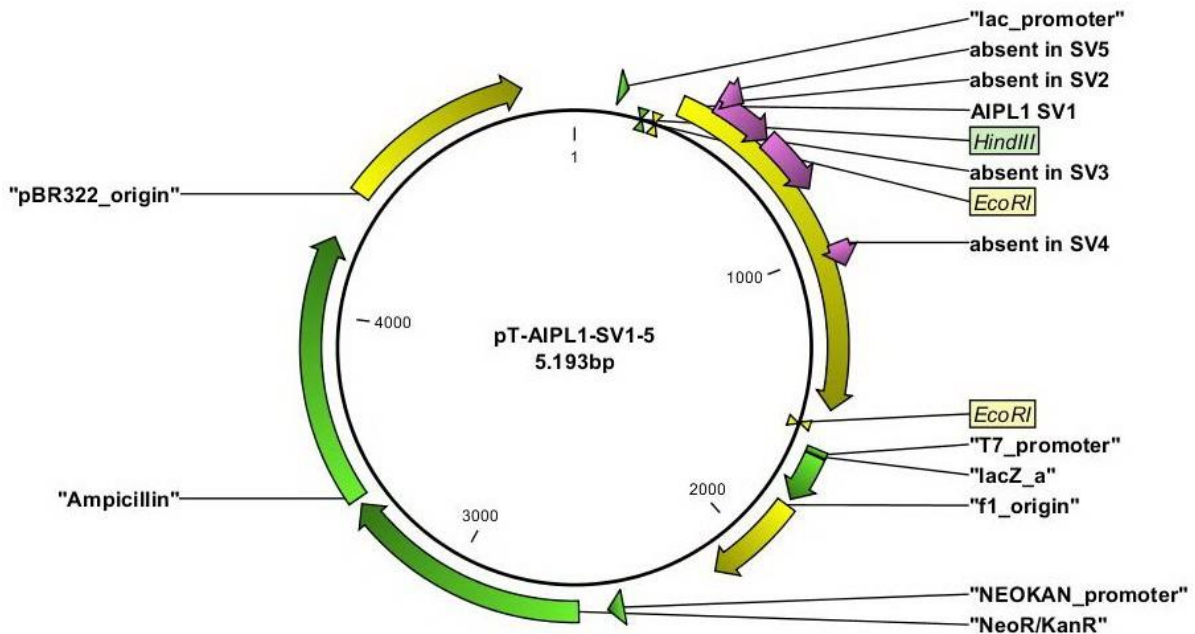


**Figure 8: pCR<sup>®</sup> 2.1-TOPO-TA vector map with AIPL1 cloned into the TA-site**

The vector map represents all the 5 *AIPL1* splice variants (SV1 - SV5) cloned with restriction enzymes *EcoRI* and *HindIII*. Functional elements of the vector: *lac\_promoter*, *T7\_promoter*, *lacZ\_a*, *f1\_origin*, *NEOKAN\_promoter*, *NeoR/KanR*, *Ampicillin*: *Ampicillin* resistance ORF and *pBR322\_origin*.

### 3.1.2 Cloning of splice variants

*pQE-TriSystemHis.Strep 1* is an expression vector possessing a His and a Strep tag along with the advantage of having prokaryotic promoter (T5) and eukaryotic promoter (CMV) to over express the recombinant constructs both in prokaryotic and eukaryotic systems. For subcloning the inserts were amplified with a Phusion<sup>™</sup> Hot start High-Fidelity DNA polymerase (Finnzymes) by using the primer set *AIPL1-For* and *AIPL1-Rev* (2.1.2) having internal *EcoRI* and *HindIII* restriction sites.

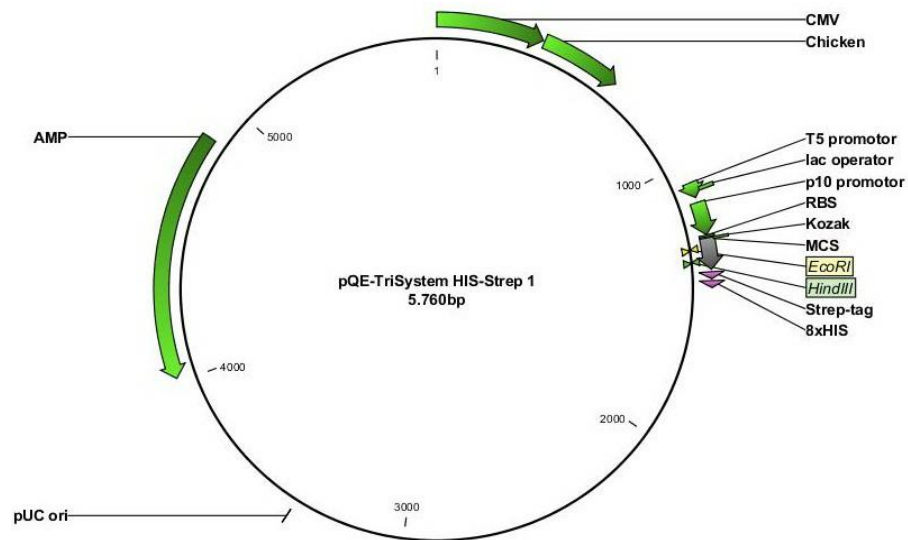


**Figure 9: pQE-TrisSystem His.Strep 1 vector map and its elements** - CMV: immediate early enhancer region, chicken: chicken actin promoter, T5 promoter, lac operator element, p10 promoter: promoter elements, RBS: ribosome binding site, Kozak: translation start, MCS: Multiple cloning site including EcoRI and HindIII sites, Strep-tag: Strep-tag coding sequence, 8xHis: 8xHis tag coding sequence, AMP: Ampicillin resistance coding sequence.

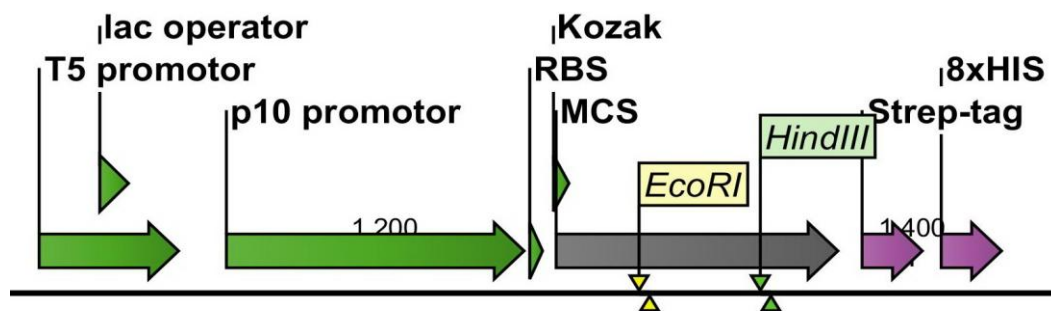


**Figure 10: Multiple cloning site of pQE-TrisSystem His.Strep 1 vector with restriction enzymes *EcoRI* and *HindIII* used for sub cloning of *AIPL1* splice variants (SV1-SV5).** T5 promoter, lac operator element, p10 promoter: promoter elements, RBS: ribosome binding site, Kozak: translation start, MCS: Multiple cloning site, Strep-tag: Strep-tag coding sequence, 8xHis: 8xHis tag coding sequence

These restriction sites were chosen because the multiple cloning site sequence of the expression vector possesses EcoRI and HindIII sites which were used as target sites for sub

cloning the amplified PCR products of AIPL1. The PCR products were cut out from an agarose gel and purified with the NucleoSpin<sup>®</sup> Extract II kit (Macherey Nagel). Later the purified pCR2.1-TOPO<sup>®</sup>-AIPL1 splice variant clones were digested with EcoRI and HindIII (NEB) restriction enzymes according to chapter 2.3.4.1 and dephosphorylation was done as mentioned in chapter 2.3.4.2. Dephosphorylated products were ligated according to chapter 2.3.4.3 into EcoRI and HindIII sites of the expression vector pQE-TriSystem His.Strep 1 (Qiagen, Hilden) that codes for an additional C-terminal 8xHis tag. The ligated products were transformed into XL1-Blue competent cells as mentioned in chapter 2.3.4.5 and 100 µl of the transformation set up was plated on LB-Agar supplemented with ampicillin. LB-agar plates were incubated overnight at 37 °C. Positive clones were picked and grown in overnight cultures in LB medium with ampicillin followed by plasmid mini preps. 1.5 µg of each plasmid mini prep was checked using restriction digestion of constructs with EcoRI and HindIII and were analysed on 1% agarose gel (figure 12).

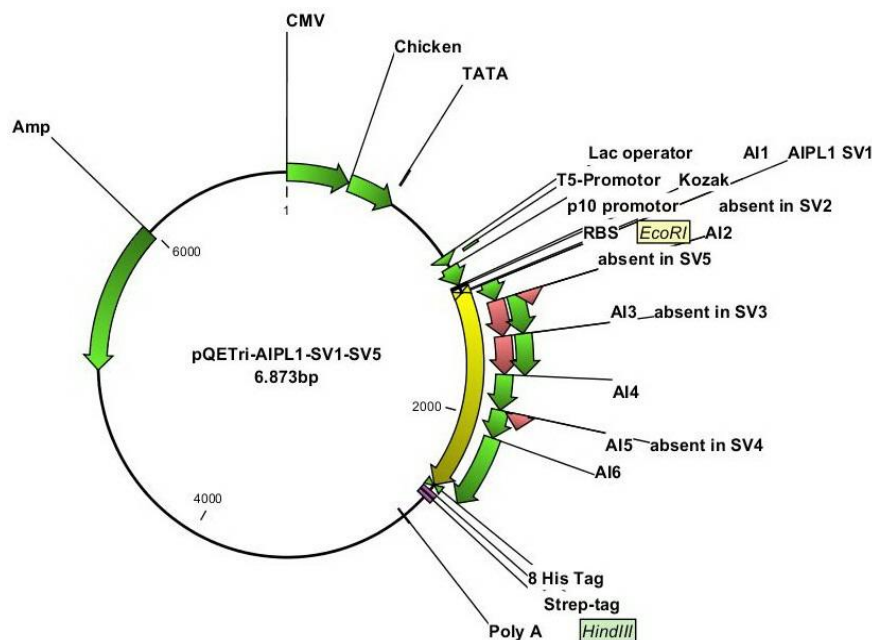


**Figure 11: Vectormap of pQE-Tri-SystemHis.Strep 1 Vector containing AIPL1 splice variants SV1 - SV5**

The vector map represents all five AIPL1 splice variants (SV1 - SV5) cloned with restriction enzymes EcoRI and HindIII. AI1 - AI6 represent AIPL1 exons (1 - 6). Functional elements of the vector are named in (Figure. 9).

### 3.1.3 Restriction digestion and sequence analysis

All cloned splice variants were analysed through restriction endonuclease digestion using EcoRI and HindIII. pQE-Tris-system His.*Strep* 1 empty vector was used as a control. All plasmids were examined after restriction digestion on a 1% (w/v) agarose and gel electrophoresis performed for 1 hour at 100 V to assure that splice variants were cloned at the right size. The expected sizes of the insert were as follows, and empty vector pQE-TriSystem His.*Strep* 1 at 5.8 kb.

Splice variant	Insert size	Construct size
SV1	1,155 bp	6873 bp
SV2	975 bp	6693 bp
SV3	966 bp	6684 bp
SV4	1,083 bp	6801 bp
SV5	1,089 bp	6807 bp

**Table 4: Expected sizes of cloned *AIPL1* splice variant fragments.**

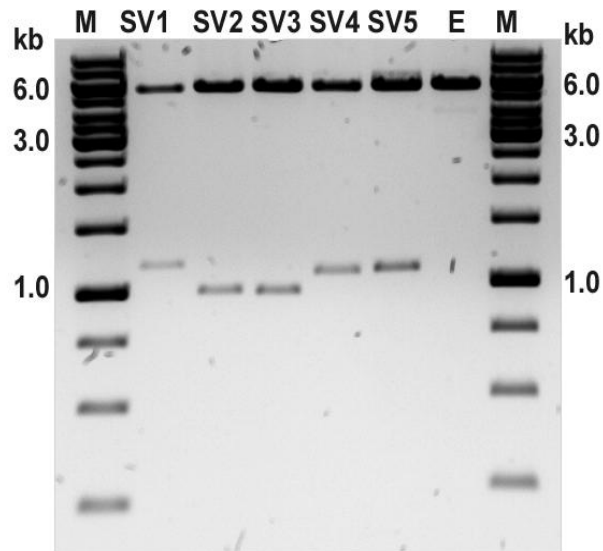
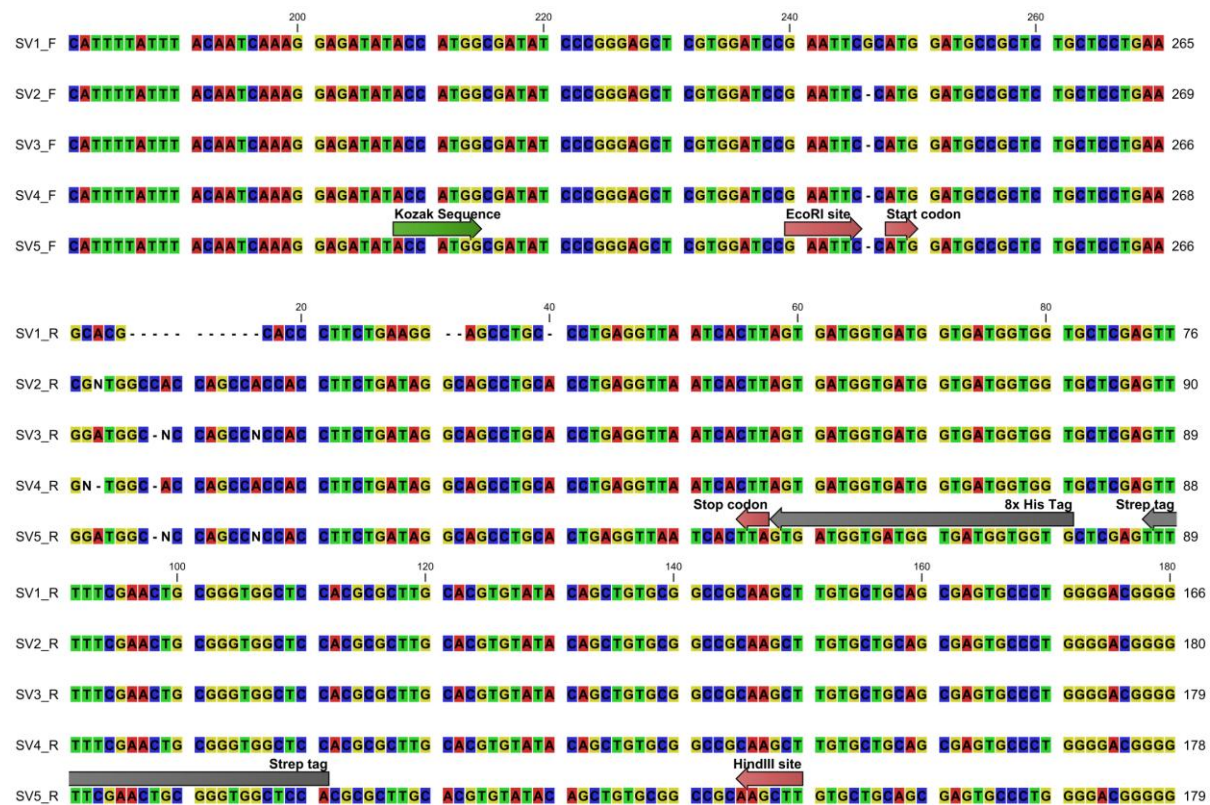


**Figure 12: Restriction endonuclease analysis of *AIPL1* splice variant pQE-TriSystem 1 His.*Strep* clones (SV1 - SV5). Vector backbone size was 5718 bp and the inserts were sized according to table 4.**

PCR and restriction enzyme analysis of the constructs of pQE-Tris\_AIPL1 on 1% agarose gel. Lane 1 and 8, M: DNA 1 kb molecular weight standard; lane 2, pQE-Tris plasmid with SV1 insert (pQE-Tris\_SV1); lane 3, pQE-Tris\_SV2; lane 4, pQE-Tris\_SV3; lane 5, pQE-Tris\_SV4; lane 6, pQE-Tris\_SV5; lane 7, pQE-Tris plasmid without insert.

Plasmid mini preps showing the expected fragment sizes of vector and insert were sequenced which revealed that all splice variants were cloned in frame along with the specified restriction enzymes added and with the His tag.

### A



### B

**Figure 13: A.** Verification of forward frame conservation of the inserts towards start codon of the vector with chosen restriction site EcoRI.

**B.** Verification of reverse frame conservation of the inserts towards stop codon of the vector with tags 8x His and Strep along with the chosen restriction site HindIII. SV1\_R to SV5\_R: splice variant specific clone for SV1 - SV5.

### **3.2 Over expression of *AIPL1* splice variants in a prokaryotic expression system using the Enbase® Flo cultivation system:**

For purification of His tagged proteins high amounts of protein yield were required. The Enbase® Flo cultivation system was used to over express the probes for achieving a higher yield of protein as mentioned in chapter **2.3.9.2**.

#### **3.2.1 Recombinant protein purification and pull down experiments**

##### **3.2.1.1 SDS-PAGE of Ni-NTA agarose purified probes of SV1 - SV5**

All identified AIPL splice variants (SV1 - SV5) were purified using Ni\_NTA agarose as mentioned in chapter **2.3.12**. All purification steps (Flow-through FT, wash 1, wash 2, elution 1, elution 2, elution 3, and elution 4) were tested for AIPL1 by SDS-page. Equal volumes of the protein sample were loaded in all lanes. Proteins were analysed on SDS-PAGE and stained with LabSafe™ GEL Blue (figure 14) as given in methods section chapter **2.3.14 and 2.3.15**.

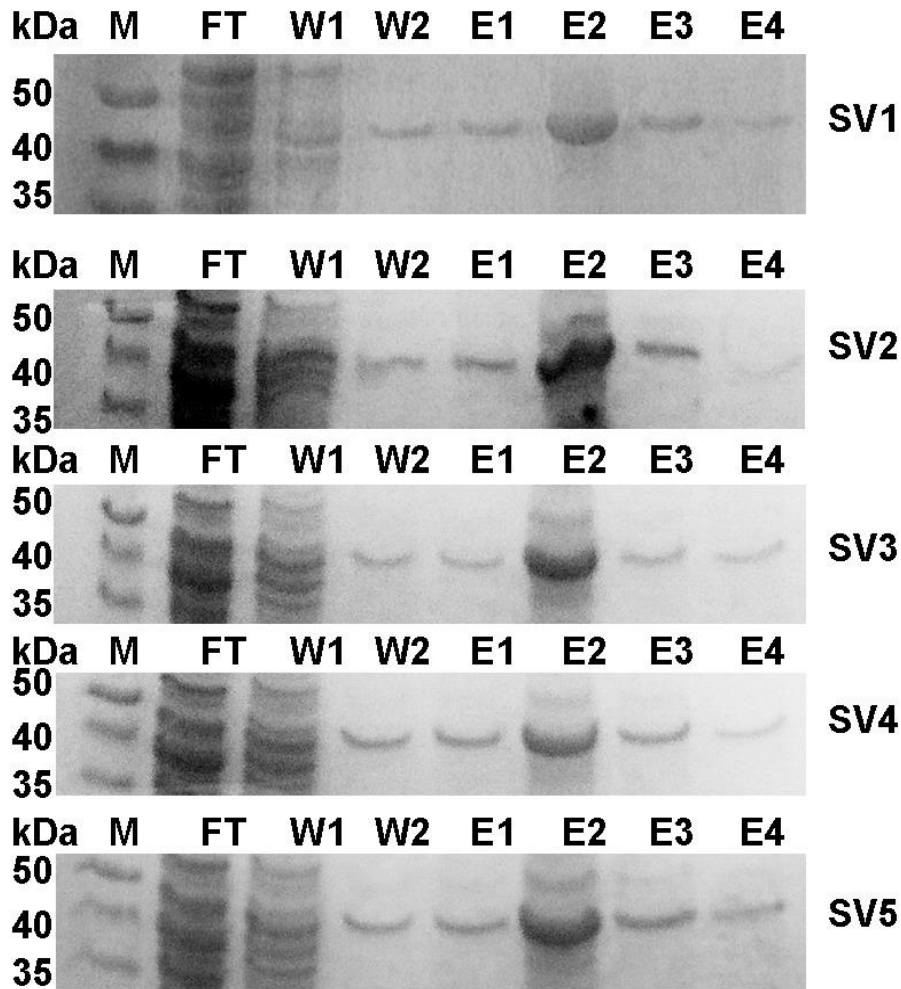


**Figure 14:** Coomassie-stained SDS-PAGE analysis of over expressed His tagged AIPL1 (SV1 - SV5) purified by Ni-NTA agarose. M: molecular mass marker (kDa), FT: Flowthrough, W1: wash 1, W2: wash 2, E1: Elution 1 E2: Elution 2, E3: Elution 3, E4: Elution 4, kDa: kilo Dalton.

### 3.2.1.2 SDS-PAGE of His tag purified and centriprep concentrated prokaryotic samples of *AIPL1* splice variants SV1 - SV5

The protein concentrations of over expressed *AIPL1* splice variants (SV1 - SV5) with His tag in prokaryotic system were measured through Bradford assay and revealed the highest concentration of purified His-tagged protein in elution fraction two (E2) as clearly depicted in SDS-PAGE analysis (figure 14). Therefore, E2 fractions of all splice variants were used for further analysis.

To further increase the concentration of recombinant protein, E2 fractions were concentrated using centiprep columns (Millipore) as given in 2.3.19. The concentrated E2 fractions were analysed by SDS-PAGE with comassie blue staining (figure 15). The results shown in the SDS\_PAGE (figures: 14 & 15) revealed that the chosen expression system was suitable for expressing the AIPL1 splice variants. The bands seen on the PAGE gels support that the expressed and purified proteins are of the expected size from the group of endogenous proteins produced along with the His tagged AIPL1 splice variants during the process of protein over expression. Further analysis was carried out by Western-blot.



**Figure 15: Coomassie-stained SDS-PAGE analysis of His tagged AIPL1 purified by Ni-NTA agarose and concentrated samples of E2 fractions of (SV1 - SV5).** Equal amounts of protein (10  $\mu$ g) from each indicated extract were separated on SDS-PAGE. Lane 1: Molecular mass marker (kDa). SV1 – SV5: Elution step E2 from overexpressed and purified AIPL1.

### 3.2.3 Immunoblot analysis of *AIPL1* splice variants

All overexpressed, purified, and concentrated *AIPL1* splice variants were validated through Western blotting to confirm correct expression and to reveal size differences in splice variants.. The expression pattern of splice variants was analyzed both in a prokaryotic expression system and an eukaryotic expression system. Protein extracted from human retinal tissue as given in chapter 2.3.10.1 was used as a positive control in the western blots.

#### 3.2.3.1 Western blot analysis of *AIPL1* splice variants (SV1 - SV5) expressed in prokaryotic system

The protein concentration of all splice variants from the prokaryotic expression system was measured using a Bradford assay and equal amounts of the protein (10  $\mu$ g) were loaded on to each lane. Human protein from a retinal tissue sample was used as positive control and protein extract from HEK293 non-transfected cells was used as negative control. SDS PAGE was performed using the gradient SERVAGel™ TG gels. Fermentas broad range

multispectrum colour marker was applied as molecular weight marker. Electrophoresis was performed at 50 V for 30 min until the protein samples entered the stacking gel. The electrophoresis proceeded further at 120 volts for 90 min.

After electrophoresis the gel was transferred onto a Protan<sup>®</sup> nitrocellulose membrane (Whatman<sup>®</sup>) using the blotelutor (Biometra). Blotting was performed for 45 min at 200 mA. Transfer of proteins was confirmed through Ponceau S staining as given in chapter 2.3.17. Here a Ponceau S staining is exemplified and will not be shown in further chapters. Immunoblot detection of AIPL1 was carried out according to chapter 2.3.18 with a primary antibody against human AIPL1 [81]. The antibody was applied in 1% milk powder in 1x TBS-0.2% Triton X 100 blocking solution at a dilution of 1:5000. Secondary peroxidase-conjugated Anti-Rabbit IgG (whole molecule) antibody from goat (SIGMA A0545) was applied at a dilution of 1:80,000 in 1% milk powder in 0.2% 1x TBS-Triton X 100 blocking solution. The blot was developed using the luminol reagent according to chapter 2.3.18.

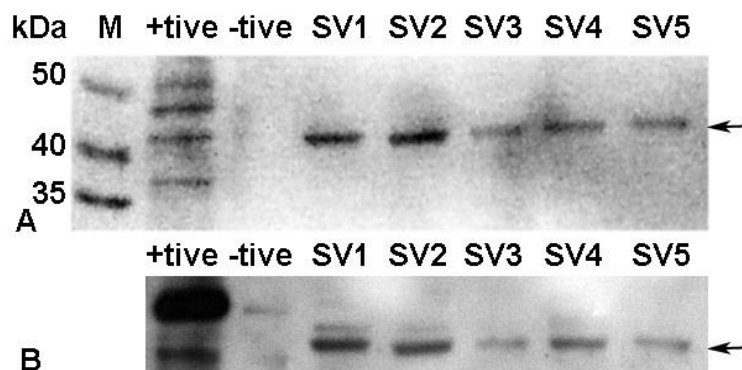


**Figure 16: Western blot analysis of overexpressed and purified His tagged AIPL1 splice variants SV1 - SV5 in prokaryotic system.**

Equal amounts of protein from each splice variant extract were separated on SDS-PAGE and transferred onto nitrocellulose membrane. **A:** Ponceau S staining of the nitrocellulose membrane following electrophoretic transfer of proteins by SDS-PAGE gel separation.

**B:** Western blot probed with an affinity purified rabbit anti-AIPL1 antibody at 1:5000 dilution & Secondary Ab: Peroxidase-conjugated Anti-Rabbit IgG (whole molecule) antibody from goat (SIGMA A0545) at 1:80,000 dilution. M: molecular mass marker (kDa), +tive: retina protein as positive control, -tive: HEK293 non-transfected as negative control), *AIPL1* Splice Variants (SV1 - SV5). **Note:** A subtle difference in size could be seen for splice variants SV1 vs SV2 and SV3 as well as SV4 and SV5.

### 3.2.3.2 Immunoblot detection of His tags in *AIPL1* splice variants from SV1-SV5

After over expression of recombinant *AIPL1* with His tag in prokaryotic system the raw lysate contained the recombinant *AIPL1* protein along with many other proteins originating from the bacterial host. To detect the His tagged proteins from raw lysate affinity purification was carried out using Ni-NTA agarose according to chapter 2.3.12. Ni-NTA agarose binds His-tagged fusion proteins from a mixture of endogenous proteins. The elute obtained from purification was used to detect the *AIPL1* proteins with His tag using immunoblot analysis.

Immunoblot detection of His tag was carried out according to chapter 2.3.16 with a polyclonal HRP tagged Rabbit anti-His antibody to 6X His (Abcam ab 1187). The antibody was applied in 1% milk powder in 1x TBS-0.2% Triton X 100 blocking solution at a dilution of 1:5000. The blot was developed using the luminol reagent according to chapter 2.3.18.

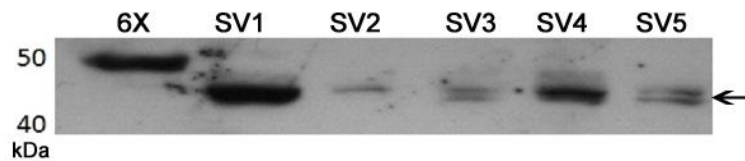


**Figure 17: Western blot analysis of over expressed and purified His tagged *AIPL1* splice variants (SV1 - SV5) in prokaryotic system:**

6x: His-tagged molecular mass protein ladder as positive control, SV1 – SV5: *AIPL1* Splice Variants (SV1 - SV5). Equal amounts of protein (10  $\mu$ g) from each indicated extract were run on SDS-PAGE and were blotted onto nitrocellulose membranes. The blot was probed with HRP tagged His Ab-Rabbit polyclonal to 6X His (Abcam ab 1187) at 1:5000 dilution. Protein molecular mass markers (in kDa) are indicated on the left.

From the immunoblot it was revealed that all the splice variants (SV1 - SV5) were possessing the His-tag since anti-His antibody detected all the splice variants of *AIPL1*. The size of the bands on the blot (figure 17) reveals all splice variants of *AIPL1* were fully expressed including His tag within the limits of their sequence but did not show detectable size differences in this separation system.

### 3.2.3.3 Expression and purification of recombinant proteins in eukaryotic HEK293 cell lines

All splice variants (SV1 - SV5) of AIPL1 were expressed in HEK293 cell lines. The reason for choosing HEK293 cell line was that *AIPL1* is not expressed endogenously in this cell line [81] and that transfection levels are higher in this cell line, resulting in a higher level of AIPL1 expression. Protein extraction was carried out using M-PER (PIERCE) kit according to chapter 2.3.10.3. The concentrations of the extracted protein were measured by Bradford assay and equal amounts of protein (10 µg) were loaded onto each well. Bradford assay revealed the highest concentration of purified His-tagged protein in elution fraction two (E2) as clearly depicted in SDS-PAGE analysis (figure 18). Therefore, E2 fractions of all splice variants were used for further analysis. Human retinal protein was used as positive control and non transfected HEK293 cell were used as negative control.

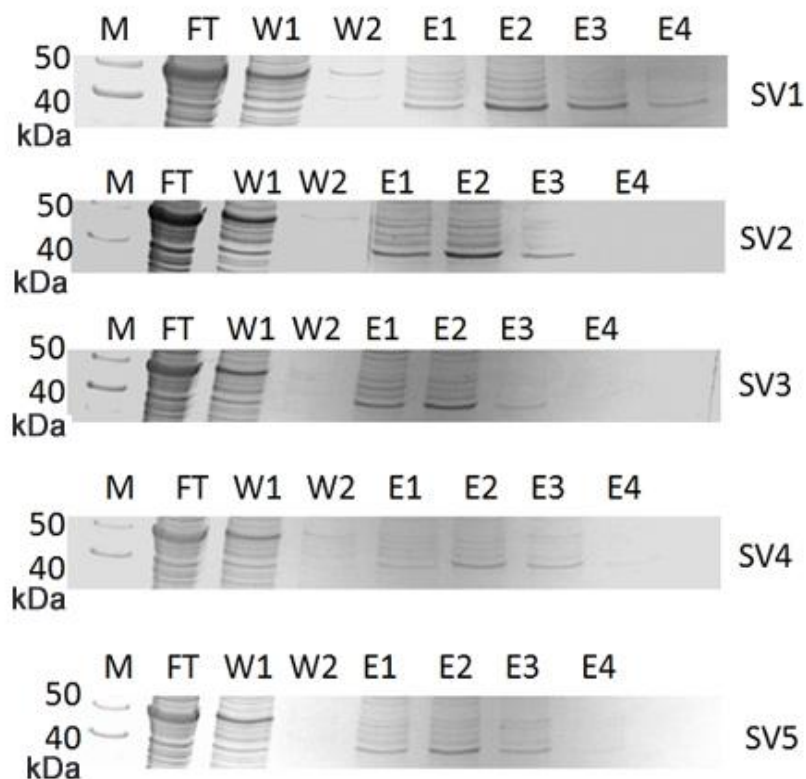


**Figure 18: SDS-PAGE of Ni-NTA agarose purified probes (SV1 - SV5) from expression in eukaryotic HEK293 cell lines**

Coomassie-stained SDS-PAGE analysis of over expressed His tagged AIPL1 purified by Ni-NTA agarose. M: Molecular mass marker (kDa), FT: Flowthrough, W1: wash 1, W2: wash 2, E1: Elution1 E2: Elution, E3:Elution 3, E4:Elution 4, kDa: Kilodalton.

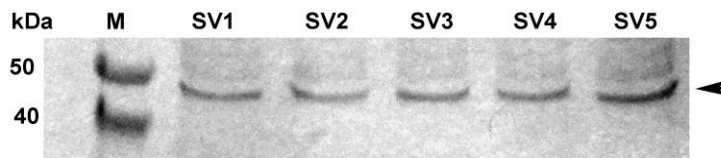


**Figure 19: SDS-PAGE of centriprep concentrated probes of AIPL1 SV1 - SV5 from expression in eukaryotic HEK293 cell lines**

Coomassie-stained SDS-PAGE analysis of His tagged AIPL1 purified by Ni-NTA agarose and concentrated samples of E2 fractions of (SV1 - SV5). M: Molecular mass markers (kDa). SV1 - SV5: Elution step E2 of eukaryotic SV1 - SV5 expression.



**Figure 20: Western blot analysis of AIPL1 splice variants (SV1 - SV5) (Eukaryotic)**

Western blot analysis of His tag purified protein from total cell extracts expressed in HEK293 cells. Western blot probed with an affinity purified rabbit anti-AIPL1 antibody at 1:5000 dilution & Secondary Ab: Peroxidase-conjugated Anti-Rabbit IgG (whole molecule) antibody from goat (SIGMA A0545) at 1:80,000 dilution. -tive: non transfected HEK293 cells as negative control, +tive: retinal protein extract as positive control, SV1 - SV5: expressed His tagged AIPL1. Equal amount of protein (10 µg) from each extract were loaded onto each lane. Protein molecular mass markers (in kDa) are indicated on the left.

Immunoblot results conclude the expression of all the AIPL1 splice variants (SV1 - SV5) in HEK293 cell lines. Anti-AIPL1 antibody detected all the splice variants over expressed and purified in mammalian cell lines HEK293. Compared to the prokaryotic protein expression system the mammalian protein expression system was less effective because The pQE-Tri-SystemHis.*Strep* 1 system is optimized for bacterial culture and expresses suboptimal in human cells. In both systems double bands (figure 16 B, 17 and 20) were seen with Anti-AIPL1 and Anti-His antibodies. The post translational modifications or the antibody used which is not a splice variant specific antibody could be possible reasons for the appearance of double bands. A subtle difference in size could be seen for splice variants SV1 vs SV2 and SV3 as well as SV4 and SV5 (Figure 16 B, 17 & 20)

### **3.3. Intracellular localization of human AIPL1 splice variants SV1-SV5 in HeLa cells:**

The pQE-TriSystemHis.*Strep* 1 based His tagged recombinant AIPL1 expression constructs (SV1 - SV5) were prepared to transfect HeLa cells to locate the expression of AIPL1 at the cellular level. Transfection of all the five splice variants, SV1 - SV5 was carried out as given in methods **2.3.21.1** and **2.3.21.2**. Initially lipofectamine was used. It was substituted by Roti<sup>®</sup>-Fect PLUS in repeat applications. For detection, hybridization with primary antibodies against AIPL1 and His-tag were carried out independently to confirm that the immunoreactivity was not specific to the AIPL1 antibody compared to the anti-His-tag antibody. Alexa Fluor labeled secondary antibodies were used to visualize bound primary antibodies. HeLa cells were examined on a Keyence (BZ-8100<sup>E</sup>) fluorescence microscope after 24 hrs of transfection and immunocytochemistry was performed as given in chapter **2.3.22**. DAPI was used as a nuclear counterstain as described.

Chicken anti-human AIPL1-Ab was applied at a dilution of 1:100 and probed with a secondary Alexa Fluor<sup>®</sup> 488-labeled goat anti-chicken IgG (H+L) antibody (Invitrogen, Darmstadt A11039) at 1:1000 dilution. Incubation was carried out for 1 h. His-tagged AIPL1 was detected by an anti-His antibody (ab1187, Rabbit, Abcam, Cambridge UK) and an Alexa Fluor<sup>®</sup> 488-labeled secondary antibody donkey anti-rabbit IgG (H+L) (Invitrogen, Darmstadt A11039). Incubation of both primary and secondary antibody was done for 1 h each. All procedures were carried out at room temperature. Finally, slides were covered with Dako Fluorescence Mounting Medium (DAKO, Hamburg) and immunoreactivity (IR) was recorded on a Keyence (BZ-8100<sup>E</sup>) wide-field microscope with epifluorescence.

Transient expression of splice variants SV1 - SV5 was detected in HeLa cells transfected with pQE-TriSystemHis.*Strep* 1 constructs. Fluorescent immunohistochemical labeling disclosed expression throughout the cytoplasm as could be seen by AIPL1-specific antibody and His-tag specific antibody (fig. 21 and 22). A splice variant specific localization pattern could not be obtained from evaluation of *AIPL1* expression alone.

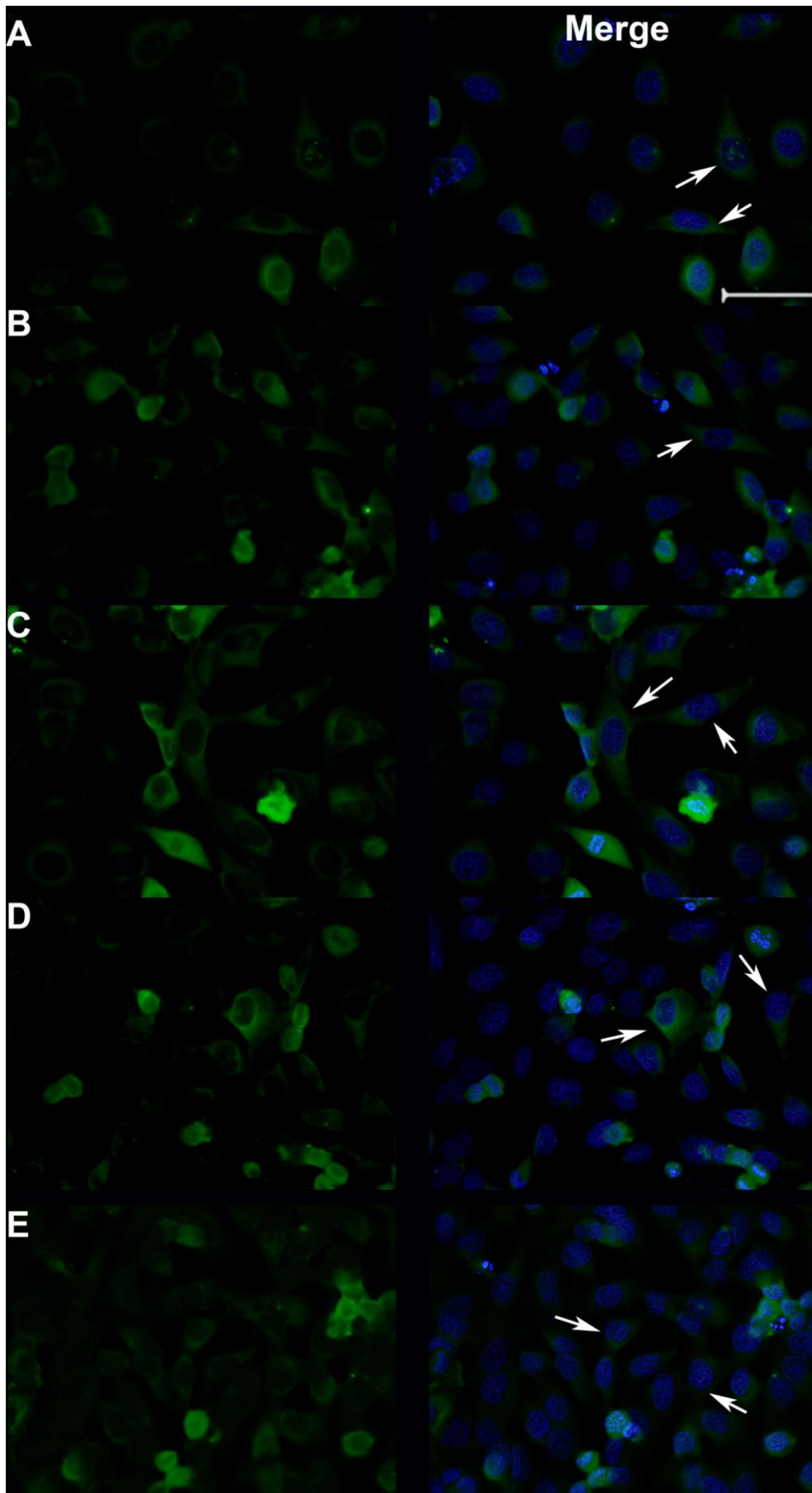


**Figure 21:** Heterologous expression of *AIPL1* splice variants in HeLa cells: Immunofluorescent images showing intracellular localisation of AIPL1 proteins expressed in HeLa cells. Cells transfected with pQE-TriSystemHis.*Strep* 1-AIPL1 splice variant constructs (SV1 - SV5) were cultured for 24 h and then processed for immunofluorescence using Chicken anti-human AIPL1-Ab followed by Alexa Fluor® 488-labeled goat anti-chicken IgG (H+L) antibody (Invitrogen, Darmstadt A11039). Nuclei were counterstained with DAPI (blue). A: SV1, B: SV2 C: SV3, D: SV4, E:SV5. Fluorescent labeling disclosed expression of AIPL1 throughout the cytoplasm. The scale bar represents 20 µm. Arrows: Indicate AIPL1 expression throughout the cytoplasm.

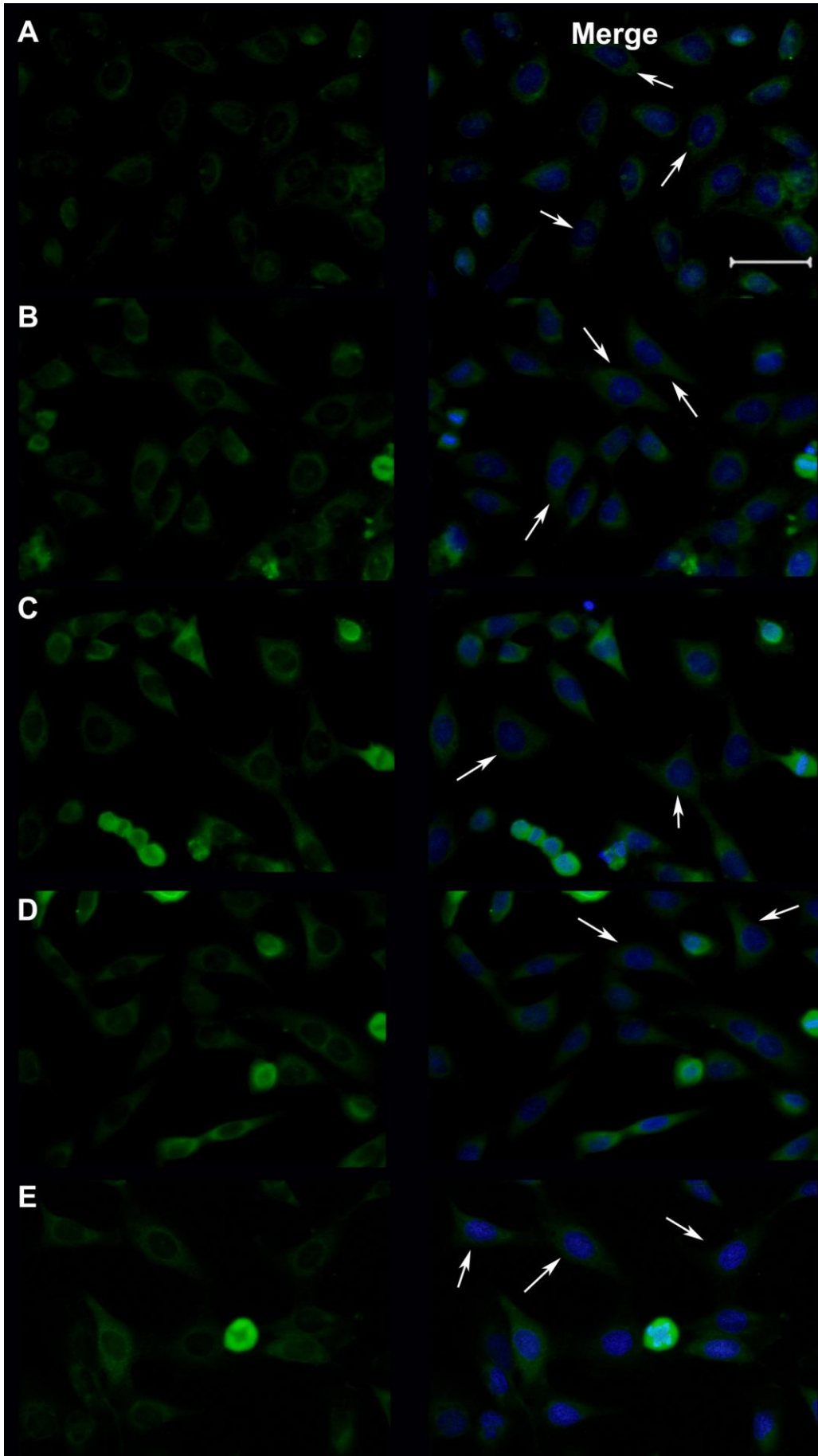
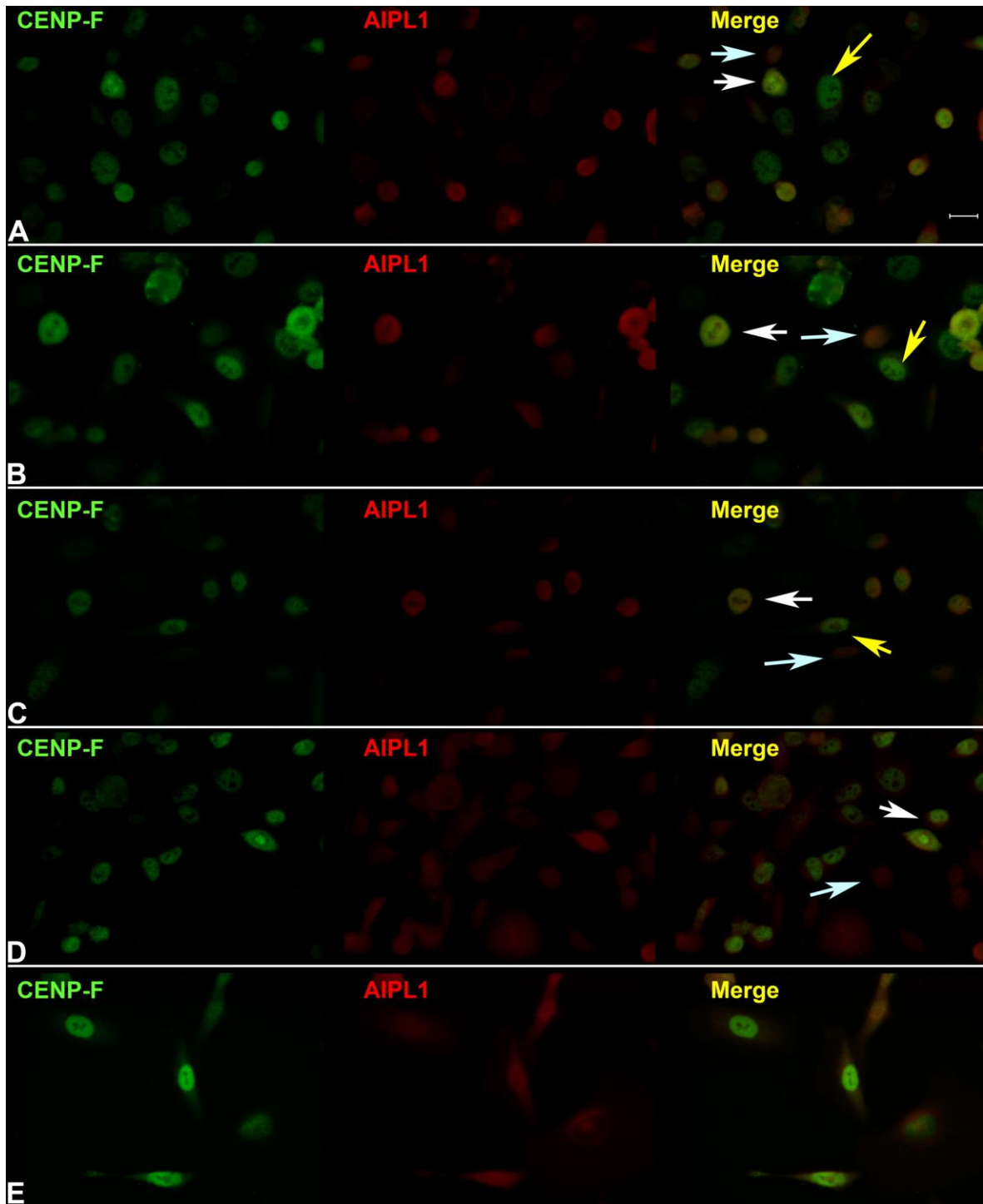


**Figure 22: Heterologous expression of His-tagged AIPL1:** Immunofluorescent images showing cellular localisation of AIPL1 proteins expressed in HeLa cells. Cells transfected with pQE-TriSystemHis.*Strep* 1-AIPL1 splice variant constructs (SV1 - SV5) were cultured for 24 h and then processed for immunofluorescence using anti-His antibody followed by Alexa Fluor® 488-labeled secondary antibody donkey anti-rabbit IgG (H+L) (Invitrogen, Darmstadt A21206). Nuclei were counterstained with DAPI (blue). A: SV1, B: SV2 C: SV3, D: SV4, E:SV5 Fluorescent labeling disclosed expression throughout the cytoplasm as could be seen by His-tag specific antibody. The scale bar represents 20 µm. Arrows: Indicate His-tagged AIPL1 expression throughout the cytoplasm.

### 3.3.1 Immunohistochemical co-detection of heterologously expressed AIPL1 and intrinsic CENP-F

To check whether AIPL1 is colocalizing with CENP-F inside the cell transfection studies were performed in HeLa cell lines and transfected cells were probed for AIPL1 expression and CENP-F expression by immunohistochemistry. Colocalization between AIPL1 and CENP-F was evaluated for full length AIPL1 and different splice variants of AIPL1. The transfected recombinant AIPL1 and the intrinsic CENP-F were detected using AIPL1 and CENP-F antibodies.

HeLa cells were seeded in silicone frames on microscope slides (PAA, Cölbe) and grown at 37 °C and 5% CO<sub>2</sub> over night in an incubator. Full length *AIPL1* cloned in pQE-TriSystemHis.*Strep* 1 vector (Qiagen) with a His-tag added at the C-terminus was transfected and expressed in HeLa cells as mentioned in chapter 2.3.21. His-tagged AIPL1 was detected by Anti-HIS antibody (ab1187, Abcam) and anti-AIPL1-ab (Chicken IgY against purified whole protein). CENP-F was detected by anti-CENPF-ab (sc-135865, Santa Cruz). Immunoreactivity (IR) was recorded on a Keyence (BZ-8100<sup>E</sup>) microscope by epifluorescence using the Z-stack feature. Digital images were evaluated for co-localization by Pearson's coefficient using the JACoP plugin in ImageJ (V. 1.44p).



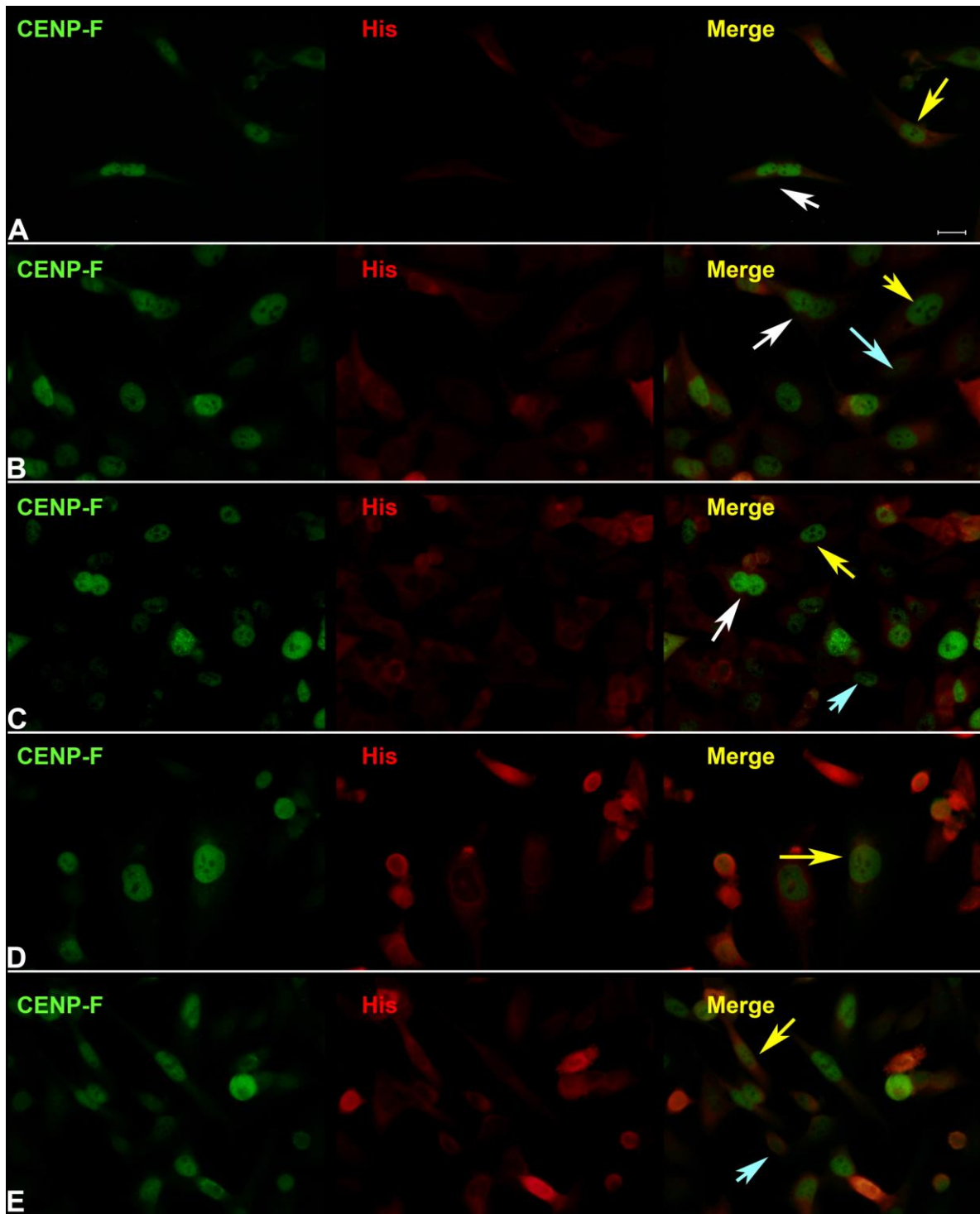
	SV1	SV2	SV3	SV4	SV5
Pearson's coefficient	$r = 0.735$	$r = 0.836$	$r = 0.795$	$r = 0.675$	$r = 0.655$

**Figure 23: Immunohistochemical detection of intrinsic *CENPF* expression and transient *AIPL1* expression in HeLa cells**

First column shows intrinsic CENPF expression, second column shows heterologous AIPL1 expression, third column shows digital overlays of the single coloured images. Antibodies used- Primary: anti-AIPL1-ab (Chicken IgY against purified whole protein) & Primary Ab: anti-CENPF-ab (sc-135865, Santa Cruz). Secondary (for AIPL1)-red lable: goat IgG anti-chicken IgY (Alexa Fluor 564, Invitrogen A11040) & (For CENP-F) Secondary Ab-green lable: Goat anti- mouse IgG (H+L), Alexa Fluor 488, Invitrogen A11001). A: SV1, B: SV2 C: SV3, D: SV4, E:SV5. The scale bar represents 20  $\mu$ m. Arrows indicate: White - dividing cell, Yellow - pre-division cell and light Blue - resting cell.

In HeLa cells heterogeneously expressed AIPL1 is spread for all splice variants throughout the cytoplasm in all stages of the cell cycle (figure 23A-E). Intrinsically expressed CENP-F is localized in the nucleus of the cells and to a lesser extent in the perinuclear cytoplasm especially during certain stages of cell divison (figure 23A-E). In the resting phase of cell divison CENP-F is almost absent. Co-localization of AIPL1 and CENP-F is seen in the perinuclear region and in the nucleus at certain stages of the cell cycle.

Immunoreactivity (IR) against the AIPL1-specific antibody and the His-tag-specific antibody for AIPL1 was seen in the cytoplasm of HeLa cells. IR to intrinsically expressed CENP-F also localized to the cytoplasm in HeLa cells overlapping with the IR of AIPL1.



	SV1	SV2	SV3	SV4	SV5
Pearson's coefficient	$r = 0.694$	$r = 0.558$	$r = 0.434$	$r = 0.543$	$r = 0.658$

**Figure 24: Immunohistochemical detection of intrinsic *CENPF* expression and transient expression of His-tagged AIPL1 in HeLa cells**

First column shows intrinsic CENP-F expression by a CENP-F specific antibody (green), second column shows heterologous expression of His-tagged AIPL1 by a His-tag-specific antibody (red), third column shows digital overlays of single coloured images. Antibodies used- Primary: polyclonal HRP tagged Rabbit anti-His antibody to 6X His (Abcam ab 1187) & anti-CENPF-ab (sc-135865, Santa Cruz). Secondary (for His)-red lable: goat anti-rabbit IgG(H+L), Alexa Fluor 546, Invitrogen A11010 & (For CENP-F)-green lable: Goat anti-mouse IgG (H+L), Alexa Fluor 488, Invitrogen A11001). A: SV1, B: SV2 C: SV3, D: SV4, E:SV5. The scale bar represents 20  $\mu$ m. Arrows indicate: white -dividing cell, yellow - pre-division cell, and light blue - resting cell.

CENP-F, as stated earlier, takes part in cell cycle regulation. The influence of cell cycle regulating check points on CENP-F is huge. They control the vital functions of CENP-F, in other words they decide the fate of CENP-F. These check points control the CENP-F functions like stability, delay to the next phase or sometimes leads to depletion of CENP-F. During the co-localization studies it was seen that few cells were prepared to divide (Figure 23 A,B & C yellow arrows) and few of them showed cell divison (Figure 23 A,B,C & D white arrows) and the remaining cells are in the resting phase (Figure 23 A,B,C & D light blue arrows). It was envisaged that splice variants (SV1 - SV5) of AIPL1 are colocalizing with CENP-F at different stages of cell cycle.

# CHAPTER 4

---

## 4. Discussion

The research of the past two decades on both *AIPL1* and *CENP-F* has revealed various roles of these genes in retinal dystrophies and cell cycle activities respectively. This is the first study on human *AIPL1* splice variants. The existence of splice variants identified in *AIPL1* was investigated through various biochemical techniques at the molecular level.

With approximately 7% *AIPL1* mutations cover a major share of mutations causing Leber congenital amaurosis (LCA) compared to other known LCA genes. [17,20,89]. Knowledge on *AIPL1* has progressed through various steps, from gene identification [88,89] followed by the clinical characterization of the phenotype [20,31,72,102] towards an increasing understanding of the molecular mechanism [37,54,65,67,80,99,100] cumulating in a treatment strategy [91,96]. *AIPL1* mutations have been described to cause several types of retinal dystrophies such as LCA, juvenile Cone-rod dystrophy (CRD) and milder forms of EOSRD [20,89]. The prevalence of *AIPL1* mutations in LCA and the severity of the resulting phenotype generate an interest in the function and pathofunction of *AIPL1*. The results obtained in this study provide information on *AIPL1* interaction with centromere protein *CENP-F* and opens perspectives for further research on *AIPL1* interactions with centromere genes.

### 4.1 Impact of splicing on *AIPL1* protein function

The splicing pattern observed in *AIPL1* lead into the question what impact this splicing will have on the function of the *AIPL1* protein. The identified alternative exons are encoding presumptively important structural domains. In exons 2 and 3 (Figure 3) this is a peptidylprolyl isomerase domain, that may act in folding of nascent proteins. So skipping of exon 2 or 3 could result in *AIPL1* protein isoforms with diminished or even without chaperone function which was suggested to play a role in rod phosphodiesterase activation. The alternatively expressed aminoacids encoded from the beginning of exon 5 lie within the binding site of one established interaction partner of *AIPL1*, the *NUB1* protein and their exclusion might change the affinity for *NUB1*. So minor *AIPL1* isoforms derived from the identified alternative transcripts are supposed to have individual properties and might even possess mutually exclusive chaperone and *NUB1*-binding activity.

## 4.2 Protein expression and purification studies of AIPL1

As described in the introduction about the importance of splicing and identification of the *AIPL1* splice variants, various molecular biology techniques were used to validate these identified splice variants. To study the role of splice variants of *AIPL1* at protein level splice variants (SV1 - SV5) were sub cloned from pCR<sup>®</sup>2.1-TOPO-TA vector to pQE-TriSystemHis.*Strep* 1. The idea behind sub cloning the splice variants into the Tris-System is to use them for expressing in both prokaryotic and eukaryotic systems. For recombinant protein expression studies the QIAexpress System (pQETriSystemHis.*Strep* 1) has been chosen. In this system genes could be expressed in prokaryotic and eukaryotic systems due to the presence of both T7 (prokaryotic) and CMV (eukaryotic) promoters. For over expression of proteins in prokaryotic system an enzyme-based glucose release system (EnBase<sup>®</sup>) was opted [56]. Enbase system boosts the production of proteins in higher amounts when compared to the normal prokaryotic protein production. The higher amounts of the crude protein could be used in protein purification assays to achieve the higher amounts of His-tagged AIPL1 protein. The presence of His tag helps in producing the proteins with high purity. To pick only the His tagged AIPL1 proteins from the pellet of endogenous proteins produced during the expression, purification of expressed proteins was carried out by Ni-NTA agarose where the divalent Ni ions bind specially to the His tagged AIPL1 proteins. The expressed proteins were purified and the concentration of protein fractions (FT, W1, W2, E1, E2, E3 & E4) revealed that E2 fraction possess the highest amount of protein. To analyze whether the system opted for expressing the AIPL1 splice variants yielded the right sized His tagged AIPL1 proteins, SDS-PAGE was performed from the various fractions obtained in the Ni-NTA agarose purification (FT, W1, W2, E1, E2, E3 & E4) (Figure 14 & 18).

Further the eluted E2 fractions (Figure 15 & 19) were concentrated using the centripres for Western blot studies. In the prokaryotic system the cultures could be done in bulk amount and the production of protein in the system would be higher compared to the eukaryotic system. The expression of each splice variant was tested individually and all the splice variants were expressed in the similar fashion. In human cell lines, like HEK293 which was used in this study for eukaryotic protein expression, the enhancement of protein production in higher amounts was not possible like in the prokaryotic system. Therefore, the quantity of the expressed protein from whole cell pellet possess less AIPL1 protein. Quantity of protein is always directly proportional to the transfection rate. Repeated transfections were carried out by optimizing the conditions to obtain a good transfection efficiency. That was the one major

issue faced when expression studies were done in the eukaryotic system. Compared to the prokaryotic protein expression system the mammalian protein expression system was additional less effective because The pQE-Tri-SystemHis.*Strep* 1 system is optimized for bacterial culture and expresses suboptimal in human cells. All the expressed proteins were validated using the anti-AIPL1 antibodies as well as anti-His antibodies (Figure 16B, 17 & 20). In both systems, double bands (Figure 16 B, 17 and 20) were seen with Anti-AIPL1 and Anti-His antibodies. Post translational cleavage is one of the reasons for the appearance of double bands. In this study double bands were seen in immunoblot detection with all the splice variants (SV1-SV5). Sometimes the double bands were not detected, it was envisaged that splice variants are acting differently during protein expression based on the protein domains present in these splice variants.

#### **4.2.1 Role of imidazole and FKBP in protein purification**

Further to perform protein interaction studies a purified AIPL1 protein in higher amounts is required. To purify a desired protein, His-tagged AIPL1 in this study from a complex mixture, various factors play role in the protein purification. Among these factors protein domains and buffers used for protein purification play vital role in obtaining a high quality protein. Previously a contamination of the elute with increased imidazole concentrations was reported using Ni-NTA spin columns. The studies identified an *E. coli* protein containing a domain homologous to FK506-binding proteins (FKBPs) as a persistent contaminant in immobilized metal affinity chromatography of recombinant proteins that were expressed in *E. coli* [36]. A band of the expected size 44 kDa and the other band of 30 kDa are observed frequently in our study. A cocktail of protease inhibitors was suggested to solve the problem of extra bands, later optimization of the imidazole concentrations and application of a cocktail of protease inhibitors solved this problem (figure 16B, 17 & 20).

#### **4.3 Immunoblot analysis of AIPL1 splice variants**

The presence of all splice variants was demonstrated through immunoblot analysis, both in the prokaryotic and eukaryotic systems (Figures: 16, 17 & 20). All splice variants expressed and analyzed through the western blot migrated at about the same size corresponding to full length of AIPL1. The various size differences SV1 - 43.9 kd, SV2 - 36.8 kd, SV3 - 35.0 kd, SV4 - 40.9 kd and SV5 - 41.2 kd of the AIPL1 splice variants could not be separated. The size difference between the splice variants varies from 0.3 kDa to 8.9 kDa. The small size differences of the splice variants may explain why the splice variants could not be separated

on PAGE gels using *in vivo* samples. This could be one major reason why the various splice variants were not identified in previous studies [23]. When observed in the positive control used for all the immunoblots a slightly bigger size of the wild type protein compared to the splice variants could be shown (Figure 16). The positive control sample was extracted from protein from human retinal tissue which is eukaryotic. Eukaryotic proteins are post translationally modified. This may be the reason for the greater molecular weight of human retinal protein and compared to proteins expressed in a prokaryotic host.

#### **4.4 Choosing CENP-F as a possible interaction partner of AIPL1**

In a preceding study using a Yeast two hybrid system an interaction of the C-terminal 120 amino acids of CENP-F with AIPL1 was shown [40]. It arose interest in the influence of centromere proteins on photoreceptor maturation, while *AIPL1* playing a key role in maintaining the morphology of the neuroretina by processing farnesylated proteins [81] and CENP-F playing a role in the segregation of cells. The interest lies in knowing what happens if AIPL1 is interacting with CENP-F and the influence of interaction on retinal cytoarchitecture.

#### **4.5 Features that support interaction between AIPL1 and CENP-F**

Prenylation is important for protein interaction and function. Protein farnesylation plays important roles in the membrane association and protein-protein interaction of a number of eukaryotic proteins[94]. During Farnesylation which is catalyzed through Farnesyltransferase (FTase) an isoprenoid is added to proteins terminating in a CAAX motif at the carboxyl terminus of the protein. Previous studies concluded that *AIPL1* may interact with the C-terminal prenylation motif in the cytosol dependent on the presence of farnesyltransferase [51]. CENP-F has a C-terminal CAAX motif [4] which is required for isoprenylation and carboxy methylation. It was shown that *AIPL1* interaction enhanced the post translational farnesylation of proteins in the retina [81]. Various functions were assigned to AIPL1 which include protection of farnesylated proteins from proteasomal degradation in the cytosol, facilitated targeting of the protein to the ER for further protection or chaperone the farnesylated proteins to the target membrane. From this it was envisaged that AIPL1 farnesylation could initiate protein interaction with CENP-F through C-terminal CAAX motif during photoreceptor proliferation, which protects and guide CENP-F towards its target.

Further Yeast-two hybrid studies, determined that *AIPL1* interacts with NUB1 (NEDD8 Ultimate Buster-1), a protein involved in regulating cell-cycle progression and proliferation [2]. In cell cycle progression NUB1 functions through down-regulating NEDD8 expression post-translationally by targeting NEDD8 and its conjugates for proteasomal degradation [52]. NEDD8 is involved in the degradation of many proteins including Cyclin D1 and p27kip1, acting in the regulation of cell cycle progression in the developing retina [24,25]. Recent studies suggested that *AIPL1* regulates the ubiquitin like FAT10 pathway by interaction with FAT10 E1 activating enzyme UBA6 [6]. Ubiquitin which is a house keeping gene and plays role in cell cycle regulation, which supports the hypothesis that *AIPL1* may show partial or complete interaction with cell cycle regulating proteins.

#### **4.6 Colocalization studies of AIPL1 and CENP-F**

Transfection studies were carried out to check the subcellular localization of *AIPL1* and *CENP-F* using HeLa and HEK293 cell lines, which are not expressing *AIPL1* intrinsically. *CENP-F* is a housekeeping gene, therefore a heterologous expression of *AIPL1* should be able to show colocalization in these cell lines. The intrinsic expression of *CENP-F* in HeLa and HEK293 cells was expected to produce sufficient protein for interaction studies. The mammalian expression studies revealed that cytoplasmic localization of *CENP-F* and *AIPL1* was overlapping upon heterologous expression of *AIPL1* in HeLa cells indicating a possible interaction. Cytoplasmic localization of *CENP-F* and *AIPL1-SV1* were overlapping upon heterologous expression of *AIPL1* in HeLa cells in perinuclear positions and in the nucleus (Figure 23 and 24). From the expression level of *CENP-F* it may be interpreted that colocalization occurs during cell division indicating a restricted interaction at certain stages of the cell cycle. Nuclear morphology implies colocalization of *AIPL1* and *CENP-F* in dividing cells. Possibly pre-dividing and resting cells do not show colocalization indicating a function of *AIPL1* upon proteins active during cell division. The reduced Pearson's coefficient for SV3 (Figure 25) may indicate important domains of *AIPL1* are involved in interacting with *CENP-F* due to the missing colocalization in the cytoplasm. From (Figure 23 and 24) it was clear that the expression of *CENP-F* differs in the cells based on the developmental stages of the pre-dividing, dividing and resting. These images emphasize the redistribution of *CENP-F* and distinct punctate *CENP-F* patterns proximally located in relation to the centromeres can be seen. The interaction studies performed between *AIPL1* and *CENP-F* through immunoblot analysis did not show any interaction. May be that the interaction is transient between *AIPL1* and *CENP-F* or that there are technical reasons that

hampered detection of interaction. The system used for the interaction studies had some limitations. An first hand the size of CENP-F (350 kDa) has to be mentioned which causes a problem in blotting with AIPL1 by overblotting of the smaller AIPL1 protein in parallel transfer. Further CENP-F may not well enter the denaturing PAGE gel and thus is not represented on the blotted gel. Finally, the interaction may be too weak and underrepresented compared to interactions of AIPL1 with other cellular proteins. In this case the detection limit of the method would be insufficient.

#### **4.7 Future aspects in validating AIPL1 splice variants and protein interaction studies**

This study revealed the presence of splice variants (SV1 - SV5) in *AIPL1* gene expression studies. One drawback to the functional studies of the variants at the protein level is the lack of specific antibodies recognizing certain variants exclusively, which would be extremely useful for delineating their overlapping and distinct functions. Further investigations are required to check the role of these splice variants in interaction studies with centromere proteins and for the maintenance of photoreceptor development. For performing interaction studies between AIPL1 and CENP-F full length cloning of CENP-F into an expression vector could be one option to add a tag to the protein which may ease the access to the interaction studies. On the other hand a tag may also interrupt important protein-protein or protein-membrane interactions and may interfere with its physiological function.

## CHAPTER 5

---

### SUMMARY

In this study an investigation of splice variants in human *AIPL1*, the fourth gene underlying Leber Congenital Amurosis (LCA), in relation to cell cycle regulating centromere protein CENP-F was accessed.

The study addressed the presence of the splice variants (SV1 - SV5) of *AIPL1* at the protein level and the activity of these splice variants in relation to CENP-F. The existence of these splice variants may play a vital role in interactions of *AIPL1* with other proteins in retinal cells and may influence the activity of some *AIPL1* mutations at various developmental stages of the retina.

*AIPL1* splice variants (SV1 - SV5) were cloned into an expression vector possessing an 8xHis-tag and their expression was validated by transformation of prokaryotic cells and transient transfection into eukaryotic cells. The evaluation of the splice variants was assessed using protein over expression, purification by Ni-NTA agarose, and immunoblot studies. Ni-NTA agarose was used to purify the expressed splice variants by their His-tag. The study confirmed that the splice variants were not prone to removal by protein quality control mechanisms of eukaryotic cells indicating a functional relevance. Unfortunately, the splice variants could not be distinguished by polyacrylamide gel electrophoresis hampering their proof in tissue samples. Colocalization between *AIPL1* and CENP-F was shown in human cell lines probably upon cell division but the envisaged interaction between these two proteins could not be confirmed in immunoblot studies.

CENP-F interaction with *AIPL1* may open new views in revealing the link between photoreceptor maturation and segregation. Functional studies will have to clarify whether *AIPL1* function is influenced by these variants in the development and maintenance of photoreceptors as well as to the pathogenicity of mutations located within the alternatively spliced exons.

## **Zusammenfassung**

In dieser Studie wurden Spleißvarianten des *AIPL1*, dem vierten Gen das mit der Leberschen kongenitalen Amaurose (LCA) assoziiert ist, auf ihre Beziehung zum Zellzyklusregulator Zentromerprotein F (CENP-F) untersucht.

Die Studie befasste sich mit der Darstellung der *AIPL1* Spleißvarianten (SV1 - SV5) auf Proteinebene und deren Aktivität in Bezug auf CENP-F. Die Existenz der Spleißvarianten könnte einen grundlegenden Einfluß auf die Interaktionen des *AIPL1* mit anderen Proteinen der retinalen Zellen haben und die Funktion von *AIPL1* Mutationen in verschiedenen Entwicklungsstadien der Netzhaut beeinflussen.

*AIPL1* Spleißvarianten (SV1 - SV5) wurden in einen Expressionsvektor kloniert, der einen 8xHis-tag exprimiert und ihre Expression wurde durch Transformation in prokaryotische Zellen und transiente Transfektion in eukaryotische Zelle bewertet. Dies wurde mittels Proteinüberexpression, Aufreinigung mit Ni-NTA Agarose und Immunoblotstudien untersucht. Ni-NTA Agarose wurde zur Aufreinigung der exprimierten Proteine über den 8xHis-tag angewandt. Es zeigte sich, dass die Spleißvarianten exprimiert wurden und nicht in Proteinqualitätskontrollen der eukaryotischen Zellen entfernt wurden. Dies unterstützte die funktionelle Relevanz der Spleißvarianten. Eine Unterscheidung der Spleißvarianten über polyacrylamidgelelektrophoretische Auftrennungsverfahren konnte nicht durchgeführt werden, was die Möglichkeit eines Nachweises in Gewebeproben deutlich einschränkte.

Eine Kolokalisation von *AIPL1* und CENP-F konnte in humanen Zelllinien mutmaßlich während der Zellteilung gezeigt werden. Eine direkte Interaktion zwischen diesen beiden Proteinen konnte im Immunoblot nicht bestätigt werden.

Die Interaktion von CENP-F und *AIPL1* eröffnet neue Interpretationsmöglichkeiten über die Verknüpfung von *AIPL1* mit der Photorezeptorreifung und -verteilung. Funktionelle Studien werden klären müssen, ob *AIPL1*-Spleißvarianten die Funktion von *AIPL1* in der Entwicklung und Unterhaltung der Photorezeptoren beeinflussen und inwieweit Mutationen in den alternativ gespleißten Exons Einfluß auf deren Pathogenität nehmen.

## References

- 1 Akey DT, Zhu X, Dyer M, Li A, Sorensen A, Blackshaw S et al. The inherited blindness associated protein AIPL1 interacts with the cell cycle regulator protein NUB1. *Hum Mol Genet* 2002; 11(22):2723-2733
- 2 Akey DT, Zhu X, Dyer M, Li A, Sorensen A, Fukada-Kamitani T et al. Functional studies of AIPL1: potential role of AIPL1 in cell cycle exit and/or differentiation of photoreceptors. *Adv Exp Med Biol* 2003; 533:287-95.:287-295
- 3 Anant JS, Ong OC, Xie HY, Clarke S, O'Brien PJ, Fung BK. In vivo differential prenylation of retinal cyclic GMP phosphodiesterase catalytic subunits. *J Biol Chem* 1992; 267(2):687-690
- 4 Ashar HR, James L, Gray K, Carr D, Black S, Armstrong L et al. Farnesyl transferase inhibitors block the farnesylation of CENP-E and CENP-F and alter the association of CENP-E with the microtubules. *J Biol Chem* 2000; 275(39):30451-30457
- 5 Ashe M, Pabon-Pena L, Dees E, Price KL, Bader D. LEK1 is a potential inhibitor of pocket protein-mediated cellular processes. *J Biol Chem* 2004; 279(1):664-676
- 6 Bett JS, Kanuga N, Richet E, Schmidtke G, Groettrup M, Cheetham ME et al. The Inherited Blindness Protein AIPL1 Regulates the Ubiquitin-Like FAT10 Pathway. *PLoS One* 2012; 7(2):e30866
- 7 Blatch GL, Lassel M. The tetratricopeptide repeat: a structural motif mediating protein-protein interactions. *Bioessays* 1999; 21(11):932-939
- 8 Bowne SJ, Sullivan LS, Mortimer SE, Hedstrom L, Zhu J, Spellicy CJ et al. Spectrum and frequency of mutations in IMPDH1 associated with autosomal dominant retinitis pigmentosa and leber congenital amaurosis. *Invest Ophthalmol Vis Sci* 2006; 47(1):34-42
- 9 Carver LA, Bradfield CA. Ligand-dependent interaction of the aryl hydrocarbon receptor with a novel immunophilin homolog in vivo. *J Biol Chem* 1997; 272(17):11452-11456
- 10 Casiano CA, Humbel RL, Peebles C, Covini G, Tan EM. Autoimmunity to the cell cycle-dependent centromere protein p330d/CENP-F in disorders associated with cell proliferation. *J Autoimmun* 1995; 8(4):575-586
- 11 Chiang PW, Wang J, Chen Y, Fu Q, Zhong J, Chen Y et al. Exome sequencing identifies NMNAT1 mutations as a cause of Leber congenital amaurosis. *Nat Genet* 2012; 44(9):972-974
- 12 Cote RH. Characteristics of photoreceptor PDE (PDE6): similarities and differences to PDE5. *Int J Impot Res* 2004; 16 Suppl 1:S28-33.:S28-S33
- 13 Cremers FP, van den Hurk JA, den Hollander AI. Molecular genetics of Leber congenital amaurosis. *Hum Mol Genet* 2002; 11(10):1169-1176
- 14 D'Andrea LD, Regan L. TPR proteins: the versatile helix. *Trends Biochem Sci* 2003; 28(12):655-662

- 15 den Hollander AI, Koenekoop RK, Mohamed MD, Arts HH, Boldt K, Towns KV et al. Mutations in LCA5, encoding the ciliary protein lebercilin, cause Leber congenital amaurosis. *Nat Genet* 2007; 39(7):889-895
- 16 den Hollander AI, Koenekoop RK, Yzer S, Lopez I, Arends ML, Voeselek KE et al. Mutations in the CEP290 (NPHP6) Gene Are a Frequent Cause of Leber Congenital Amaurosis. *Am J Hum Genet* 2006; 79(3):556-561
- 17 den Hollander AI, Roepman R, Koenekoop RK, Cremers FP. Leber congenital amaurosis: genes, proteins and disease mechanisms. *Prog Retin Eye Res* 2008; 27(4):391-419
- 18 den Hollander AI, ten Brink JB, de Kok YJ, van Soest S, van den Born LI, van Driel MA et al. Mutations in a human homologue of Drosophila crumbs cause retinitis pigmentosa (RP12). *Nat Genet* 1999; 23(2):217-221
- 19 den Hollander AI, van Lith-Verhoeven JJ, Arends ML, Strom TM, Cremers FP, Hoyng CB. Novel compound heterozygous TULP1 mutations in a family with severe early-onset retinitis pigmentosa. *Arch Ophthalmol* 2007; 125(7):932-935
- 20 Dharmaraj S, Leroy BP, Sohocki MM, Koenekoop RK, Perrault I, Anwar K et al. The phenotype of Leber congenital amaurosis in patients with AIPL1 mutations. *Arch Ophthalmol* 2004; 122(7):1029-1037
- 21 Dryja TP, Adams SM, Grimsby JL, McGee TL, Hong DH, Li T et al. Null RPGRIP1 alleles in patients with leber congenital amaurosis. *Am J Hum Genet* 2001; 68(5):1295-1298
- 22 Du J, Zhang Y, Liu Y, Li Y, Zhu X. Involvement of Cenp-F in interphase chromatin organization possibly through association with DNA-dependent protein kinase. *Acta Biochim Biophys Sin (Shanghai)* 2010; 42(12):839-846
- 23 Du Z, Zhao D, Zhao Y, Wang S, Gao Y, Li N. Identification and characterization of bovine regulator of telomere length elongation helicase gene (RTEL): molecular cloning, expression distribution, splice variants and DNA methylation profile. *BMC Mol Biol* 2007; 8:18.:18
- 24 Dyer MA, Cepko CL. p57(Kip2) regulates progenitor cell proliferation and amacrine interneuron development in the mouse retina. *Development* 2000; 127(16):3593-3605
- 25 Dyer MA, Cepko CL. p27Kip1 and p57Kip2 regulate proliferation in distinct retinal progenitor cell populations. *J Neurosci* 2001; 21(12):4259-4271
- 26 Falk MJ, Zhang Q, Nakamaru-Ogiso E, Kannabiran C, Fonseca-Kelly Z, Chakarova C et al. NMNAT1 mutations cause Leber congenital amaurosis. *Nat Genet* 2012; 44(9):1040-1045
- 27 Franceschetti A, MONNIER M, Dieterle P. [Analysis of oculomotor disorders with electro-oculography]  
Analyse des troubles de l'appareil oculo-moteur par l'electro-oculographie (EOG). *Bull Schweiz Akad Med Wiss* 1954; 10(2):124-134

- 28 Freund CL, Wang QL, Chen S, Muskat BL, Wiles CD, Sheffield VC et al. De novo mutations in the CRX homeobox gene associated with Leber congenital amaurosis. *Nat Genet* 1998; 18(4):311-312
- 29 Friedman JS, Chang B, Kannabiran C, Chakarova C, Singh HP, Jalali S et al. Premature truncation of a novel protein, RD3, exhibiting subnuclear localization is associated with retinal degeneration. *Am J Hum Genet* 2006; 79(6):1059-1070
- 30 Fukada Y, Kokame K, Okano T, Shichida Y, Yoshizawa T, McDowell JH et al. Phosphorylation of iodopsin, chicken red-sensitive cone visual pigment. *Biochemistry* 1990; 29:10102-10106
- 31 Galvin JA, Fishman GA, Stone EM, Koenekoop RK. Clinical phenotypes in carriers of Leber congenital amaurosis mutations. *Ophthalmology* 2005; 112(2):349-356
- 32 Gonzalez-Barrios R, Soto-Reyes E, Herrera LA. Assembling pieces of the centromere epigenetics puzzle. *Epigenetics* 2012; 7(1):3-13
- 33 Goodwin RL, Pabon-Pena LM, Foster GC, Bader D. The cloning and analysis of LEK1 identifies variations in the LEK/centromere protein F/mitosin gene family. *J Biol Chem* 1999; 274(26):18597-18604
- 34 Graham FL, Smiley J, Russell WC, Nairn R. Characteristics of a human cell line transformed by DNA from human adenovirus type 5. *J Gen Virol* 1977; 36(1):59-74
- 35 Gu S, Thompson DA, Srisailapathy Srikumari CR, Lorenz B, Finckh U, Nicoletti A et al. Mutations in RPE65 cause autosomal recessive childhood-onset severe retinal dystrophy. *Nat Genet* 1997; 17(2):194-197
- 36 Hengen P. Purification of His-Tag fusion proteins from *Escherichia coli*. *Trends Biochem Sci* 1995; 20(7):285-286
- 37 Hidalgo-de-Quintana J, Evans RJ, Cheetham ME, van der SJ. The Leber congenital amaurosis protein AIPL1 functions as part of a chaperone heterocomplex. *Invest Ophthalmol Vis Sci* 2008; 49(7):2878-2887
- 38 Hiller M, Platzer M. Widespread and subtle: alternative splicing at short-distance tandem sites. *Trends Genet* 2008; 24(5):246-255
- 39 Inglese J, Glickman JF, Lorenz W, Caron MG, Lefkowitz RJ. Isoprenylation of a protein kinase. Requirement of farnesylation/alpha-carboxyl methylation for full enzymatic activity of rhodopsin kinase. *J Biol Chem* 1992; 267(3):1422-1425
- 40 Janke B, Lorenz B, Preising M. Functional Analysis of AIPL1 Mutations and Splice Variants. *ARVO Meeting Abstracts* 48[5], 4667. 10-5-2007.
- 41 Janke B, Lorenz B, Preising MN. Alternative Splicing in AIPL1 - Implications On Function And The Mutational Spectrum. (Abstract) *ARVO Meeting Abstracts* (Abstract) 45(5), 2481. 1-5-2004. Online Reference: <http://abstracts.iovs.org/cgi/content/abstract/45/5/2481>.

- 42 Janke B, Lorenz B, Preising MN. Alternative Splicing of LCA Gene AIPL1 Is Conserved in Mammals. (Abstract) ARVO Meeting Abstracts (Abstract) 46(5), 3101. 1-5-2005. Online Reference: <http://abstracts.iovs.org/cgi/content/abstract/46/5/3101>.
- 43 Kanaya K, Sohocki MM, Kamitani T. Abolished interaction of NUB1 with mutant AIPL1 involved in Leber congenital amaurosis. *Biochem Biophys Res Commun* 2004; 317(3):768-773
- 44 Kaplan J, Bonneau D, Frezal J, Munnich A, Dufier JL. Clinical and genetic heterogeneity in retinitis pigmentosa. *Hum Genet* 1990; 85:635-642
- 45 Karni R, de SE, Lowe SW, Sinha R, Mu D, Krainer AR. The gene encoding the splicing factor SF2/ASF is a proto-oncogene. *Nat Struct Mol Biol* 2007; 14(3):185-193
- 46 Kay BK, Williamson MP, Sudol M. The importance of being proline: the interaction of proline-rich motifs in signaling proteins with their cognate domains. *FASEB J* 2000; 14(2):231-241
- 47 Kim E, Goren A, Ast G. Alternative splicing and disease. *RNA Biol* 2008; 5(1):17-19
- 48 Kim E, Goren A, Ast G. Alternative splicing: current perspectives. *Bioessays* 2008; 30(1):38-47
- 49 Kim E, Magen A, Ast G. Different levels of alternative splicing among eukaryotes. *Nucleic Acids Res* 2007; 35(1):125-131
- 50 Kimmins S, MacRae TH. Maturation of steroid receptors: an example of functional cooperation among molecular chaperones and their associated proteins. *Cell Stress Chaperones* 2000; 5(2):76-86
- 51 Kirschman LT, Kolandaivelu S, Frederick JM, Dang L, Goldberg AF, Baehr W et al. The Leber congenital amaurosis protein, AIPL1, is needed for the viability and functioning of cone photoreceptor cells. *Hum Mol Genet* 2010; 19(6):1076-1087
- 52 Kito K, Yeh ET, Kamitani T. NUB1, a NEDD8-interacting protein, is induced by interferon and down-regulates the NEDD8 expression. *J Biol Chem* 2001; 276(23):20603-20609
- 53 Koenekoop RK, Wang H, Majewski J, Wang X, Lopez I, Ren H et al. Mutations in NMNAT1 cause Leber congenital amaurosis and identify a new disease pathway for retinal degeneration. *Nat Genet* 2012; 44(9):1035-1039
- 54 Kolandaivelu S, Huang J, Hurley JB, Ramamurthy V. AIPL1, a protein associated with childhood blindness, interacts with alpha-subunit of rod phosphodiesterase (PDE6) and is essential for its proper assembly. *J Biol Chem* 2009; 284(45):30853-30861
- 55 Kosmaoglou M, Schwarz N, Bett JS, Cheetham ME. Molecular chaperones and photoreceptor function. *Prog Retin Eye Res* 2008; 27(4):434-449
- 56 Krause M, Ukkonen K, Haataja T, Ruottinen M, Glumoff T, Neubauer A et al. A novel fed-batch based cultivation method provides high cell-density and improves yield of soluble recombinant proteins in shaken cultures. *Microb Cell Fact* 2010; 9:11
- 57 Kuksa V, Imanishi Y, Batten M, Palczewski K, Moise AR. Retinoid cycle in the vertebrate retina: experimental approaches and mechanisms of isomerization. *Vision Res* 2003; 43(28):2959-2981

- 58 Lai RK, Perez-Sala D, Canada FJ, Rando RR. The gamma subunit of transducin is farnesylated. *Proc Natl Acad Sci U S A* 1990; 87(19):7673-7677
- 59 Lamb TD, Pugh EN, Jr. Dark adaptation and the retinoid cycle of vision. *Prog Retin Eye Res* 2004; 23(3):307-380
- 60 Landschulz WH, Johnson PF, McKnight SL. The leucine zipper: a hypothetical structure common to a new class of DNA binding proteins. *Science* 1988; 240(4860):1759-1764
- 61 Leber T. Über Retinitis pigmentosa und angeborene Amaurose. *Albrecht von Graefes Arch Ophthal* 1869; 15:1-25
- 62 Li J, Zoldak G, Kriehuber T, Soroka J, Schmid FX, Richter K et al. Unique proline-rich domain regulates the chaperone function of AIPL1. *Biochemistry* 2013; 52(12):2089-2096
- 63 Liao H, Winkfein RJ, Mack G, Rattner JB, Yen TJ. CENP-F is a protein of the nuclear matrix that assembles onto kinetochores at late G2 and is rapidly degraded after mitosis. *J Cell Biol* 1995; 130(3):507-518
- 64 Liu M, Zack D. Alternative splicing and retinal degeneration. *Clin Genet* 2013;10
- 65 Liu X, Bulgakov OV, Wen XH, Woodruff ML, Pawlyk B, Yang J et al. AIPL1, the protein that is defective in Leber congenital amaurosis, is essential for the biosynthesis of retinal rod cGMP phosphodiesterase. *Proc Natl Acad Sci U S A* 2004; 101(38):13903-13908
- 66 Ma L, Zhao X, Zhu X. Mitosin/CENP-F in mitosis, transcriptional control, and differentiation. *J Biomed Sci* 2006; 13(2):205-213
- 67 Makino CL, Wen XH, Michaud N, Peshenko IV, Pawlyk B, Brush RS et al. Effects of low AIPL1 expression on phototransduction in rods. *Invest Ophthalmol Vis Sci* 2006; 47(5):2185-2194
- 68 Mataftsi A, Schorderet DF, Chachoua L, Boussalah M, Nouri MT, Barthelmes D et al. Novel TULP1 mutation causing leber congenital amaurosis or early onset retinal degeneration. *Invest Ophthalmol Vis Sci* 2007; 48(11):5160-5167
- 69 Modrek B, Lee CJ. Alternative splicing in the human, mouse and rat genomes is associated with an increased frequency of exon creation and/or loss. *Nat Genet* 2003; 34(2):177-180
- 70 Palczewski K, Kumasaka T, Hori T, Behnke CA, Motoshima H, Fox BA et al. Crystal structure of rhodopsin: a G protein-coupled receptor. *Science* 2000; 289:739-745
- 71 Parker RO, Fan J, Nickerson JM, Liou GI, Crouch RK. Normal cone function requires the interphotoreceptor retinoid binding protein. *J Neurosci* 2009; 29(14):4616-4621
- 72 Pasadhika S, Fishman GA, Stone EM, Lindeman M, Zelkha R, Lopez I et al. Differential macular morphology in patients with RPE65-, CEP290-, GUCY2D-, and AIPL1-related Leber congenital amaurosis. *Invest Ophthalmol Vis Sci* 2010; 51(5):2608-2614
- 73 Perrault I, Hanein S, Gerard X, Delphin N, Fares-Taie L, Gerber S et al. Spectrum of SPATA7 mutations in Leber congenital amaurosis and delineation of the associated phenotype. *Hum Mutat* 2010; 31(3):E1241-E1250

- 74 Perrault I, Hanein S, Gerber S, Barbet F, Ducroq D, Dollfus H et al. Retinal dehydrogenase 12 (RDH12) mutations in leber congenital amaurosis. *Am J Hum Genet* 2004; 75(4):639-646
- 75 Perrault I, Hanein S, Zanlonghi X, Serre V, Nicouleau M, foort-Delhemmes S et al. Mutations in NMNAT1 cause Leber congenital amaurosis with early-onset severe macular and optic atrophy. *Nat Genet* 2012; 44(9):975-977
- 76 Perrault I, Rozet JM, Calvas P, Gerber S, Camuzat A, Dollfus H et al. Retinal-specific guanylate cyclase gene mutations in Leber's congenital amaurosis. *Nat Genet* 1996; 14(4):461-464
- 77 Perrault I, Rozet JM, Gerber S, Ghazi I, Leowski C, Ducroq D et al. Leber Congenital Amaurosis. *Mol Genet Metab* 1999; 68(2):200-208
- 78 Petrulis JR, Perdew GH. The role of chaperone proteins in the aryl hydrocarbon receptor core complex. *Chem Biol Interact* 2002; 141(1-2):25-40
- 79 Preising MN, Hausotter-Will N, Solbach MC, Friedburg C, Rüschenhoff F, Lorenz B. Mutations in RD3 are associated with an extremely rare and severe form of early onset retinal dystrophy EOSRD. *Invest Ophthalmol Vis Sci* 2012; 53(7):3463-3472
- 80 Ramamurthy V, Niemi GA, Reh TA, Hurley JB. Leber congenital amaurosis linked to AIPL1: a mouse model reveals destabilization of cGMP phosphodiesterase. *Proc Natl Acad Sci U S A* 2004; 101(38):13897-13902
- 81 Ramamurthy V, Roberts M, Van Den AF, Niemi G, Reh TA, Hurley JB. AIPL1, a protein implicated in Leber's congenital amaurosis, interacts with and aids in processing of farnesylated proteins. *Proc Natl Acad Sci U S A* 2003; 100(22):12630-12635
- 82 Rando RR. The biochemistry of the visual cycle. *Chem Rev* 2001; 101(7):1881-1896
- 83 Rattner JB, Rao A, Fritzler MJ, Valencia DW, Yen TJ. CENP-F is a .ca 400 kDa kinetochore protein that exhibits a cell-cycle dependent localization. *Cell Motil Cytoskeleton* 1993; 26(3):214-226
- 84 SCHAPPERT-KIMMIJSER J, HENKES HE, Van Den Bosch J. Amaurosis congenita (Leber). *AMA Arch Ophthalmol* 1959; 61(2):211-218
- 85 Sergouniotis PI, Davidson AE, Mackay DS, Li Z, Yang X, Plagnol V et al. Recessive Mutations in KCNJ13, Encoding an Inwardly Rectifying Potassium Channel Subunit, Cause Leber Congenital Amaurosis. *Am J Hum Genet* 2011; 89(1):183-190
- 86 Serio G, Margaria V, Jensen S, Oldani A, Bartek J, Bussolino F et al. Small GTPase Rab5 participates in chromosome congression and regulates localization of the centromere-associated protein CENP-F to kinetochores. *Proc Natl Acad Sci U S A* 2011; 108(42):17337-17342
- 87 Smith RL, Redd MJ, Johnson AD. The tetratricopeptide repeats of Ssn6 interact with the homeo domain of alpha 2. *Genes Dev* 1995; 9(23):2903-2910

- 88 Sohocki MM, Bowne SJ, Sullivan LS, Blackshaw S, Cepko CL, Payne AM et al. Mutations in a new photoreceptor-pineal gene on 17p cause Leber congenital amaurosis. *Nat Genet* 2000; 24(1):79-83
- 89 Sohocki MM, Perrault I, Leroy BP, Payne AM, Dharmaraj S, Bhattacharya SS et al. Prevalence of AIPL1 mutations in inherited retinal degenerative disease. *Mol Genet Metab* 2000; 70(2):142-150
- 90 Stamm S, Ben-Ari S, Rafalska I, Tang Y, Zhang Z, Toiber D et al. Function of alternative splicing. *Gene* 2005; 344:1-20
- 91 Sun X, Pawlyk B, Xu X, Liu X, Bulgakov OV, Adamian M et al. Gene therapy with a promoter targeting both rods and cones rescues retinal degeneration caused by AIPL1 mutations. *Gene Ther* 2010; 17(1):117-131
- 92 Swaroop A, Kim D, Forrester D. Transcriptional regulation of photoreceptor development and homeostasis in the mammalian retina. *Nat Rev Neurosci* 2010; 11(8):563-576
- 93 Sweeney MO, McGee TL, Berson EL, Dryja TP. Low prevalence of lecithin retinol acyltransferase mutations in patients with Leber congenital amaurosis and autosomal recessive retinitis pigmentosa. *Mol Vis* 2007; 13:588-593
- 94 Tamanoi F, Kato-Stankiewicz J, Jiang C, Machado I, Thapar N. Farnesylated proteins and cell cycle progression. *J Cell Biochem Suppl* 2001; Suppl 37:64-70.:64-70
- 95 Tan MH, Mackay DS, Cowing J, Tran HV, Smith AJ, Wright GA et al. Leber Congenital Amaurosis Associated with AIPL1: Challenges in Ascribing Disease Causation, Clinical Findings, and Implications for Gene Therapy. *PLoS One* 2012; 7(3):e32330
- 96 Tan MH, Smith AJ, Pawlyk B, Xu X, Liu X, Bainbridge JB et al. Gene therapy for retinitis pigmentosa and Leber congenital amaurosis caused by defects in AIPL1: effective rescue of mouse models of partial and complete Aipl1 deficiency using AAV2/2 and AAV2/8 vectors. *Hum Mol Genet* 2009; 18(12):2099-2114
- 97 van der Spuy J, Chapple JP, Clark BJ, Luthert PJ, Sethi CS, Cheetham ME. The Leber congenital amaurosis gene product AIPL1 is localized exclusively in rod photoreceptors of the adult human retina. *Hum Mol Genet* 2002; 11(7):823-831
- 98 van der Spuy J, Cheetham ME. The chaperone function of the LCA protein AIPL1. AIPL1 chaperone function. *Adv Exp Med Biol* 2006; 572:471-476
- 99 van der Spuy J, Kim JH, Yu YS, Luthert PJ, Chapple JP, Cheetham ME. Spatial and Temporal Expression of AIPL1 and NUB1 Protein in Human Retina (Abstract). Ft. Lauderdale, 4. - 9.5.2003: The Association For Research In Vision And Ophthalmology (ARVO), 2003.
- 100 van der Spuy J, Kim JH, Yu YS, Szel A, Luthert PJ, Clark BJ et al. The expression of the Leber congenital amaurosis protein AIPL1 coincides with rod and cone photoreceptor development. *Invest Ophthalmol Vis Sci* 2003; 44(12):5396-5403

- 101 Varis A, Salmela AL, Kallio MJ. Cenp-F (mitosin) is more than a mitotic marker. *Chromosoma* 2006; 115(4):288-295
- 102 Walia S, Fishman GA, Jacobson SG, Aleman TS, Koenekoop RK, Traboulsi EI et al. Visual acuity in patients with Leber's congenital amaurosis and early childhood-onset retinitis pigmentosa. *Ophthalmology* 2010; 117(6):1190-1198
- 103 Wang GS, Cooper TA. Splicing in disease: disruption of the splicing code and the decoding machinery. *Nat Rev Genet* 2007; 8(10):749-761
- 104 Wang H, den Hollander AI, Moayed Y, Abulimiti A, Li Y, Collin RW et al. Mutations in SPATA7 cause Leber congenital amaurosis and juvenile retinitis pigmentosa. *Am J Hum Genet* 2009; 84(3):380-387
- 105 Wright AF, Chakarova CF, bd El-Aziz MM, Bhattacharya SS. Photoreceptor degeneration: genetic and mechanistic dissection of a complex trait. *Nat Rev Genet* 2010; 11(4):273-284
- 106 Young JE, Gross KG, Khani SC. A Short Enhancer Segment of the Human Rhodopsin Kinase (Rk) Promoter Drives Robust Expression of Green Fluorescent Protein and Other Reporters in Transgenic Mouse Photoreceptors and Retinoblastoma Cell Lines (Abstract). Ft. Lauderdale, 4. - 9.5.2003: The Association For Research In Vision And Ophthalmology (ARVO), 2003.
- 107 Zhou X, Wang R, Fan L, Li Y, Ma L, Yang Z et al. Mitosin/CENP-F as a negative regulator of activating transcription factor-4. *J Biol Chem* 2005; 280(14):13973-13977
- 108 Zhu X. Structural requirements and dynamics of mitosin-kinetochore interaction in M phase. *Mol Cell Biol* 1999; 19(2):1016-1024
- 109 Zhu X, Chang KH, He D, Mancini MA, Brinkley WR, Lee WH. The C terminus of mitosin is essential for its nuclear localization, centromere/kinetochore targeting, and dimerization. *J Biol Chem* 1995; 270(33):19545-19550
- 110 Zhu X, Mancini MA, Chang KH, Liu CY, Chen CF, Shan B et al. Characterization of a novel 350-kilodalton nuclear phosphoprotein that is specifically involved in mitotic-phase progression. *Mol Cell Biol* 1995; 15(9):5017-5029

## **Acknowledgements**

First and foremost I express special thanks to my principal supervisor, PD Dr. Dipl-Biol. Markus Preising, who provided me the opportunity to pursue my research and for his professional guidance throughout my doctoral endeavor.

My sincere thanks go to Professor Birgit Lorenz for providing lab space and funding for my research. I would like to thank Prof Dr. Dr. Jürgen Henning who is my co-supervisor for my PhD studies. I would like to thank PD Dr. Dr. med. vet. Knut Stieger for his valuable suggestions in the lab meetings during my research career. I thank Dr. P Sundaresan with whom I had a wonderful time during his visit to Giessen, Germany as well my visits to the Aravida eye clinic Madhurai, India.

My special thanks go to Anabella who helped me in getting acquainted with the equipment and softwares in the lab during my early days of PhD. My heartfelt thanks go to Tobias Wimmer, whose suggestions helped in solving various technical aspects of my research work. A word of gratitude goes to all my colleagues for their insightful discussions and cooperation throughout my research work.

I would like to extend my sincere thanks to “Giessen Graduate College of Life sciences” (GGL), where I had the opportunity to acquire scientific knowledge as well as soft skills. I thank all my wg-mates who are very cheerful and made my life all the time happening. I would like to thank my grandfather who always encouraged me in choosing the path for higher studies. I take this as an opportunity to thank my beloved parents Parise Satya Vara Prasad & Krishna Kumari, brothers Ajay Kumar and Chaitanya Kishore living miles away in my home country but still extending their immense support, constant encouragement, love and affection.

I am greatly indebted to my beloved wife Devi for her huge support during tough times of my career. I thank my dear friends Ramesh, P.V, Purushotham, Neelam, Balaji, Ravi Kumar, Raj Kumar, Kokila, Seemun Ray and all my buddies who gave immense support during my research.

## **Declaration**

I declare that I have completed this dissertation single-handedly without the unauthorized help of a second party and only with the assistance acknowledged therein. I have appropriately acknowledged and referenced all text passages that are derived literally from or are based on the content of published or unpublished work of others, and all information that relates to verbal communications. I have abided by the principles of good scientific conduct laid down in the charter of the Justus Liebig University of Giessen in carrying out the investigations described in the dissertation.

Place and Date

Bhupesh Parise